2-8-2011

Nano-scale evaluation of moisture damage in asphalt

Md Arifuzzaman

Md Arifuzzaman
Candidate

Civil Engineering
Department

This dissertation is approved, and it is acceptable in quality and form for publication:

Approved by the Dissertation Committee:

Rafi Tarefder, Chairperson

NANO-SCALE EVALUATION OF MOISTURE DAMAGE IN ASPHALT

BY

MD ARIFUZZAMAN

B. Sc. in Civil Engineering

Bangladesh University of Engineering and Technology, Dhaka, Bangladesh

M.Sc. in Civil (Geotechnical) Engineering

Asian Institute of Technology (AIT), Thailand

DISSERTATION

Submitted in Partial Fulfillment of the
Requirements for the Degree of

Doctor of Philosophy
Engineering

The University of New Mexico
Albuquerque, New Mexico

December 2010

DEDICATION

This dissertation is dedicated to my parents, wife, and daughter.

ACKNOWLEDGMENTS

I would like to thank my supervisor Dr. Rafiqul A. Tarefder for his support and encouragement throughout the study. I would like to express my sincere thanks to my Ph.D. committee members: Professors Arup Maji, Percy Ng, and Gabriel Huerta for their valuable time and advice. I am thankful to Dr. Thomas Rotter of Center for High Tech Materials (CHTM) for Atomic Force Microscopy (AFM) training and suggestion. I would like to thank Ms. Angie Alvarado and Mr. Bob McGennis of Holy Asphalt Company for providing me with asphalt binder, Styrene-Butadine (SB) and Styrene-Butadine-Styrene (SBS) polymer materials. Special thanks to Mr. Hal Panabaker, manager of DuPont Company for providing me with Elvaloy modifier. I would like to thank Mr. Richard Teran, Mr. Thomas Mueller, Mr. Chris Orsulak, Ms. Lisa Fukunaga and Mr. Alan Ponder of Veeco for valuabale suggestion regarding AFM tip selection and parameters for testing throughout the whole testing period. I would like to thank Mr. Lynn Smith of Novascan for custom-made functionalization of AFM tips.

I am thankful to my colleagues and friends at the Civil Engineering and Mechanical Engineering Departments. Support for this study came from the National Science Foundation.

NANO-SCALE EVALUATION OF MOISTURE DAMAGE IN ASPHALT

BY

MD ARIFUZZAMAN

ABSTRACT OF DISSERTATION

Submitted in Partial Fulfillment of the
Requirements for the Degree of

Doctor of Philosophy

Engineering

The University of New Mexico
Albuquerque, New Mexico

December 2010

Nano-scale Evaluation of Moisture Damage in Asphalt

BY

MD ARIFUZZAMAN

B.S., Civil Engineering, Bangladesh University of Engineering and Technology, BANGLADESH, 2003

M.S., Civil (Geotechnical) Engineering, Asian Institute of Technology, THAILNAD, 2005

Ph.D., Engineering, University of New Mexico, USA, 2010

ABSTRACT

Moisture damage is one of the major problems of asphalt pavements in United States. Moisture damage problem in asphalt has been studied for decades; still it remains an unsolved problem. Traditional macro-scale tests and methods failed to describe how and what factors affect moisture damage. Because moisture damage in asphalt is related to asphalt chemistry and adhesion characteristics, which are below micron scale phenomena. To this end, asphalt chemistry and adhesion values are studied at nano-scale to understand moisture damage in this study. Nano-scale measurements are conducted using an Atomic Force Microscope (AFM) in the laboratory.

In an AFM test, adhesion forces of dry and wet asphalt samples are measured by probing the sample surface with AFM tips. Nano-scale pull-off force or adhesion between sample molecules and tip molecules are measured. To facilitate the study of asphalt chemistry, AFM tips are modified using chemical functional groups such as carboxyl (-COOH), hydroxyl (-OH), ammin ($-NH_3$) and methyl ($-CH_3$), representing the chemistry of asphalt binder. Thus functionalized tips facilitate the measurement of adhesion within the asphalt binder. In addition, silicon nitride (Si_3N_4) tips are used. Silicon nitride resembles to aggregate molecules (e.g. silica aggregate) that are used to produce asphalt concrete or pavements. Thus adhesion value measured using a silicon nitride tip can be considered as the adhesion value of asphalt-aggregate interface. It is shown in this study that the adhesion within the asphalt binder varies depending on the chemistry of asphalt.

AFM testing on asphalt is non-trivial and very challenging as AFM tips stick to the asphalt surface due to viscous and soft nature of asphalt binder. AFM testing also requires smooth surface of a test sample. This study has developed a methodology for asphalt sample preparation for AFM testing. Simply, pouring asphalt binder on a glass substrate and melting to free flow and then cooling it generates an AFM asphalt sample with a root mean square surface roughness below 10 nm. Such sample surface is smooth enough for AFM testing. Through trial and error, this study has calibrated a set of AFM testing parameters that are suitable for successful adhesion measurement in asphalt binder. In all cases, a set of AFM samples are tested under dry condition, and a set of identical samples are tested after wet conditioning.

Polymer is almost an essential component of asphalt binders now-a-days. However it is not known whether polymer modification helps reduce moisture damage potential of asphalt. Therefore, both base binder and polymer modified asphalt binder are characterized herein using AFM. Two common polymers Styrene-Butadyne (SB) and Styrene-Butadyne-Styrene (SBS) are used to modify the base asphalt. The goal is to examine whether polymer modification helps reduce moisture damage at nano-scale. In addition to polymer, a chemical modifier known as Elvaloy is included in this study to examine whether Elvaloy is more effective than polymer in regards to moisture damage. It is shown that both base and modified asphalt binders are vulnerable to moisture damage to some degree. However, base binder is the most susceptible to moisture damage among all the binders. It is evident that the SB polymer modification of asphalt is good for interface adhesion, whereas the SBS polymer modification is good for achieving higher adhesion within the asphalt binder.

Antistripping agents are commonly used to reduce moisture damage potential of an asphalt binder. A number of antistripping agents are available in the market. However, it is not know which antistripping works better than others. To examine, five common antistripping agents such as lime, klingbeta, wetfix, morlife and unichem are considered for AFM testing in this study. It is evident from this study that moisture damage occurs in asphalt binder having an antistripping agent. Hydrated lime provides higher moisture damage resistance to asphalt binders that the liquid antistripping agents such as morlife, unichem, klingbeta, and wetfix. Statistical analysis of the adhesion test results is performed. Based on Pearson's p-value (significance test), it is concluded that the

adhesion value measure by an AFM varies with the type and amount of antistripping agent present in an asphalt sample.

Finally, an attempt is made to correlate nano-scale adhesion value of an asphalt binder to macro-scale strength value representing moisture damage. Only polymer modified binders are considered for examining such correlations. Macro-scale indirect tension tests are conducted on wet and dry asphalt concrete samples. A good correlation exists between the macro-scale indirect tensile strength ratio, and nano-scale adhesion ratio of wet and dry samples.

TABLE OF CONTENTS

ABSTRACT vii

CHAPTER 1 1
Introduction 1
1.1 General 1
1.2 Hypotheses, Objectives and Scope 5
1.2.1 Hypotheses One 5
1.2.2 Hypotheses Two 5
1.2.3 Hypotheses Three 5
1.2.2 Objectives and Scope 5

CHAPTER 2 8
Literatures Review 8
2.1 Introduction 8
2.1 Moisture Damage Test and Methods 8
2.1.1 Boil Test (ASTM D 3625) 9
2.1.2 Static Immersion Test (ASTM D 1664, AASHTO T 182) 9
2.1.3 Environmental Conditioning System (ECS) 9
2.1.5 Indirect Tensile Test (ASTM D 4867, AASHTO T 283) 10
2.1.6 Immersion and Compression Test (ASTM D1075, AASHTO T 165) 11
2.1.7 Freeze-Thaw Pedestal Test 11
2.1.8 Hamburg Wheel Testing Device (HWTD) 12
2.1.9 Asphalt Pavement Analyzer (APA) 12
2.1.10 Traffic Simulation Testing 13
2.1.11 Moisture Damage in Antistripping Modified Binder and AC 14
2.1.11.1 Performance of Modified Binder and AC 14
2.1.11.2 Performance of Lime Modified AC 15
2.1.11.3 Long Term Performance of Lime and Liquid Modified Binder and AC 15
2.1.11.4 Effective Percentages of Antistipping Agents 16

2.2 Atomic Force Microscopy (AFM) for Adhesion Measurement 17
2.2.1 AFM Study on Polymer 17
2.2.2 AFM on Asphalt 17
2.3 Factors that Affect Moisture Damage 19

CHAPTER 3 20
Laboratory AFM Testing 20
3.1 Introduction 20
3.2 Objective 20
3.2 Test Matrix: Without Antistripping Agents 20
3.3 Description of Asphalt Binders 21
3.4 Description of Polymers 22
3.4.1 Styrene-Butadiene (SB) Polymer 23
3.4.2 Styrene-Butadiene-Styrene (SBS) Polymer 24
3.4.3 Elvaloy 25
3.5 Polymer Mixing 27
3.5.1 SB and SBS 27
3.5.2 Elvaloy 28
3.6 AFM Sample Preparation 29
3.7 Laboratory Testing 30
3.7.1 The AFM Testing 30
3.7.2 Description of Cleanroom 30
3.8 Tip Functionalization 31
3.9 Sample Conditioning 32
3.10 Tip Calibration 33
3.11 Selection of AFM Test Parameters 33
3.12 Asphalt Surface Imaging 34
3.13 Conclusions 35

CHAPTER 4 44
Moisture Damage Evaluation on Polymer Modified Asphalt 44

4.1 Introduction 44
4.2 Objective 45
4.3 Test Matrix 46
4.4 Adhesion Measurements from Force-Distance Graph 46
4.4.1 Explanation of Force-Distance Graph and Mechanical Strength 47
4.5 Results and Discussions 47
4.5.1 Repeatability of Test Results 47
4.5.2 Adhesion Force in Dry and Wet Base Asphalts 48
4.5.2.1 Adhesive Force in Dry and Wet Asphalt Samples Using - Si_3N_4 Tip 49
4.5.2.1.2 SB Modified Asphalts 49
4.5.2.1.3 SBS Modified Asphalts 49
4.5.2.1.4 Elvaloy modified Asphalts 50
4.5.2.2 Adhesion Force in Dry and Wet Asphalt Samples Using -COOH Tips 50
4.5.2.2.1 SB Modified Asphalts 50
4.5.2.2.2 SBS Modified Asphalts 51
4.5.2.2.3 Elvaloy Modified Asphalts 52
4.5.2.3 Adhesion Force in Dry and Wet Asphalt Samples Using -CH_3 Tips 52
4.5.2.3.1 SB Modified Asphalts 52
4.5.2.3.2 SBS Modified Asphalts 52
4.5.2.3.3 Elvaloy Modified Asphalts 53
4.5.2.4 Adhesion Force in Dry and Wet Asphalt Samples Using -OH Tips 53
4.5.2.4.1 SB Modified Asphalts 53
4.5.2.4.2 SBS Modified Asphalts 54
4.5.2.4.3 Elvaloy Modified Asphalts 54
4.5.2.5 Adhesion Force in Dry and Wet Asphalt Samples Using –NH_3 Tips 54
4.5.2.5.1 SB Modified Asphalts 54
4.5.2.5.2 SBS Modified Asphalts 55
4.5.2.5.3 Elvaloy Modified Asphalts 55
4.5.3 Comparing Adhesion Force in SB and SBS Samples 55
4.5.4 The Ratio of Wet to Dry Adhesion Forces in Base, SB, and SBS Samples 56
4.6 Statistical Analysis of AFM Data 57

4.6.1 SB Samples 57
4.6.2 SBS Samples 57
4.6.3 Elvaloy Samples 58
4.7 Conclusions 58

CHAPTER 5 87
Adhesion Loss in Antistripping Treated Asphalt Binders Due to Moisture 87
5.1 Introduction 87
5.1.1 Past Study on Anstripping Agents and Moisture Damage 87
5.1.2 Objectives 89
5.2 Test Matrix 89
5.3 Statistical Analysis of AFM Data 90
5.3.1 Statistical Analysis with Pearson Value 90
5.3.2 p- Value 91
5.4 Antistripping Agents 92
5.4.1 Lime 92
5.4.2 Kling Beta 93
5.4.3 WetFix 93
5.4.4 Unichem 94
5.4.5 Morlife 94
5.5 Wet vs. Dry: Base Asphalt with Lime 95
5.6 Wet vs. Dry: Elvaloy Modified Asphalt with Lime 95
5.6.1 On 0.5% Elvaloy Binder 96
5.6.2 On 0.75% Elvaloy Binder 97
5.6.3 On 1.5% Elvaloy Binder 98
5.6.4 On 2.0% Elvaloy Binder 99
5.7 Wet vs. Dry: Elvaloy Modified Asphalt with Klingbeta (KB) 100
5.7.1 On 0.5% Elvaloy Modified KB 100
5.7.2 On 0.75% Elvaloy Modified KB 101
5.7.3 On 1.5% Elvaloy Modified KB 101
5.7.4 On 2.0% Elvaloy Modified KB 102

5.8 Wet vs. Dry: Elvaloy Modified Asphalt with WetFix 103
5.9 Wet vs. Dry: Elvaloy Modified Asphalt with Morlife 104
5.10 Wet vs. Dry: Elvaloy Modified Asphalt with Unichem 105
5.11 Wet vs. Dry: SB Modified Asphalt with Lime 106
5.12 Wet vs. Dry: SB Modified Asphalt with Kling Beta 107
5.13 Wet vs. Dry: SB Modified Asphalt with WetFix (WF) 107
5.14 Wet vs. Dry: SB Modified Asphalt with Unichem 107
5.15 Wet vs. Dry: SB Modified Asphalt with Morlife 108
5.16 Wet vs. Dry: SBS Modified Asphalt with Lime 108
5.17 Wet vs. Dry: SBS Modified Asphalt with Kling Beta 109
5.18 Wet vs. Dry: SBS Modified Asphalt with Wet Fix 109
5.19 Wet vs. Dry: SBS Modified Asphalt with Unichem 109
5.20 Wet vs. Dry: SBS Modified Asphalt with Morlife 110
5.21 Lime vs. Liquid Antistripping Agents 110
5.21.1 Base Binder 110
5.22 Error Data for Lime Modified SB Binders 111
5.23 Effect of Antistripping Agent on SB Modified Asphalt 111
5.24 Effect of Antistripping Agent on SB Modified Asphalt 112
5.25 Conclusions 112

CHAPTER 6 163
Relation between AFM Results to Mechanical Testing Results 163
6.1 Introduction 163
6.2 Objectives 164
6.3 Description of Test and Materials 164
6.4 Test Matrix 164
6.5 Superpave Gyratory Compactor and Sample Preparation 165
6.6 Moisture Damage Determination using AASHTO T 283 Method 166
6.7 Summary of Test 167
6.8 Sample Preparation 167
6.9 Determination of Bulk Specific Gravity (Gmb) 168

6.10 Maximum Specific Gravity (G*mm*)..... 169
6.11 Results of the Tests on AC..... 171
6.12 Moisture Damage Correlations between Binders and AC..... 172
6.12.1 On 4% SB Binder and AC..... 172
6.12.2 On 5% SB Binder and AC..... 172
6.12.3 On 4% SBS Binder and AC..... 173
6.12.4 On 5% SBS Binder and AC..... 173
6.13 Conclusions..... 173

CHAPTER 7..... 190
Conclusions and Recommendations..... 190
7.1 Summary..... 190
7.2 Conclusions..... 193
7.3 Recommendations for future study..... 195

REFERENCES..... 196

APPENDIX

APPENDIX A1 Elvaloy and Lime modified binder raw data.....203

APPENDIX A2 Elvaloy and KlingBeta modified binder raw data 204

APPENDIX A3 Elvaloy and Wetfix modified binder raw data 205

APPENDIX A4 Elvaloy and Morlife modified binder raw data 206

APPENDIX A5 Elvaloy and Unichem modified binder raw data.....207

Determining Hardness and Elastic Modulus of Asphalt by Nanoindentation.....208

LIST OF TABLES

Table 3.1 The AFM Testing Parameters 36

Table 3.2 The Roughness Values of AFM samples 37

Table 4.2 Variation of adhesion force at 9-point tests per sample with – Si_3N_4 tip 61

Table 4.3 Comparison of average adhesion force (nN) values 62

Table 4.4 All the test results with significance test results for SB 63

Table 4.5 All the test results with significance test results for SBS 65

Table 4.6 All the test results with significance test results for Elvaloy 67

Table 5.2 Statistical Analysis on AFM test results of SB and Lime modified asphalts with –COOH tip 114

Table 5.3 Properties of hydrated lime (Gorkem and Sengoz, 2009) 115

Table 5.4 AFM test results of SB and Lime modified asphalts (with –COOH and –OH tip) 116

Table 5.5 AFM test results of SB and Lime modified asphalts (with $–NH_3$ and $–CH_3$ tip) 117

Table 5.6 AFM test results of SB and Kling Beta modified asphalts (with –COOH and –OH tip) 118

Table 5.7 AFM test results of SB and Kling Beta modified asphalts (with $–NH_3$ and $–CH_3$ tip) 119

Table 5.8 AFM test results of SB and WetFix modified asphalts (with –COOH and –OH tip) .. 120

Table 5.9 AFM test results of SB and WetFix modified asphalts (with $–NH_3$ and $–CH_3$ tip) 121

Table 5.10 AFM test results of SB and Unichem modified asphalts (with –COOH and –OH tip) 122

Table 5.11 AFM test results of SB and Unichem modified asphalts (with $–NH_3$ and $–CH_3$ tip). 123

Table 5.12 AFM test results of SB and Morlife modified asphalts (with –COOH and –OH tip) 124

Table 5.13 AFM test results of SB and Morlife modified asphalts (with $–NH_3$ and $–CH_3$ tip) ... 125

Table 5.14 AFM test results of SBS and Lime modified asphalts (with –COOH and –OH tip) . 126

Table 5.15 AFM test results of SBS and Lime modified asphalts (with $–NH_3$ and $–CH_3$ tip) 127

Table 5.16 AFM test results of SBS and KlingBeta modified asphalts (with –COOH and –OH tip) 128

Table 5.17 AFM test results of SBS and KlingBeta modified asphalts (with –NH3 and –CH3 tip) 129

Table 5.18 AFM test results of SBS and WetFix modified asphalts (with –COOH and –OH tip) 130

Table 5.19 AFM test results of SBS and WetFix modified asphalts (with $–NH_3$ and $–CH_3$ tip) . 131

Table 5.20 AFM test results of SBS and Unichem modified asphalts (with –COOH and –OH tip) 132

Table 5.21 AFM test results of SBS and Unichem modified asphalts (with $–NH_3$ and $–CH_3$ tip) 133

Table 5.22 AFM test results of SBS and Morlife modified asphalts (with –COOH and –OH tip) 134

Table 5.23 AFM test results of SBS and Morlife modified asphalts (with $–NH_3$ and $–CH_3$ tip). 135

Table 6.1 Selection of number of gyrations for Superpave Gyratory Compactor 175

Table 6.2 Dry and wet SB modified AC cylinder samples results..... 176

Table 6.3 Dry and wet SBS modified AC cylinder samples results 177

Table 6.4 Adhesion loss of dry/wet SB and SBS samples..... 178

LIST OF FIGURES

Figure 1.1 Adhesion and cohesion in asphalt concrete 7

Figure 3.1 Elvaloy molecular arrangement 38

Figure 3.2 AFM sample 39

Figure 3.3 Schematic of an AFM 40

Figure 3.4 Picture of cleanroom at CHTM 41

Figure 3.5 Main AFM setup 42

Figure 4.1 Force-distance characteristics of asphalt samples (5% SBS, dry sample) 68

Figure 4.3 Dry vs. Wet: adhesion in base binder (0% polymer) 70

Figure 4.4 Dry vs. wet: adhesion forces in asphalt samples by -Si_3N_4 tip on SB polymer modified sample 71

Figure 4.5 Dry vs. wet: adhesion forces in asphalt samples by -Si_3N_4 tip on SBS polymer modified sample 72

Figure 4.6 Dry vs. wet: adhesion forces in asphalt samples by -Si_3N_4 tip on Elvaloy modified sample 73

Figure 4.7 Dry vs. wet sample adhesion forces using –COOH tip on SB sample 74

Figure 4.8 Dry vs. wet sample adhesion forces using –COOH tip on SBS sample 75

Figure 4.9 Dry vs. wet sample adhesion forces using –COOH tip on Elvaloy sample 76

Figure 4.10 Dry vs. wet sample adhesion force using –CH_3 tip on SB modified asphalt 77

Figure 4.11 Dry vs. wet sample adhesion force using –CH_3 tip on SBS modified asphalt 78

Figure 4.12 Dry vs. wet sample adhesion force using –CH_3 tip 79

Figure 4.13 Dry vs. wet sample adhesion force using –OH tip on SB modified sample 80

Figure 4.14 Dry vs. wet sample adhesion force using –OH tip on SBS modified sample 81

Figure 4.15 Dry vs. wet sample adhesion force using –OH tip 82

Figure 4.16 Dry vs. wet sample adhesion force using –NH_3 tip on SB modified sample 83

Figure 4.17 Dry vs. wet sample adhesion force using –NH_3 tip on SBS modified sample 84

Figure 4.18 Dry vs. wet sample adhesion force using $–NH_3$ tip on Elvaloy modified sample 85
Figure 4.19 Adhesion forces in wet SB vs. wet SBS polymer modified asphalt samples 86
Figure 5.1 Adhesion force comparison with –COOH tip on base binder 136
Figure 5.2 Adhesion force comparison with –OH tip on base binder 137
Figure 5.3 Adhesion force comparison with $–NH_3$ tip on base binder 138
Figure 5.4 Adhesion force comparison with $–CH_3$ tip on base binder 139
Figure 5.5 Adhesion forces loss in 0.5% Elvaloy samples 140
Figure 5.6 Adhesion forces loss in 0.75% Elvaloy samples 141
Figure 5.7 Adhesion forces loss in 1.5% Elvaloy samples 142
Figure 5.8 Adhesion forces loss in 2.0% Elvaloy samples 143
Figure 5.9 Adhesion forces loss in 0.5% Elvaloy samples 144
Figure 5.10 Adhesion forces loss in 0.75% Elvaloy samples 145
Figure 5.11 Adhesion forces loss in 1.5% Elvaloy samples 146
Figure 5.12 Adhesion forces loss in 2.0% Elvaloy samples 147
Figure 5.13 Adhesion forces loss in 0.5% Elvaloy samples 148
Figure 5.14 Adhesion forces loss in 0.75% Elvaloy samples 149
Figure 5.15 Adhesion forces loss in 1.5% Elvaloy samples 150
Figure 5.16 Adhesion forces loss in 2.0% Elvaloy samples 151
Figure 5.17 Adhesion forces loss in 0.5% Elvaloy samples 152
Figure 5.18 Adhesion forces loss in 0.75% Elvaloy samples 153
Figure 5.19 Adhesion forces loss in 1.5% Elvaloy samples 154
Figure 5.20 Adhesion forces loss in 2.0% Elvaloy samples 155
Figure 5.21 Adhesion forces loss in 0.5% Elvaloy samples 156
Figure 5.22 Adhesion forces loss in 0.75% Elvaloy samples 157
Figure 5.23 Adhesion forces loss in 1.5% Elvaloy samples 158
Figure 5.24 Adhesion forces loss in 2.0% Elvaloy samples 159

Figure 5.25 Adhesion force comparison for the base binder with –COOH and –OH tips..... 160

Figure 5.26 Adhesion force comparison for the base binder with – NH_3 and – CH_3 tips..... 157

Figure 5.27 Error bar plot for lime mixed 3% SB samples..... 158

Figure 5.28 Error bar plot for lime mixed 4% SB samples..... 159

Figure 5.29 Error bar plot for lime mixed 5% SB samples..... 160

Figure 5.30 Adhesion losses comparison for the 4% SB binder modified with lime using –CH_3 tips..... 161

Figure 5.31 Adhesion losses comparison for the 5% SB binder modified with KB using –CH_3 tips 162

Figure 6.1 Superpave Gyratory Compactor 179

Figure 6.2 Top view of water bath..... 180

Figure 6.3 Vacuum machine setup..... 181

Figure 6.4 Gyratory compacted cylinder sample 182

Figure 6.5 A part of laboratory setup for measuring G*mb* 183

Figure 6.6 Loose mix sample..... 184

Figure 6.7 IDT setup 185

Figure 6.8 Adhesion loss comparison on 4% SB binder and AC sample 186

Figure 6.9 Adhesion loss comparison on 5% SB binder and AC sample 187

Figure 6.10 Adhesion loss comparison on 4% SBS binder and AC sample..... 188

Figure 6.11 Adhesion loss comparison on 5% SBS binder and AC sample..... 189

CHAPTER 1

Introduction

1.1 General

Asphalt pavement is one of the biggest infrastructures in US. There are about 4 million miles of asphalt roads and nationally we spend billions of dollars to keep our highway and roadway pavements functional. An asphalt pavement shows several distresses including fatigue cracking, rutting and moisture damage. While in the last decades several experiments and models were developed to tackle cracking and rutting, moisture damage in asphalt remained vastly unexplored. Even, the new mechanistic pavement design guide has established models for fatigue cracking and rutting but not for moisture damage. Moisture damage is yet a poorly understood phenomenon in asphalt engineering.

Moisture induced-damage is caused by moisture interaction with bonds in an asphalt system. The main difficulty in understanding moisture damage lies in the fact that the moisture interaction with bonds in an asphalt system is a phenomenon that occurs at the nano-scale level. Moisture-induced damage in asphalt concrete can be attributed to two prime mechanisms, namely, the loss of adhesion, and the loss of cohesion as shown in Figure 1.1. Loss of adhesion, also called stripping, is caused by breaking of the adhesive bonds between the aggregate surface and the asphalt binder primarily due to the action of water and water vapor (Jo et al. 1997, Little and Jones 2003). Loss of cohesion is caused

by the softening or breaking of cohesive bonds within the asphalt binder due to the action of water or water diffusion. When bonds are damaged or broken, asphalt pavement weakens and develops failure such as particle disintegration, degradation, eventually leading to potholes, cracking and raveling. There is a need for measuring loss of adhesion/cohesion in asphalt-aggregate system.

Up until today, numerous test methods have been developed and used to predict moisture-induced damage in asphalt concrete (Masad et al. 2006, Kanitpong and Bahia 2005, Cheng 2002, Solaimanian et al. 1993). In the last two decades, there have been significant improvements in moisture damage test methods and our understanding the micro to macro-scale behavior of asphalt concrete (Hicks et al. 2004, Solaimanian et al. 1993). There exists evidence that moisture-induced damage in asphalt concrete is influenced by factors such as asphalt grade, viscosity, modifiers, phenol group concentrations, aggregate surface chemistry, minerals, roughness, porosity, clay coatings, mix air voids, asphalt content, permeability, and binder thickness (Hicks 2004). Yet, a combination of asphalt and aggregate that would be compatible enough to produce moisture damage-free asphalt concrete is not available (Hicks et al. 2004, Park 2000). Consequently, the pavement engineering community continues to place faith in available asphalt-aggregate mixtures, which leads to construction of damage prone pavements. There is an urgent need for the development and assessment of testing methods capable of examining the effect of moisture on asphalt concrete. To this end, this study employs an atomic force microscope (AFM) for measuring adhesion/cohesion forces in an asphalt

system. There is a need for determining type of polymer and antistripping agent that can reduce moisture damage in asphalt.

Moisture damage tests have been developed largely through micro-scale testing. For example, according to AASHTO T283 method, asphalt concrete cylindrical samples are tested under wet and dry conditions. Similarly, Boil test (ASTM D 3625), Static Immersion test (ASTM D 1664, AASHTO T182), Indirect Tensile Test (ASTM D 4867, AASHTO T 283) etc. are done at macro-scale. Very recently, a study has attempted to measure surface force of asphalt cast onto glass slide substrates using AFM (Huang et al. 2005). Their study was limited to asphalt morphology. This preliminary AFM tests were done using -Si_3N_4 tips. The present study has included functionalized tips to measure weak intermolecular forces (i.e., adhesion/cohesion) in polymer modified asphalt systems. To the authors' knowledge, such a study has not been attempted yet in the asphalt area. No real attempts have been made to match the functional groups exists in asphalt binder. There is a need for understanding the effect of those functionals on moisture damage in asphalt.

Moisture damage within the binder and/or at asphalt-aggregate interfaces has been studied by several researchers (Sadd et al. 2003, Cheng et al. 2002, Masad et al. 2006, Little et al. 2004). Recently, surface free energy of asphalt and aggregate has been empirically related to the moisture-induced damage of asphalt concrete (Cheng et al. 2002, Wasiuddin et al. 2008). Surface free energy of asphalt and aggregate is indirectly measured using the Wilhelmy plate, sorption device, and Youn-Dupré equation. However, the Wilhelmy plate method cannot differentiate between the functional groups.

For example, the surface free method fails to differentiate between actions of carboxylic acid (bad) and carbonyls (good), or carboxylic acid (bad) and nitrogen compound (good) under wet condition. Also, the Wilhelmy plate technique cannot clearly distinguish between untreated asphalt and asphalt treated with amine antistrip. By the same token, the universal sorption device requires vacuum degas preconditioning, which is very different from the mixing plant conditions (Wasiuddin et al. 2008). Very recently, a study has attempted to measure surface force of asphalt cast onto glass slide substrates using AFM (Huang et al. 2005). Their study was limited to asphalt morphology and did not include functionalized tips. The present study has included functionalized tips to measure intermolecular forces (i.e., adhesion/cohesion) in polymer modified asphalt systems. To the author's knowledge, such a study has not been attempted yet in the asphalt area.

Though various macro-micro scale tests and models of moisture damage of HMA have been suggested, the fact is that these test and models cannot explain why moisture damage occurs in HMA mixtures. As moisture related damage initiates from the atomic and molecular level, it is hypothesized in this study that a nano and micro level testing is necessary element in estimating the moisture damage problem. However, most of these tests did not develop an understanding of the bond damage phenomena, and so as a result moisture damage is still one of the most common and complex unsolved problems. Hence, the need for a fundamental approach, which would elucidate and quantify bond strength in asphalt concrete is evident (Little and Jones 2003, Hicks et al. 2004).

1.2 Hypotheses, Objectives and Scope

1.2.1 Hypotheses One

Asphalt binder contains carboxyl (-COOH), hydroxyl (-OH), methyl ($–CH_3$), and ammin ($-NH_3$) functionals. How these functional groups affect adhesion/cohesion properties is not known yet. It is hypothesized that adhesion within asphalt can be determined using chemically functionalized AFM tips.

1.2.2 Hypotheses Two

Antistripping agents are commonly used in asphalt binders to guard against moisture damage. However, it is not known how effective these agents are in reducing adhesion and cohesion. It is hypothesized that AFM test results can be interpreted to measure the effect of antistripping agents.

1.2.3 Hypotheses Three

Moisture damage in macro-scale is quantified using wet and dry sample strength ratio. Such ratio can be defined by adhesion of wet and dry samples. It is not known where macro-scale wet/dry ratio can be correlated to the nano-scale wet/dry adhesion ratio, called bond damage index in this study.

1.2.2 Objectives and Scope

The objectives are to:

- Measure the magnitude of the intermolecular interactions (i.e. adhesion) between asphalt and silicon-nitride (i.e. resembles aggregate) molecules by proving the asphalt surface with a silicon nitride AFM tip.

- Quantify the magnitude of the intermolecular interactions (i.e. cohesion) between asphalt molecules and carboxyl (–COOH), methyl ($–CH_3$), ammin ($-NH_3$) and hydroxyl (–OH) functional groups by proving the asphalt surface with chemically functionalized tips.
- Determine the effect of antistripping agents on adhesion/cohesion
- Examine whether there is a correlation between macro-scale wet/dry strength ration and nano-scale wet/dry bond damage ratio

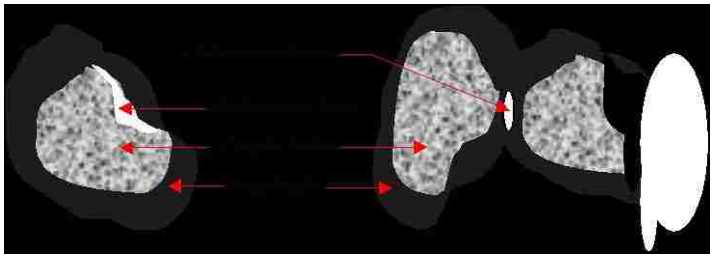

Figure 1.1 Adhesion and cohesion in asphalt concrete

CHAPTER 2

Literatures Review

2.1 Introduction

Asphalt concrete, being a compacted mix of asphalt coated aggregates and air voids, derives its strength mainly from two phenomena: adhesion/cohesion resistance of the asphalt binder, and interlock and frictional resistance of the aggregate particles. Under traffic and environmental loading, the stress imposed on the asphalt-aggregate system is a key factor that leads to bond damage. When bonds are damaged or broken, asphalt pavement weakens and develops failure such as particle disintegration, degradation, eventually leading to potholes, cracking, and raveling. The breaking of bonds between two asphalt or aggregate molecules occurs at a nano-scale. Therefore, a nano-scale understanding of the bond breaking, in other words, the intermolecular forces in an asphalt-aggregate system is important. To date, only the rheological properties such as viscosity, and penetration, and mechanical properties such as dynamic shear, phase angle, and stiffness of polymer modified asphalt binder are measured (WRI, 2003).

2.1 Moisture Damage Test and Methods

Several researchers have developed various test methods and devices to study moisture damage in asphalt. Some of these test methods are discussed below:

2.1.1 Boil Test (ASTM D 3625)

Boil test is done on loose asphalt mix is accordance to ASTM D3625. A total of about 250 grams of loose Hot Mix Asphalt (HMA) is added to boiling water for 10 minutes and the percentage of the total of aggregate visible surface area that retains its original coating after boiling is estimated. It is considered that this HMA has the potential to fail by stripping if this value is below 95%. This test has been modified by considering various methods of stirring the mixture, various sample sizes, and various procedures for adding water.

2.1.2 Static Immersion Test (ASTM D 1664, AASHTO T 182)

In this method, the specimen of HMS is immersed in distilled water (77°F) for 16 to 18 hours and is observed under water to visually estimate the total surface area of the aggregate on which asphalt coating remains according to both ASTM D 1664 and AASHTO T 182.

2.1.3 Environmental Conditioning System (ECS)

It can simulate the field condition up to certain level. The ECS is a product of SHRP project A-003A. It is consisted of three subsystems such as fluid conditioning, an environmental conditioning cabinet, and a loading system. The HMA sample experienced various conditioning cycles in these subsystems to simulate real field conditions. After conditioning the sample, the modular ratio, water permeability, and percent stripping based on visual inspection are measured to evaluate the moisture susceptibility of HMA (Terrel and Al-Swailmi 1994).

2.1.4 Net Adsorption Test (NAT)

This test determines the aggregate potential for moisture sensitivity of HMA. It was developed through the SHRP project A-003B that was focused on the fundamental aspects of the bond between aggregates and asphalt binders. In this process, aggregate (passed #4 sieve) are kept in a 135°C oven for 15 hours for drying. A solution of asphalt in toluene is added to 50 grams of aggregate sample and subsequently removed after specific times with or without the introduction of further water. The differential amount of absorption of asphalt into the aggregate from asphalt/toluene solution between the "with water" and "without water" cases can be measured using the difference in the amount of asphalt binder concentration from the supernatant solution (Curtis et al. 1991).

2.1.5 Indirect Tensile Test (ASTM D 4867, AASHTO T 283)

Here, cylindrical samples are prepared for testing for moisture suceptibility. One-third of the prepared sample is kept in the dry condition and the remaining two-thirds of the samples are exposed to vacuum saturation. After that, one half of the vacuum saturated samples are exposed to secondary conditioning consisting of a single freeze–thaw cycle (0ºF–140ºF) or repeated freeze–thaw cycles (18 cycles of 0ºF–120ºF–0ºF). After the two sample groups—dry conditioned and moisture conditioned—are tested for indirect tensile strength and instantaneous E-modulus at 55°F and 73°F, the data are normalized by expressing them in the form of a tensile strength ratio (TSR) and an E–modulus ratio (EMODR), where the tensile strength and E-modulus of the conditioned specimens are expressed as percentages of the dry (unconditioned) results. Field evaluation, involving 17 in-service pavements in 14 states, indicated that a minimum tensile strength ratio of 0.7 provided good reliability in identifying good stripping resistance (Lottman, 1982).

According to Tunnicliff and Root, the induced damage could be attributed to the conditions of the test rather than to the moisture susceptibility of the mixtures tested in Lottman's test. Thus, conditioning after vacuum saturation was modified to simulate more accurate locally prevalent climatic conditions. AASHTO T283, which is generally referred to as the "modified Lottman" test, was developed by Kandhal and adopted by AASHTO in 1985 (Kandhal 1992). It is a combination of the Lottman and the Root-Tunnicliff tests. Work by Kiggunndu and Roberts indicate this test is the most accurate test method currently available for predicting moisture damage in HMA mixtures.

2.1.6 Immersion and Compression Test (ASTM D1075, AASHTO T 165)

This method is type of mechanical test in the laboratory. It has similarities with the indirect tensile test. The main difference is the way to apply the load. In indirect tension, samples are loaded diametrically to apply tension. In compression test, sample is subjected to indirect compression. In this approach, the ratio of retained indirect compressive strengths between the conditioned and unconditioned samples is used as the acceptance criterion.

2.1.7 Freeze-Thaw Pedestal Test

This test was developed by Kennedy and Anagnos in 1984. Uniform size aggregate (0.50 –0.85 mm) are cured for 2 hours at 150°C before compaction. Then compact under 28 KN to 19 mm X 41 mm size. After compaction the sample was cured for three days at room temperature. Thermal Cycling –12°C (15 hrs), 49°C (9 hrs) for causing crack initiation in an asphalt mixture.

2.1.8 Hamburg Wheel Testing Device (HWTD)

This test was developed by Helmut-Wind Incorporated of Hamburg, Germany (Takallou et al. 1985). HWTD is used as a specification requirement for some of the most traveled roadways in Germany to evaluate rutting and stripping. The results obtained from the Hamburg Wheel Testing Device consist of rut depth, stripping, creep slope, inflection point, and stripping slopes. The stripping inflection point is the number of wheel passes corresponding to the intersection of the creep slope and the stripping slope. The values are used to estimate the relative resistance of the HMA sample to moisture-induced damage. The HMA mixture that survives the HWTD test should be rut resistant in the field; however mixtures that do not survive the test may also perform well in the field as well. Use of this device in mixture pass/fail situations can result in the rejection of acceptable HMA mixtures. However, if the criteria are set correctly this should be a reasonable test to evaluate rutting and/or stripping. Potential user agencies need to develop their own evaluation of test results using local conditions. Izzo and Tahmoressi evaluated the laboratory repeatability of the HWTDs among different laboratories throughout the United States. Their results indicated that the device has good repeatability when testing a gravel mixture, but it has poor repeatability when testing a limestone slab compacted mixture. Currently, the Utah DOT and Texas DOT use the HWTD to evaluate mix design or plant produced mix (Fromm 1974).

2.1.9 Asphalt Pavement Analyzer (APA)

The APA has been used in an attempt to evaluate rutting, fatigue, and moisture resistance of the HMA mixtures. This method was first manufactured in 1996 by Pavement

Technology, Inc. The test specimens for the APA can be either beam or cylindrical. Tests can also be performed on cores or slabs taken from an actual pavement. Test configurations for cylinders include 4% air voids, standard PG temperature, and standard hose and test configurations for beams include 5% air voids, standard PG temperature and standard hose were recommended in NCHRP Project 9-17 to develop the APA rut test. Recently, various agencies have utilized APA to evaluate moisture damage of asphalt mixes (ASTM-Road and Paving Material 1998). Samples were tested at 40°C using four different preconditioning procedures: dry, soaked, saturated, and saturated with a freeze cycle. The test results indicated that only dry and soaked conditioning appeared to be adequate and saturation with a freeze cycle did not result in increased wet rut depths. As a conclusion, it was found that the APA can be utilized to evaluate the moisture susceptibility of asphalt mixes with precautions.

2.1.10 Traffic Simulation Testing

This test tries to simulate the traffic condition over pavement. Here the load condition on pavement derives from the passage of traffic wheel loads passing over the pavement surface. Although most performance tests have been developed to simulate this condition through many hypotheses, only several tests can closely simulate this condition. The common element of these tests is the application of a wheel loading over the surface of the sample. Some of these include the Asphalt Pavement Analyzer (APA), the Georgia Loaded Wheel Tester (GLWT), and the Hamburg Wheel Tracking Device (HWTD). In the evaluation of stripping using the HWTD, a rectangular slab specimen (10.2 x 12.6 x 1.6 in) is compacted to 7% ± 1% air voids using a laboratory rolling compactor and tested

with a 47 mm wide steel wheel under a load of 705 N. The wheel is moved back and forth over the specimen while submerged under water. The results are plotted on a graph of the permanent deformation (rut depth) versus the number of wheel passes for calculation purpose. As the number of wheel passes increases, the permanent deformation increases slowly until up to some point a rapid increase in the rate of deformation is observed. A bi-linear plot is observed, and it has been hypothesized that the point at which the slopes change (referred to as the stripping inflection point) indicates the initiation of stripping within the mixture. The number of loaded wheel passes needed to achieve the stripping inflection point is used as a relative measure of susceptibility to stripping. Unfortunately, the various equipment used (i.e., Asphalt Pavement Analyzer, Hamburg Wheel Tracking Device, and Georgia Loaded Wheel Tester) rank mixtures differently with respect to moisture susceptibility (Sunghwan and Brian 2005).

2.1.11 Moisture Damage in Antistripping Modified Binder and AC

2.1.11.1 Performance of Modified Binder and AC

Huang et al. (2010) performed laboratory experiment to investigate the effectiveness of cementitious fillers on moisture susceptibility of HMA mixtures. They utilized five types of cementitious fillers namely, fly ash, cement kiln dust, and three types of hydrated lime with different finenesses. The laboratory performance of HMA mixtures subjected to moisture conditioning was evaluated through the following tests: dynamic modulus test; superpave indirect tensile tests; and tensile strength ratio test. The test results indicate that the cementitious fillers were generally effective in reducing the moisture susceptibility of HMA mixtures. The finer the hydrated lime particle, the more resistant the asphalt

mixtures. In addition, dynamic shear rheometer test was conducted on asphalt mastics to explore the stiffening effect of different cementitious fillers.

2.1.11.2 Performance of Lime Modified AC

Sebaaly et al. (2002) evaluated field samples and pavement performance data from untreated and lime treated pavements. The properties of untreated and lime-treated mixtures from field projects in the southern and north-western parts of Nevada indicated that lime treatment of Nevada's aggregates significantly improves the moisture sensitivity of HMA mixtures. The study showed that lime treated HMA mixtures become significantly more resistant to multiple freeze-thaw than the untreated mixtures. The long term pavement performance data indicated that under similar environmental and traffic conditions, the lime-treated mixtures provided better performing pavements with fewer requirements for maintenance and rehabilitation activities. The analysis of the impact of lime on pavement life indicated that lime treatment extends the performance life of HMA pavements by an average of 3 years. This represents an average increase of 38% in the expected pavement life.

2.1.11.3 Long Term Performance of Lime and Liquid Modified Binder and AC

Putman and Amirkhanian (2006) studied the effects of conditioning the mixes for longer durations. Their report addresses two issues, by preparing and testing mixtures made with fresh binder for indirect tensile strength after conditioning the samples for 1, 7, 28, 90 and 180 days, and samples prepared from binder stored for 3 days at 163^{o}C after conditioning them for 1, 28 and 90 days. The results of this study indicated that hydrated

lime and the liquid anti-stripping agents were equally effective for the mixes used in this research when conditioned beyond 1 day. In the case of samples prepared from stored binder, there was no significant difference in the effectiveness of hydrated lime and the liquid anti-stripping agents even after conditioning for 1 day. Though it was observed that none of the ASA treatments performed better than others in the case of samples prepared with stored binder, it was also observed that almost all mixes gave significantly similar wet ITS and TSR values as samples prepared from fresh binder.

2.1.11.4 Effective Percentages of Antistipping Agents

Kandhal and Rickards (2001) classified stripping as a physio-chemical incompatibility of the asphalt system, and the classical moisture sensitivity tests are relevant. They suggested that under saturated conditions all asphalt mixes may fail as a consequence of cyclical hydraulic stress physically scouring the asphalt binder from the aggregate. They classified this stripping as a mechanical failure of the asphalt pavement system and the classical moisture sensitivity tests are irrelevant. This study documented four such case histories from Pennsylvania, Oklahoma, and New South Wales in Australia. Case histories gave the details of construction, visual observation of pavement distress, sampling and testing of pavement, and conclusions/recommendations. Moisture profile within the pavement structure was also determined by dry sampling with a jack hammer. The phenomenon of stripping was investigated from a global perspective, looking at the relative permeability of the pavement components, subsurface drainage system, and the interaction between different asphalt courses including open-graded friction courses. Hypotheses were presented to explain the mechanisms that will result in the pavement

saturation observed. They recommended using the percentage of lime as 1-1.5% in the HMA.

2.2 Atomic Force Microscopy (AFM) for Adhesion Measurement

2.2.1 AFM Study on Polymer

AFM has been used in polymer science for long time. Adhikari et al. (2001) studied the morphology of different styrene/butadiene (SB) block copolymers with triblock architectures using tapping mode scanning force microscopy (SFM). Comparative analysis of the morphology of the samples at the polymer/substrate interface of solution-cast films and in bulk was performed. They found that, besides the total phase volume ratio, the interfacial structure between the incompatible chains determines the phase morphology and mechanical properties of the investigated block copolymers.

2.2.2 AFM on Asphalt

Recently, a study has attempted to measure surface force of asphalt cast onto glass slide substrates using the AFM (Huang et al. 2005). Their study was limited to asphalt morphology and did not include functionalized tips. Abraham et. al (2002) used an atomic force microscope (AFM) to directly measure the interaction between asphaltenes and silica surfaces in aqueous solutions. The electrokinetic properties of these surfaces were determined to establish a link between conventional electrokinetic studies and AFM results. The Western Research Institute (WRI) has reported use of Atomic Force Microscopy to develop quantifiable images of asphalts and asphalt with additives (Huang 2005) and their adhesive properties with aggregate at interfacial region. Loeber et. al (1996) has reported that the structure of asphalts can be studied without any pre-

preparation with AFM. Abraham et. al (2002) has also reported use of AFM to directly measure the interaction between asphaltenes and silica surfaces in aqueous solutions. The electrokinetic properties of these surfaces were determined to establish a link between conventional electrokinetic studies and AFM results. Liu et al. (2006) studied and characterized the morphology of asphaltene films with AFM. Ren et al (2009) studied the effect of weathering on colloidal interactions between bitumen and oil sands solids by atomic force microscopy (AFM). Western research institute has studied the surface energy study of SHRP asphalt with AFM (Pauli et al. 2003). They investigated surface energies with the help of AFM. Moraes et al. studied the AFM study on asphalt high temperatures. AFM was used to reveal the structure of the surface of a sample of asphalt cement (CAP 30/45) derived from a blend of Arabian Light asphalting residue with aromatic extract of Bright Stock. Images of phase contrast and topography were obtained at different temperatures and after different thermal treatment and it was observed that the overall sample morphology is highly dependent on the thermal history and analysis temperature (Moraes et al. 2009). Some AFM work on asphalts, a bee-like structure, called catana phase, was attributed to asphaltene (Loeber et al. 1996; Masson et al. 2006). This model was supported by Pauli et al. (2001) who doped bitumen with asphaltene and observed an increase in the density of the catana phase in the doped material. The bee structure does not have a defined pattern but usually it can be visualized by AFM as composed of a series of aligned protrusions and depressions (Moraes et al. 2009). Work at Council for Scientific and Industrial Research (CSIR) is focusing on the correlation between the aging of bituminous binders on the road (a property that severely affects the deterioration of the pavement surface) and the elastic stiffness of the binders as measured

using the AFM (Steyn 2007). Initial data focused on the surface morphology and a clear difference could be observed between the surface morphology of a bituminous binder that was aged at different temperatures.

2.3 Factors that Affect Moisture Damage

Moisture damage in asphalt concrete pavements is a complex phenomenon and does not relate to a single factor. This is affected by a variety of factors like asphalt binder type, mix composition, percentages of air void ratio, pavement drainage condition, traffic loading, and some environmental factors.

If asphalt pavement is impermeable then it could prevent the penetration and movement of moisture through it. But in practical we design the pavement with certain percentages of air void in order to handle some other distresses. For conventional dense-graded mixes, excess rutting and bleeding typically occur if the air-void content is less than three percent. Moisture in asphalt pavement may also affect cohesion through saturation and expansion of the void system due to freeze-thaw cycles under temperature changes (Stuart 1990).

CHAPTER 3

Laboratory AFM Testing

3.1 Introduction

This chapter deals with the materials description, sample mixing and preparation of the AFM testing. In this study the AFM is used to evaluate adhesion between asphalt-aggregate molecules. The word 'adhesion' based on the Latin word adhaerere (means 'to stick to'). According to ASTM D907 the definition of adhesion is "the state in which two surfaces are held together by valence forces or interlocking forces, or both" (Hefer and Little 2005). The testing parameters are prerequisite for acquiring successful force-distance curve. The parameters are not trivial hence it needs a lot of trial for successful reading for the AFM lab testing.

3.2 Objective

The objectives of the study are:

1. Quantification of the AFM testing parameters for asphalt binder
2. To capture AFM Image and analysis of dry and conditioned asphalt binders.
3. To select good smooth samples from surface roughness analysis.

3.2 Test Matrix: Without Antistripping Agents

This study explores three polymers namely, styrene-butadiene (SB), styrene-butadiene-styrene (SBS) and Elvaloy. SB was SBS were mixed at 1%, 2%, 3%, 4% and 5% (by

weight) of a base asphalt binder. The total of four (0.5%, 0.75%, 1.5% and 2.0%) different percentages of Elvaloy was modified with the base binder for testing. Polymer-modified asphalt films or samples are prepared on glass substrate. One set of sample is tested under dry condition, and the other set tested after wet conditioning. A total of five different AFM tips are used. One is a silicon nitrite (Si_3N_4) tip, and other tips are modified with asphalt functionals such as carboxyl (–COOH), hydroxyl (–OH), ammin (-NH_3) and methyl (–CH_3). All the tips were classified as either hydrophobic and or hydrophilice types. The –COOH and –OH are hydrophilic tips and the –NH_3, -CH_3 and –Si_3N_4 are hydrophobic tips. Probing the asphalt (film) surface with functionalized tips facilitates the measurement of cohesion between two asphalt molecules. Whereas probing the asphalt surface with silicon nitrite -Si_3N_4 tip facilitates the measurement of adhesion between an asphalt molecule and an aggregate molecule. Silica being the most naturally abundant aggregate mineral, silicon nitrite tip is selected for this study (Park et al. 2000, Petersen and Plancher 1998).

All the AFM tests are done at room temperature. A total of 864 tests [6 (1 base, 5 percent polymer) x 2 (SB and SBS) x 2 (dry and wet) x 4 tips x 9 points] are performed.

A total of five types (lime, klingbeta, wetfix, morlife and unichem) of antistripping agents were mixed with all the binders to study the moisture damage.

3.3 Description of Asphalt Binders

The base asphalt and polymers are collected from a local supplier in New Mexico in cooperation with the New Mexico Department of Transportation. Chemically, asphalt

consists of long carbon chains and rings saturated with hydrogen atoms, which are essentially non-polar in character (Little and Jones 2003). The inert character of these molecules stems from the fact that they are saturated, made up exclusively from single C-H and C-C bonds, with relatively balanced electron distributions and therefore little tendency to move around. These non-polar molecules interact mainly through van der Waals forces. Because van der Waals forces are additive, their contribution in these large molecules is significant. Asphalt is comprised of not only non-polar hydrocarbons but also a small number of heteroatoms such as nitrogen (N), sulfur (S), and oxygen (O), which produce different functional groups in asphalt. A functional group is a group of atoms of a particular arrangement that gives the entire molecule certain characteristics. Functional groups are named according to the composition of the group. For example, −COOH is a carboxyl functional group in asphalt. The most common functional groups in asphalt are: carboxyl (–COOH), methyl ($–CH_3$), ammin ($-NH_3$) and hydroxyl (–OH) (Robertson 2000, Petersen and Plancher 1998, Park et al. 2000). Therefore, these functionals are applied to the AFM tips.

3.4 Description of Polymers

In order to accommodate the increasing traffic loadings in varying climatic environments and to resist to failures such as moisture damage, permanent deformation and cracking, major emphasis has been placed on improving the performance of asphalt mixtures. This approach has led to a fundamental variation in the design of long lasting asphalt pavements (Sengoz and Isikyakar 2008). Currently, the most commonly used polymer for bitumen modification is the styrene–butadiene–styrene (SBS) followed by other polymers

such as styrene butadiene rubber (SBR), ethylene vinyl acetate (EVA) and polyethylene (Airey 2004). For improving the asphalt binder characteristics, specific performance enhancers have been investigated in this study. These include additive modification, polymer modification and chemical reaction modification (Isacsson and Lu 1999). Polymers can be viewed as dispersed system of a polymer network (Kiridena et al. 1998, Tarefder et al. 2002). The three types of polymers used in this study are described below:

3.4.1 Styrene-Butadiene (SB) Polymer

Styrene-Butadiene (SB) is an elastomeric copolymer consisting of styrene ($C_6H_5CH=CH_2$) and butadiene ($CH_2=CH-CH=CH_2$). Its molecular formula is $C_{12}H_{14}$ and molecular weight is 158.24 g/mol. It has tensile strength of about 18 MPa with an elongation (strain) value of 70%. (Legge et al. 1987, Burnham and Kulik 1997). The SB has been widely used as a binder modifier, usually as dispersion in water (latex). Low-temperature ductility is improved, viscosity is increased, elastic recovery is improved and adhesive and cohesive properties of the pavement are improved. The benefit of latex is that the rubber particles are extremely small and regular. When they are exposed to asphalt during mixing they disperse rapidly and uniformly throughout the material and form a reinforcing network structure. In a 1999 laboratory test at the Texas Transportation Institute, it was found that coating smooth, rounded, siliceous gravel aggregates with cement plus SBR latex for use in HMA increased stability according to Hveem and Marshall standards, as well as tensile strength, resilient modulus and resistance to moisture damage. Coated aggregates have greater resistance to rutting and cracking (Kim et al. 1999). SBR latex polymers increase the ductility of asphalt

pavement (Becker et al. 2001). Water-based SBR latex has been widely used to improve chip retention in emulsions, but SBS has gradually replaced latex because of its effect of greater tensile strength at strain, and because it is compatible with a broader range of asphalts (King 1999). SBR modification also increases elasticity, improves adhesion and cohesion, and reduces the rate of oxidation, which helps to compensate for hardening and aging problems (Roque et al. 2004).

3.4.2 Styrene-Butadiene-Styrene (SBS) Polymer

Styrene-Butadiene-Styrene (SBS) is also an elastomeric polymer consisting of styrene ($C_6H_5CH=CH_2$), butadiene ($CH_2=CH-CH=CH_2$) and styrene ($C_6H_5CH=CH_2$). Its molecular formula is $C_{20}H_{22}$ and molecular weight is 262.39 g/mol. It has tensile strength of about 43 MPa with an elongation (strain) of 95% and shear modulus of 1.26 to 1.78 MPa. Both SB and SBS behave like Newtonian fluids at 163°C (Burnham and Kulik 1997). The main difference between SB and SBS is the amount of styrene (second) blocks (Legge et al. 1987). According to a 2001 review in *Vision Tecnologica* (Becker et al. 2001) it is probably the most appropriate polymer for asphalt modification, although the addition of SBS type block copolymers has economic limits and can show serious technical limitations. Although low temperature flexibility is increased, some authors claim that a decrease in strength and resistance to penetration is observed at higher temperatures. Nonetheless, "SBS is the most used polymer to modify asphalts, followed by reclaimed tire rubber" (Becker et al. 2001). The Danish Road Directorate found that an SBS-modified binder course showed no superior rut resistance compared to other Danish asphalt courses. Asphalt cores taken from the job site indicated that separation

had occurred, and that the polymer phase was not homogeneously distributed, which might have been the cause of the poor performance of the pavement. (Wagan and Nielsen 2001). As reported in the Journal of Material in Civil Engineering, transmission electron microscopy was used in 2002 to better understand the behavior of SBS in asphalt binders. Depending on the sources of asphalt and polymer, morphology varies: there can be a continuous asphalt phase with dispersed SBS particles, a continuous polymer phase with dispersed globules of asphalt, or two interlocked continuous phases. It is the formation of the critical network between the binder and polymer that increases the complex modulus, an indication of resistance to rutting (Chen et al. 2002). The Florida Department of Transportation and FHWA published a report looking at the effect of SBS modification on cracking resistance and healing characteristics of Superpave™ mixes. They found that SBS benefited cracking resistance, primarily due to a reduced rate of micro-damage accumulation. SBS did not, however, have an effect on healing or aging of the asphalt mixture. (Roque et al. 2004). The possibility of using SBS-modified binders in India has been investigated recently. Calculations indicated that the surface life of the Delhi–Ambala expressway would be almost doubled while the thickness of the bituminous layers would be reduced, although the cost per km would be greater for polymer modified binders (Shukla et al. 2003).

3.4.3 Elvaloy

Elvaloy is made of from ethylene glycidyl acrylate (EGA) terpolymer that chemically reacts with the asphalt binder during mixing. The main advantage of the chemical reaction is that it helps the base asphalt binder from the separation from the Elvaloy

during storage and transportation. Roads using Elvaloy have been in use since 1991. In 1995 Witczak et al. (1995) studied the laboratory performance of asphalt modified with Elvaloy at the University of Maryland. Two different grades of asphalt were each modified by 0%, 1.5% and 2.0% Elvaloy by weight of binder. The susceptibility of the mixtures to moisture damage was found to be greatly decreased by the addition of Elvaloy (Yildirim 2007). The Elastomeric modifier (Elvaloy in this study) was collected from DuPont. This Elvaloy based polymers are classified as plastomer that modify asphalt binders by forming a tough, rigid, three-dimensional network to resist deformation. Their characteristics lie between those of low density polyethylene, semi rigid, translucent product and those of a transparent and rubbery material similar to plasticized poly vinyl chloride (PVC) and certain types of rubbers modifiers (Mahabir and Mazumder 1999). When added in small quantities to asphalt, Elvaloy creates a permanently modified binder with improved elastomeric properties. Unlike most other plastomers and elastomers that are simply mixed into asphalt, Elvaloy has an active ingredient that chemically reacts with asphalt. The result is not a mixture of asphalt and modifier, but rather a stable, elastically improved, more resilient binder that can be stored and shipped to hot mix plants to help meet SHRP and other higher-performance specifications. Hot mix asphalts made with Elvaloy are easy to spread and compact, and provide outstanding resistant to rutting, cold cracking and fatigue. Roads made with Elvaloy have been in service since 1991, and are showing excellent long-term durability.

Ethylene polymers are characterized by a low polarity and low reactivity plastomers. They are like waxes in this respect, having a low dielectric constant and being soluble in hot oils, hot wax and hot hydrocarbons. They also are well known to be inert. For some

uses it is desirable to modify the ethylene polymers to make them flexible, to impart more polarity to the polymers, and to be able to use them in reaction with other resins. To obtain high degree of polarity (to improve the dispersion of these materials in asphalt) high level of ester are required, which turn adversely affects the inherit advantage of the long ethylene chain (low cost, good temperature behavior, etc.) while retaining the hydrocarbon chain as the major feature of the polymer. Commercially available thermosetting resins such as phenolics, epoxys etc. have been found to be useful because of retention of their performance at elevated temperatures. This retention of performance is associated with the crosslinking or curing action inherent in the structure of the thermosetting resins utilized. However, this retention of high temperature performance is accompanied by high stiffness of such material or if some stiffness is desired by providing a higher degree of toughness. For these reasons ECOPATH has developed the technology to blend flexible polymers into the thermosetting resin. Research on Elvaloy modified binders show increased high temperature viscosities but they demonstrate limited viscosity changes at colder temperatures. As such, Elvaloy modified binder enhances the high temperature properties of the asphalt mix. Furthermore, it tends to exhibit significant improvements in the moisture susceptibility properties of the asphalt mix. The molecular arrangement of Elvaloy is shown in Figure 3.1 (Ecopath Website 2010).

3.5 Polymer Mixing

3.5.1 SB and SBS

For mixing of polymers, the base binder is heated in an oven at 163°C (350°F) until it is fluid enough to pour. Approximately 4 gallons of base binder poured in a mixing pan and

heated to polymer blending temperature of 190°C (375°F). The base binder is then stirred with a lab mixer set at 60 rpm and the desired amount of polymer is added slowly to the asphalt. The blend is stirred for a total of 2 hrs, and removed from the mixer. The polymer-modified asphalt is then poured into containers. The container with a tightly covered lid is placed in an oven at 190°C (380°F) for an hour for initial setting. The binder is then ready for preparing AFM samples.

3.5.2 Elvaloy

The mixing percentage of Elvaloy is 2.0% and phosphoric acid is 0.25%. As phosphoric acid is a hydroscopic substance so it will absorb moisture from the air during operation and storage. At the time of storage and handling of the acid, care was taken to avoid contact with water and air. We did some precautions like while the dilution of phosphoric acid with water as this is highly exothermic chemical reaction. The acid dilution was carried out slowly when needed. Dilution in water causes acid to be more aggressive on skin contact. Dilution in water causes acid to more aggressively attack mild steals. A lab mix study needs to be performed to determine optimum Elvaloy® RET and acid levels prior to producing commercial pounds of product. Do not increase polymer or acid levels above laboratory levels without first running a lab test to see if PMA (Polymer Modified Asphalt) will gel at the increased levels of polymer and/or acid. DuPont has an asphalt lab that will perform initial screenings of this process on your asphalt, and will provide SHRP data for the asphalt.

3.6 AFM Sample Preparation

In AFM sample preparation, a glass substrate is coated with a polymer modified asphalt binder. As a first step, a glass slide surface is wrapped with a high temperature resistant tape. Two strips of tape are placed in parallel by keeping a small gap between them. Next, the hot polymer modified liquid asphalt is poured into the gap between the two strips of tape. It can be noted that polymer modified binders are melted by heating them to 163°C temperature for an hour. The asphalt coated glass substrate is then placed in the oven at 163°C temperature for 10 minutes in order to have a smooth surface. Next, the glass substrate is removed out of the oven, cooled down to room temperature, and peeled off the tapes. The final shape of the sample is shown in Figure 3.2. The asphalt film on glass substrate is then ready for AFM testing, and referred to as the dry conditioned sample in this paper. For preparing a wet conditioned sample, the dry sample is vacuum saturated for half an hour, and kept under 3 inches of water for 72 hours. Before AFM testing, the wet conditioned samples are dried overnight inside a draft oven at 40°C temperature. In order to have same effect of temperature on both dry and wet samples, the dry samples are also kept in the draft oven overnight at 40°C temperature. Samples are dried in order to reduce the surface wettablity effects on the test results for an AFM experiment conducted under ambient condition. The interactions in ambient air may be affected by the capillary force generated by the meniscus formed between the AFM probe and sample surface. Ideally, AFM tests in vacuum or liquid medium can measure solely the interactions between tip and asphalt molecules but unfortunately more often than not these measurements have very little to do with the real systems in which the functional groups are exposed to the ambient environment. In this study, both hydrophobic methyl

($-CH_3$) and hydrophilic carboxyl (-COOH) tips are included to circumvent the limitations imposed by the capillary force, if any.

3.7 Laboratory Testing

3.7.1 The AFM Testing

In an AFM test, the surface of an asphalt or aggregate sample is probed with a sharp tip located at the free end of a cantilever. The attractive or repulsive force between the tip and the sample surface causes the cantilever to bend or deflect. A laser beam reflection technique, which is built-in with the AFM system, measures the cantilever deflection, as the tip is brought vertically towards the sample surface, and then away from it. By multiplying the deflection by a cantilever spring constant, the attractive or repulsive force acting on the cantilever tip is measured as a function of the distance between the tip and the surface. Components of the AFM are shown in Figure 3.3.

3.7.2 Description of Cleanroom

A cleanroom is a low level of environmental pollutants i, e., dust, airborne microbes, chemical vapors and aerosol particles. All of our AFM experiments were done in a cleanroom inside Center for High Tech Materials (CHTM) as shown in Figure 3.4. The problems associated with molecular and particle contamination of spacecraft components, instruments and structures are well known and documented especially those that contain fine mechanisms and/or optics. This problem is severely exaggerated when the instrument is operating under space vacuum. A Class 10 cleanroom is defined as having less than 10 particles of more than 0.5 micron in size within a cubic foot of air. Similarly,

a Class 1000 cleanroom has less than 1000 particles of more than 0.5 micron in size within a cubic foot of air. This level of cleanliness is necessary to maintain the reproducibility of newly developed state-of-the art electronic device processes. To reach and maintain this level of cleanliness, the transfer of particle and chemical contaminations must be eliminated wherever they are found. The main AFM setup is shown in Figure 3.5**.** It has a microscope, steel cap, noise reduction chamber and tip holder.

3.8 Tip Functionalization

In this study, silicon nitride (Si_3N_4) tips are functionalized using −COOH, -OH, -NH_3 and -CH_3 functional groups. Probing a polymer modified asphalt film surface with a tip functionalized by an asphalt molecule facilitates the measurement of intermolecular forces between two asphalt molecules. Silicon nitride tips are purchased from VEECO Instruments, Inc (Veeco Instrument Inc., 2007). This tip has a beam bounce cantilever (called RFESPA-CP MPP211) with a length of 125 μm, natural frequency of 90 kHz and spring constant of 3 N/m. These tips are functionalized with carboxyl (–COOH), hydroxyl (–OH) , ammin (-NH_3) and methyl (–CH_3) functional groups with the help of a tip modifying company called Novascan Technologies in Ames, Iowa. The tip modification process includes a controlled deposition of a monolayer thin film onto the tip followed by immersion of the tip into a solution of organic thiol or chlorosilane (Biggs and Mulvaney 1994, Knoell et al. 1999, Vaidya and Chaudhury 2002, Tian et al. 2004). One end of the thiol covalently linked to the tip surface and the other end contains the appropriate functional group. Functionalization of tips by coating them with asphalt

and molecules is very new, not only in asphalt but also in polymer and nanotechnology areas for studying specific interactions at molecular level.

3.9 Sample Conditioning

Asphalt conditioning for AFM testing: AASHTO T 283 method was applied to condition the samples. In this process De-Ionized water from the Chemistry dept (UNM) was used. About 500 ml De-Ionized water was put in the vacuum bottle and then the bottle on its side (but tilted up) with gravel holding it in place so that no water spills out. Then we placed a few samples in the jar, asphalt slide side up. With the jar still on its side, we put the metal cap on it. It was critical that no water touches the hose outlet on the cap. Then we turn on the vacuum pump for 10 minutes so that we could see air bubbles form in the water. After that we turn off the pump and let the samples set in the water for another 10 minutes. We removed the samples from the water, replace any labels that came off, wrap them in Seran wrap. Placed in a ziplock bag, we added 10 ml minimum DI water and sealed the bag. Then we placed all the samples in the freezer, which was at 0^{o}F (-18^{o}C). We left them in the freezer for a minimum of 16 hours. After 16 hours, we removed the samples from the freezer and removed all plastic wrappings. Then we placed them into the 77^{o}F water bath for 10 hours. Then we used paper towel to dab off excess water and placed in the oven at 27^{o}C (80^{o}F) for 2 hours. After complete conditioning we dried the samples. The samples were put inside oven to ensure the absence of water in asphalt surface. We preheated the oven to 40^{o}C. The placed all binders slide in the oven for 8 hours.

3.10 Tip Calibration

To obtain adhesion/cohesion force values, it is required to know the exact value of the cantilever spring constants (k) of the functionalized tips (Ohler 2007). This is done through the automated tip calibration procedure (AFM Part 00-103-0990 module) available in the AFM control software (Veeco Inc. 2007). In the calibration procedure, the cantilever to be calibrated (i.e., a functionalized tip) is used to measure force curves on a platinum-coated hard sample (calibration grating, Model APCS -0001) and on a reference cantilever. The slope of the contact portion of the force curve is called stiffness, S. Thus two quantities: S_{ref} which is the deflection sensitivity of the reference cantilever, and S_{hard} which is the deflection sensitivity of the hard surface are measured. Whereas the spring constant of the reference cantilever, k_{ref} is known (Veeco Inc. 2007). The calibrated k value is determined from the following equation (Ohler 2007):

$$k = \left(\frac{S_{ref}}{S_{hard}} - 1\right) k_{ref} \qquad (1)$$

In this study, the calibrated values of the cantilever spring constants are determined to be: k_{ref} *=3.0 N/m,* k_{Si3N4} *= 3.9564 N/m,* k_{-COOH} *= 5.0889 N/m,* k_{-OH} *=3.433 N/m,* k_{-CH3} *=3.121 N/m and* k_{--NH3} *=2.428 N/m,*

3.11 Selection of AFM Test Parameters

Traditionally, the most of the AFM tests have been conducted on hard samples to measure surface roughness. As asphalt samples are relatively soft compared to typical silicon or metal samples, the AFM test on asphalt becomes non-trivial, especially when considering the stickiness of asphalt binder. Therefore, several parameters are controlled carefully in this study to minimize the contact between the tip and asphalt surface. The

final values of these parameters for successful AFM testing on asphalt sample are listed in Table 3.1.

It can be noted that the AFM is set up at a minus value to ensure that tip is not in contact with sample surface. Essentially tests are performed at non-contact mode with tip vibration off. During scanning or surface imaging, the AFM is setup in high voltage mode. A scan rate between 1 and 3 Hz is found to produce high quality images. Scan rate is defined by the frequency of the back and forth movements of the scanner beneath the AFM probe. It can be mentioned that setting up an appropriate scanning rate is important for capturing a good quality image. If a sample is scanned at a very fast rate, the feedback loop may not have enough time to respond to the change in film roughness, and hence may result in a bad quality image or smeared image (Thomas et al. 1995). A slow scan rate produces a good resolution of the image as the feedback system finds enough time to respond, while a fast scan rate can be time efficient. In this study, a total of 256 x 256 pixels are used to scan 5-μm^2 of the sample. The gain value is set 0.1 for all the tests. The gain value controls the error signal to generate a feedback signal.

3.12 Asphalt Surface Imaging

For adhesion measurement, it is important that the surface of the prepared asphalt sample on glass substrate is reasonably smooth. Surface smoothness is measured by taking a surface roughness image of the sample, know as surface imaging. A non-contact mode imaging is employed so as not to touch the asphalt surface. During imaging, the tip is vibrated by maintaining a constant distance (50-70nm) from the surface. The tip travels

over the scan area of the sample and the deflection of the cantilever tip are mapped into topographic images of the surface. For example, Figure 3.6 presents the 3D images of dry and wet 1% SB polymer modified asphalt samples.

The scan area (x and y dimensions) and the sample surface roughness (height or z dimension) are shown in Figures 3.6. Due to space limitation, only four images are shown in this paper. The wet asphalt samples surfaces seem to have more spikes as compared to the dry sample. Action of water may be responsible for such spikes. The images are analyzed using Matlab image analysis toolbox (Horacos et al. 2007). Surface roughness is measured using quantities such as average, maximum and root mean square (RMS) values of surface roughness over the entire surface. The RMS values of all the samples are listed in Table 3.2.

3.13 Conclusions

It can be seen that dry samples show the lowest RMS value of 0.12 nm (nanometer) and wet samples have high RMS value of 11 nm. For hard samples such as Aluminum, silicon, a sample surface with a RMS value less than 20 nm is acceptable for force-curve measurement in AFM (Jalili et al. 2004). For soft samples, no limiting RMS value can be found in the literature. In this study, the RMS roughness values of all dry and wet samples are found to be less than 10 nm. This confirms that the method of asphalt film preparation (dripping away) used in this study can produce a smooth surface sample, which is suitable for AFM testing.

Table 3.1 The AFM Testing Parameters

AFM Parameters	Values
Set Point	-0.12 to -0.51
Scan Area (A^o x A^o)	40 x 40
Scan Rate (Hz)	3
Amplitude	25 to 40

Table 3.2 The Roughness Values of AFM samples

Asphalt modified by:		Surface Roughness (nm)							
	Tip types	Si_3N_4		<-COOH>		<-CH_3>		<-OH>	
	% Polymer	Dry	Wet	Dry	Wet	Dry	Wet	Dry	Wet
Styrene-Butadiene (SB) polymer	1%	0.22	0.16	0.27	0.66	0.23	0.31	1.71	0.14
	2%	0.34	6.05	0.26	0.28	0.16	2.57	0.15	0.28
	3%	0.20	0.67	0.25	0.52	0.15	1.54	0.25	0.27
	4%	0.37	0.65	0.27	11.09	1.05	0.46	0.20	3.33
	5%	9.46	0.19	0.33	0.66	0.31	0.30	0.75	0.18
Styrene-Butadiene-Styrene (SBS) polymer	1%	0.30	0.23	0.58	0.23	0.32	0.38	0.58	11.00
	2%	0.45	0.16	2.21	0.31	0.80	1.60	0.97	3.90
	3%	0.13	0.17	2.53	0.15	0.32	0.29	1.18	0.80
	4%	0.66	0.18	0.91	0.23	1.23	0.32	1.15	8.81
	5%	0.28	1.45	0.33	0.30	0.26	0.65	0.19	0.12

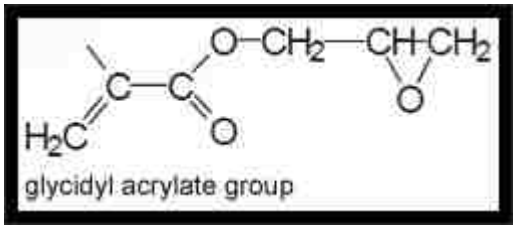

Figure 3.1 Elvaloy molecular arrangement

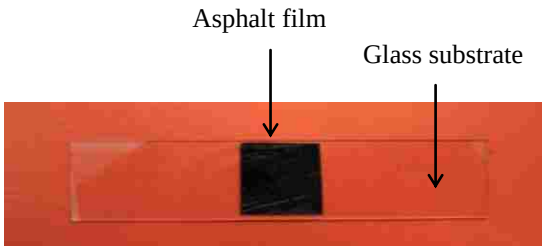

Figure 3.2 AFM sample

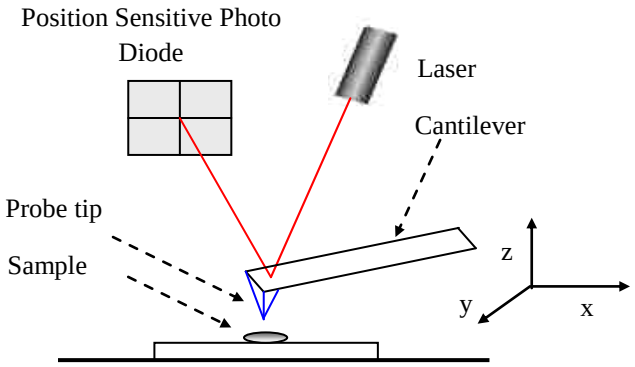

Figure 3.3 Schematic of an AFM

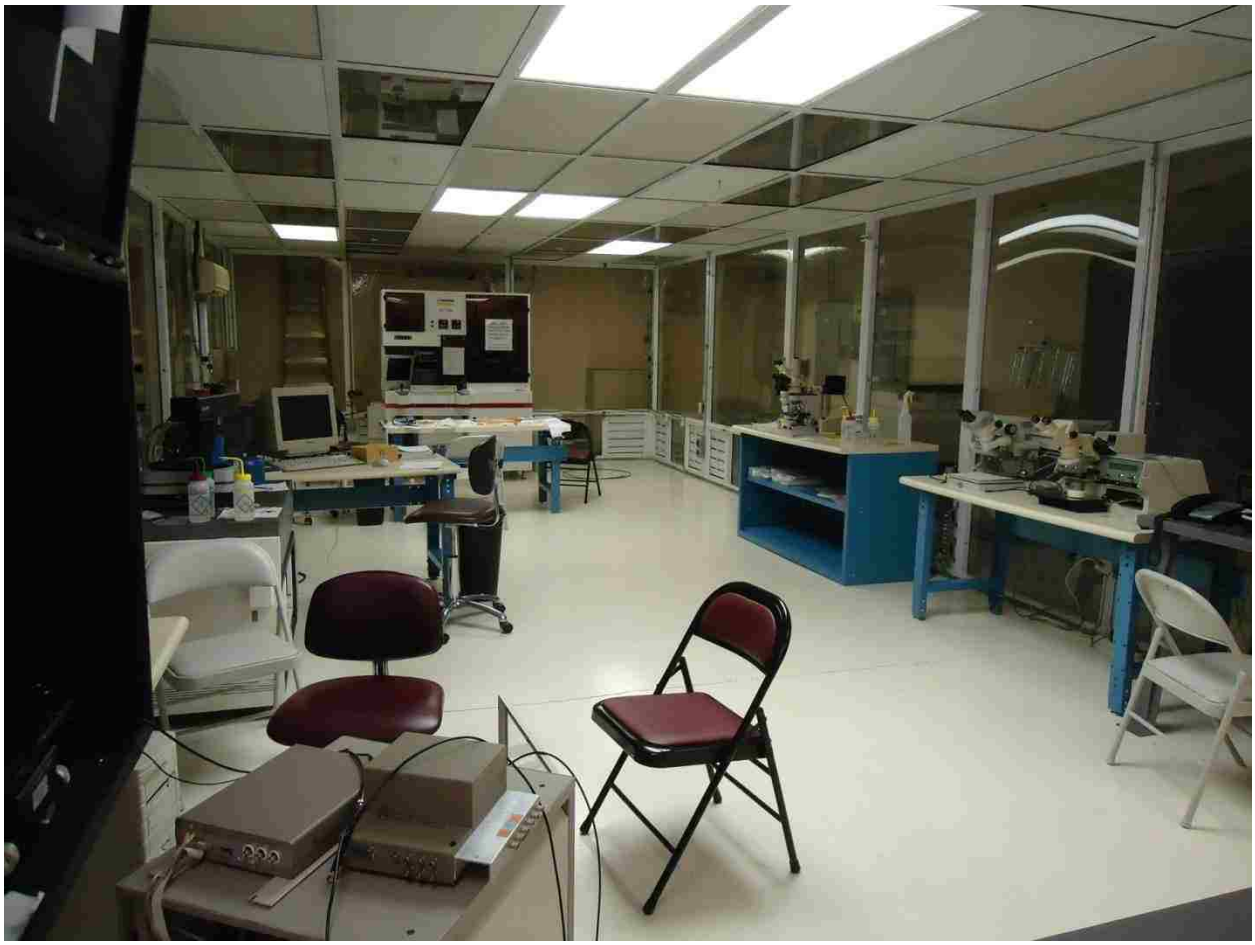

Figure 3.4 Picture of cleanroom at CHTM

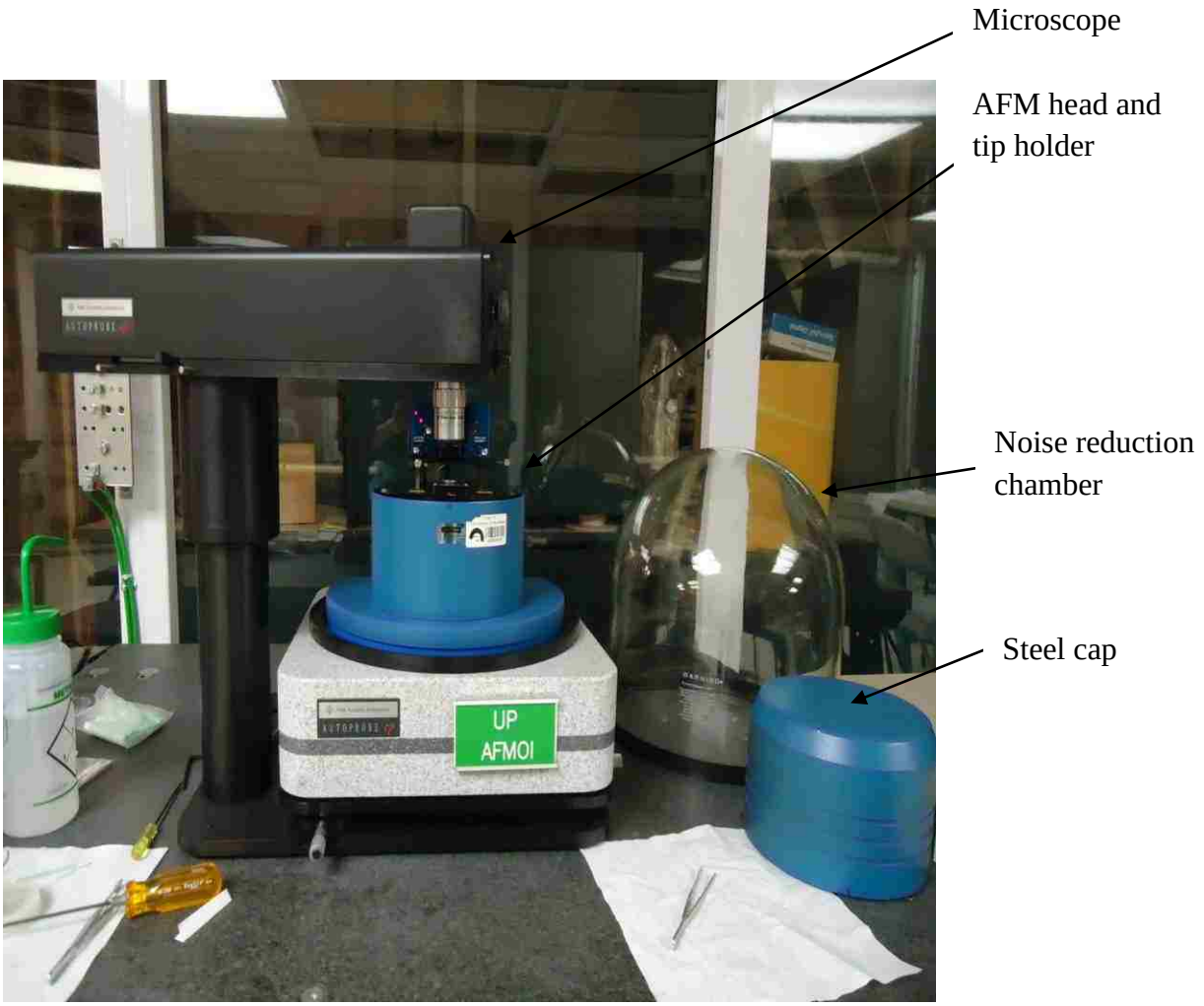

Figure 3.5 Main AFM setup

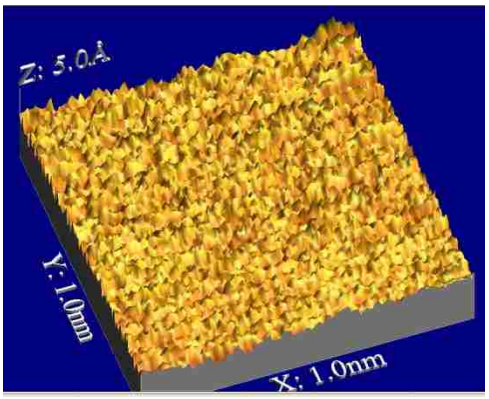

(a) Dry sample using Si_3N_4

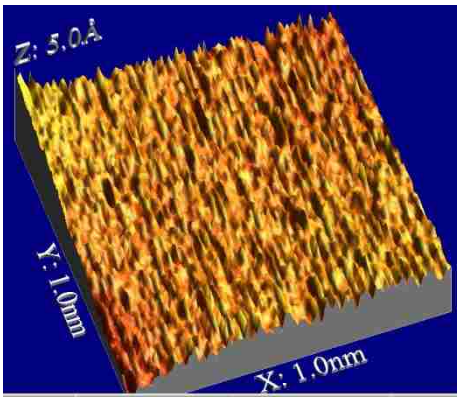

(b) Wet sample using Si_3N_4

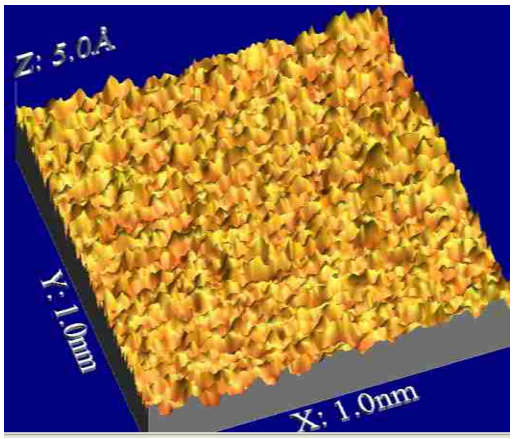

(c) Dry sample using -CH_3 tip

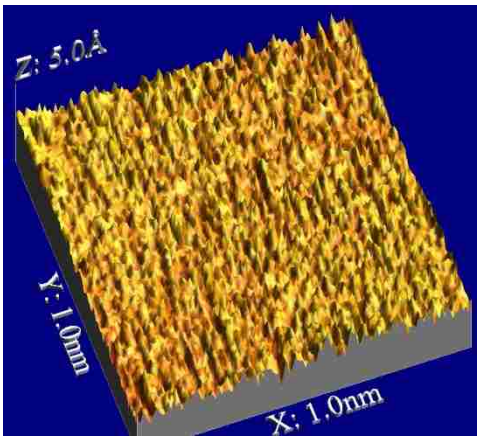

(d) Wet sample using -CH_3 tip

Figure 3.6 Surface mages of asphalt samples (1% SB)

CHAPTER 4

Moisture Damage Evaluation on Polymer Modified Asphalt

4.1 Introduction

The asphalt binder binds the smaller and larger aggregate particles together and enhances the stability of the asphalt concrete (AC) mixture that provides resistance to deformation under all kind of distresses. The performance of AC mix is a function of asphalt binder, aggregate types, its volumetric properties etc. The asphalt binder is the main element that controls the viscoelastic properties during production in the plant and service on field or road. Polymer is a common type of materials that are used to modify asphalt for better performances. The addition of polymers has gained popularity in recent years through all over the world. Study done by Isacsson and Lu (1995) showed that polymer modified asphalt achieve better asphalt pavement performance for the long service life. In their study, asphalt modifiers were used to modify the base asphalt binder. A total of two different types of modifiers are used in this study to investigate the moisture effect on asphalt thin film. The one type is called elastomer. The other type is called plastomer. Examples of elastomers are Styrene-Butadine (SB) and Styrene-Butadine-Styrene (SBS) and plastomers is Elvaloy. The history of using asphalt in constructing pavement field started from the beginning of this century. The property and quality of the asphalt binder may vary with crude oil source, refining process, chemical composition and other parameters. This type of quality and property variation may lead to distress for the pavement in real life. The engineers and experts attempted to solve many of these

distresses by establishing different criteria. One of the purposes is to establish fewer grades of asphalt binders that facilitate decision making for the pavement designers. Asphalt binder is originally a thermoplastic liquid at low service temperature. It is elastic solid in nature and behaves like a viscous liquid at high temperature. This requires the improvement to perform asphalt binder to minimize the stress cracking that occurs at low temperature and the plastic deformation occurs at high temperature. The changes in temperatures, traffic loadings, available moisture during the life of a pavement makes the design and the selection of materials to resist these stresses extremely difficult, as well as impractical. Many types of polymers are available to change asphalt binders to achieve a wider performance range for asphalt bound pavement materials in the practical field. There has been a proliferation of many types of polymers in the last 10 years for use in asphalt binder modification (Wardlaw and Shuler 1992).

This chapter deals with the materials description, polymer modification of asphalt base binder, test parameter quantification for the AFM successful testing.

4.2 Objective

The objectives of the study are:

1. Mixing polymers with base binder and to prepare sample for AFM testing.
2. To study the moisture damage in asphalt base and polymer modified binders with AFM.

4.3 Test Matrix

A total of 15 types of binders were tested with five different types of AFM tips in this study. The test matrix is like: base, 5 percentages of SB, 5 percentages of SBS and 4 types of Elvaloy modified X 2 conditions (dry and wet) X 5 tips = 150 tests.

4.4 Adhesion Measurements from Force-Distance Graph

Results from 5% dry SB sample on a glass substrate probed using all four tips in the multimode AFM is shown in Figure 4.1. The horizontal axis shows the vertical movement of cantilever tips and the vertical axis shows the force (+ve as repulsive, and – ve as attractive) acting between tip molecule and asphalt molecule. The cycle in the force measurement starts at a tip-surface separation. At a large distance, no force acts between the tip and surface, but as the tip approaches, the distance decreases and attractive forces pull the cantilever tip towards the sample. During approaching (path A-B-C) the cantilever deflects away from the surface. As the tip approaches the sample (i.e., moving from right to the left in Figure 4.1), the value of the attraction force increases and becomes the maximum at a certain distance. Further movement of the tip towards the sample increases the force magnitude but in the opposite direction. The force is theoretically very high when the tip touches the sample. Next, the tip is withdrawn back to its starting position. During retraction, the tip sticks to the surface for considerable distances because of the bonds formed during contact with the surface. At one point, it finally snaps out of contact. Path C-D-E in Figure 4.1 is the retracting path. As the cantilever tip travels away from the sample, it deflects towards the surface due to adhesion force between the sample and tip. Finally, the cantilever tip separates itself from

the sample surface, where the lowest point (point D) in retracting path or curve occurs. Upon further separation from the lowest point (moving right from left along the retracting path in Figure 4.1), the tip completely loses contact with the surface, and jumps out of the sample surface. The maximum force between tip and sample at the lowest point in Figure 4.1 (point D) is referred to as the adhesion force or pull-off force. Adhesion between the tip and the sample is mainly due to van der Waals interactions (Drelich 2006, Long et al. 2006, Vezenov et al. 2008).

4.4.1 Explanation of Force-Distance Graph and Mechanical Strength

Figure 4.2 shows the adhesion value between the $–Si_3N_4$ tip and steel, platinum and gold samples. The adhesion values are higher with the increment of mechanical strength (Young's modulus values shown in Table 4.1). As the strongest among all three metals, steel (*E* value about 200 GPa) has the lowest value of adhesion with the $– Si_3N_4$ tip as shown in Figure 4(a). Being the weakest metal the gold has the highest adhesion with the $– Si_3N_4$ tip. This is considered as the hardest material hold with smallest adhesion force for the AFM tip. The same trend also is shown with the hydrophobic tip $–CH_3$ on all the metals in Figure 4(b).

4.5 Results and Discussions

4.5.1 Repeatability of Test Results

To quantify the uncertainties in the adhesive or cohesive interactions, it always necessary to record multiple force curves for each tip-sample pair. Table 4.2 shows the adhesion values of 9 points using Si_3N_4 tip on base, 1% and 2 % (SB and SBS) modified asphalt

binders. The sample average and mean values are calculated. Clearly, the base binder has the highest value of adhesion among base, 1% and 2% modified binders. Therefore, polymer modification reduces the adhesion force in an asphalt aggregate system. The average adhesion value of 1% SB modified binder is higher than that of the 1% SBS modified binder. Therefore 1% SB modification has less effect in reducing adhesion force than the 1% modification. Again, when comparing 2% SB and 2% SBS modifications, it can be seen that both polymers have similar (almost same) effect. The average adhesion force is 25.50 nN for 2% SB binder and 23.58 nN for 2% SBS binder. When comparing 1% modification to 2% modification, increase in polymer has no effect on adhesion force in SBS sample but does on SB sample. Therefore, AFM test can distinguish the adhesion or pull-off force in asphalt binder depending on the amount of polymer and type of polymer. The standard deviation of base binder is higher than those of other samples. The percent variation is calculated by dividing the standard deviation value with the average value and expressing it as a percentage. It can be seen that percent variation is consistent and almost same in all three samples.

4.5.2 Adhesion Force in Dry and Wet Base Asphalts

Figure 4.3 is a bar plot that compares the adhesion forces in the base binder under dry and wet conditions. For all types of tips, dry samples show smaller adhesion values than the wet samples. This indicates that base asphalt binder selected in this study is susceptible to moisture damage. The noticeable change is observed with the $-NH_3$ tip for moisture damage.

4.5.2.1 Adhesive Force in Dry and Wet Asphalt Samples Using - Si_3N_4 Tip

4.5.2.1.2 SB Modified Asphalts

Figure 4.4 shows adhesion forces in dry and wet SB modified asphalt samples. Wet samples have higher adhesion values than those of dry samples. In dry samples, the adhesion force value decreases while going from 1% to 3%. The force value is the minimum at 3% SB polymer.

In wet conditioned asphalt samples, the average adhesion force is 195.0 nN in wet. The same is about 37.8 nN in dry sample. Adhesion force in wet sample increases while going from 1% to 4% and then decreases at 5% polymer. The adhesion forces increases slightly for increase in polymer percentage from 3 to 4% in both dry and wet SB samples. It can be noted that increase in percentage polymer from 4% to 5% does not increase adhesion force in wet samples but it does increase adhesion force in dry samples.

4.5.2.1.3 SBS Modified Asphalts

Figure 4.5 shows adhesion forces of dry and wet SBS polymer modified asphalt samples. It is evident that adhesion forces of wet binders are higher than those of dry binders. The average adhesion force is 28.7 nN in dry samples, and 129.0 nN in wet samples. The adhesion forces in wet SBS samples have increased significantly for 3% to 4% SBS polymer modification. Action of water has created temporary dipoles in the polymer modified asphalt sample, which has resulted in larger Van der Waal's force in the asphalt binder system. Van der Waal's forces are attraction forces between electrically neutral molecules that collide with or pass very close to each other and exist between molecules of different substances. Three types of Van Der Waal's forces are reported in literatures

(Giggs et al. 2002). The first type is called dipole-dipole force. It occurs in polar molecules, or the molecules experience momentary attractions between each other, diatomic free elements and individual atoms (Thomas et al. 1995). This is not the case here. The second type is due to induction or polarization. This interaction happens between a permanent multipole on a molecule and an induced multipole on another. The third type of Van der Waal's force is called London dispersion force. This involves the attraction between temporarily induced dipoles in nonpolar molecules (Burnham and Kulik 1997). This may be the case here. Water might have induced polarization by a repulsion of negatively charged electron clouds in nonpolar polymer modified asphalt molecules.

4.5.2.1.4 Elvaloy modified Asphalts

The adhesion forces with – Si_3N_4 tips are shown in Figure 4.6. All the wet samples adhesion forces are higher than dry samples adhesion forces. The changes in adhesion in all dry samples are consistent. The modification effect is reasonable and taking place with the adhesion variation. The changes are also similar for the wet samples.

4.5.2.2 Adhesion Force in Dry and Wet Asphalt Samples Using -COOH Tips

4.5.2.2.1 SB Modified Asphalts

Figure 4.7 shows adhesion forces between –COOH functional group and dry or wet SB polymer modified asphalt samples. Clearly, adhesion force does not differ significantly between wet and dry in SB samples when using -COOH tip. As described previously, -COOH is a hydrophilic tip. It is possible that the both dry and wet samples are affected

equally by the meniscus forming between the AFM probe and sample surface. The magnitude of the intermolecular forces affected by meniscus (i.e., capillary forces) are usually very high, which is not the case here. The average value of the adhesion force is about 75 nN in dry or wet SB polymer modified asphalt samples. It is possible that the polymer modification or water action has made the asphalt binder chemically similar to the tip group functional (i.e., -COOH). As result, the forces required to separate the tip and surface are small. It can be noted that 4% SB modified asphalt samples shows the maximum value (i.e., 95 nN) of adhesion force in both dry and wet samples. Overall, the adhesion force between asphalt sample and –COOH tip does not increase or decrease with an increase in the percentage of polymers.

4.5.2.2.2 SBS Modified Asphalts

Figure 4.8 shows adhesion forces between –COOH functional group and dry or wet SBS polymer modified asphalt samples. Again, the adhesion forces do not differ significantly in the dry and wet SBS polymer modified asphalt systems. Noticeably, the adhesion force of base binder is higher than that in modified binders under wet and dry conditions. The average value of adhesion force in SB polymer modified samples using –COOH tip is about 89.8 nN in dry sample and 105.0 in wet samples. The maximum adhesion force occurs at 3% SB polymer in dry sample. In SBS wet samples, the maximum adhesion force occurs at 4% polymer. In summary, it can be said that the –COOH functional group in SBS and SB polymer modified samples are neither susceptible nor resistant to moisture damage.

4.5.2.2.3 Elvaloy Modified Asphalts

Figure 4.9 shows the dry and wet adhesion forces comparison on the different Elvaloy modified base binders. Starting from 0.5% Elvaloy, all the wet samples shows the damage due to moisture. All the wet samples adhesion forces are more than 400 nN and the dry samples adhesion forces are close to 200 nN.

4.5.2.3 Adhesion Force in Dry and Wet Asphalt Samples Using -CH_3 Tips

4.5.2.3.1 SB Modified Asphalts

Figure 4.10 presents a comparison of adhesion forces between dry and wet SB modified asphalt samples. The average adhesion force is about 113.6 nN in wet samples and 51.0 nN in dry samples. Overall, the wet SB modified asphalt samples show higher adhesion forces compared to the SB modified dry asphalt samples. The magnitude of the adhesion force in wet samples increases with an increase in percentage polymer from 1 to 3%, whereas adhesion force decreases with the increase in percentage polymer from 3 to 5%. Therefore, 3% SB can be considered to be the optimum polymer for the highest adhesion force in wet SB modified asphalt samples. The fact that -CH_3 is a hydrophobic tip, therefore the meniscus will not affect the measured adhesion force in an ambient AFM test. In summary, it can be said that the -CH_3 functional group in SB polymer modified samples are susceptible to moisture damage, rather resistant to moisture damage.

4.5.2.3.2 SBS Modified Asphalts

Figure 4.11 shows adhesion forces between –CH_3 functional group and dry or wet SBS polymer modified asphalt samples. Clearly, adhesion forces in dry samples are higher

than those in the wet samples. Therefore, it is evident that SBS polymer modified asphalt binders are susceptible to moisture damage. The average adhesion force is 150.6 nN in dry samples and 120.9 nN in wet samples. The ratio of wet to dry adhesion forces in SBS modified sample is 0.79. From Figure 4.11, it can been seen that the adhesion force increase with an increase in percentage polymers from 1 to 3%, and further increase in polymer results in decrease in adhesion force. Therefore, 3% SBS polymer can be considered as optimum based on adhesion force between asphalt and $–CH_3$ functional group.

4.5.2.3.3 Elvaloy Modified Asphalts

The adhesion values of all dry and wet samples are shown in Figure 4.12 with the $–CH_3$ tip. The wet samples adhesion forces are higher than the dry samples. The variations of adhesion forces for dry and wet samples are noticeable here.

4.5.2.4 Adhesion Force in Dry and Wet Asphalt Samples Using -OH Tips

4.5.2.4.1 SB Modified Asphalts

Figure 4.13 is a comparison of adhesion forces in dry and wet SB polymer modified asphalt samples using –OH tips. In most cases, wet SB samples show higher adhesion forces compared to dry SB samples. The average adhesion force of dry samples is 46.1 nN, while that of dry samples is 54.1 nN. The maximum adhesion force occurs at 5% polymer is dry samples polymer, and 4% polymer in wet sample. The value of the adhesion force at 3% SB polymer is 39.1 nN in dry sample and 56.5 nN in wet sample. The increase in polymer to 4% increases the adhesion force (i.e. 69.1 nN) slightly.

Therefore, the previous consideration of 3% SB polymer as optimum is valid based on the adhesion force measured using the –OH functional group.

4.5.2.4.2 SBS Modified Asphalts

In Figure 4.14, the adhesion forces in dry and wet SBS polymer modified asphalt samples measured using -OH tips are plotted. Overall, adhesion forces in wet samples are higher than those in the dry samples. Therefore, moisture increases –OH functional related adhesion in SBS samples. The average value of adhesion is 118.3 in dry samples, and 201.5 nN in wet samples. In dry samples, the maximum adhesion force occurs at 4% SBS, whereas the minimum adhesion occurs at 1% SBS. Clearly, adhesion value increases up to 3% polymer modification, and decreases with any further increase in percentage polymer. At 3% SBS, the value of adhesion is 166.8 nN in dry samples and 252.1 nN in wet samples.

4.5.2.4.3 Elvaloy Modified Asphalts

The results with –OH tips are shown in Figure 4.15. All the wet samples adhesion forces are higher than the dry samples. The average dry adhesion force is about 120 nN and average wet adhesion force is about 230 nN.

4.5.2.5 Adhesion Force in Dry and Wet Asphalt Samples Using –NH_3 Tips

4.5.2.5.1 SB Modified Asphalts

Figure 4.16 shows the adhesion forces comparison with the –NH_3 tip. All the wet samples adhesion forces are higher than that of dry samples here. The base binder shows higher values of adhesion as compared to most of the samples.

4.5.2.5.2 SBS Modified Asphalts

Figure 4.17 shows the adhesion forces comparison on SBS modified samples with the –NH_3 tip. Here almost all wet samples are higher than that of dry samples.

4.5.2.5.3 Elvaloy Modified Asphalts

The 0.5%, 0.75%, 1.5% and 2.0% Elvaloy modified binders wet adhesion forces are higher than that of dry samples as seen from Figure 4.18. The 2.0% Elvaloy modification seems to perform better as tested with –NH_3 tip.

4.5.3 Comparing Adhesion Force in SB and SBS Samples

An attempt is made to compare the adhesion forces in the SB and SBS modified asphalt binders. As the focus of this study to evaluate the moisture damage potential of polymer modified asphalt binders, only wet samples are considered. Figures 4.19(a)-(d) compare the adhesion force using four different AFM tips. Figure 4.19(a) shows adhesion forces in wet SB modified asphalt samples are higher than those in wet SBS modified asphalt samples. Also, using silicon nitride AFM tips, adhesion force in modified binder is lower than that of base binder. Figure 4.19(b) shows the adhesion force between hydrophilic -COOH functional and of SB modified asphalt samples is slightly smaller than the adhesion force between -COOH functional and of SB modified asphalt samples. All the SB and SBS modified wet asphalt samples have smaller adhesion force than the wet base binders. From Figure 4.19(C), it is evident that the difference between adhesion forces in SB sample and adhesion forces in SBS sample is not significant overall using the hydrophobic –CH_3 tips. Figure 4.19(d) compares adhesion forces between SB and –OH

tip to the adhesion forces between SBS and –OH tip. Clearly, adhesion forces in the SBS samples are significantly higher than those in the SB sample. The adhesion forces in SB samples vary only slightly due to percentage polymer modification. Adhesion forces is SBS samples are two to three order magnitude higher than the adhesion forces in SB polymer modified samples. The difference between an SB and SBS sample is mainly the amount of styrene (second block). From Figure 4.19, it is evident that the SB polymer modification of asphalt is good achieving higher adhesion force (resembles to asphalt-aggregate interaction), whereas the SBS polymer modification is good for achieving higher adhesion force (resembles to asphalt-asphalt interaction).

4.5.4 The Ratio of Wet to Dry Adhesion Forces in Base, SB, and SBS Samples

The ratio of wet to dry adhesion forces can be used to measure the moisture-induced damage in the polymer modified asphalt binders. The mean values of the adhesion forces over the entire test data sets are presented in Table 4.3. It can be seen that the mean values do not overlap. In other words, there are differences in the magnitude of the adhesion forces among different functions groups. Therefore, it can be postulated that it is possible to differentiate intermolecular forces in asphalt due to chemically distinct functional groups by measuring the adhesion forces with a tip of defined functionality. The ratio of wet to dry samples' adhesion forces are also calculated in Table 4.3. For base binders, this ratio is approximately 0.60 for Si_3N_4, –COOH and $–CH_3$ tips, and 0.83 for –OH tip. Therefore, it can be postulated that the base binder are susceptible to moisture damage. The ratios of wet to dry adhesive forces in polymer modified binders are mostly greater than 1.0, except in one SBS sample when using $–CH_3$ tips. Base on this data, it

can be said that SB polymer modified binders are less susceptible to moisture damage compared to the SBS polymer modified asphalt binders. However, if the magnitude of the adhesion force is compared, it can be seen that there is a significant drop in the adhesion force magnitude due to polymer modification when comparing solely the value of adhesion of dry base samples to the value adhesion of dry polymer modified binders. In contrast, when comparing wet sample, the adhesion forces in base samples are mostly smaller than the adhesion of polymer modified samples.

4.6 Statistical Analysis of AFM Data

4.6.1 SB Samples

Table 4.4 shows all the values of dry and wet adhesion forces as well as the p-value and Pearson product moment correlation coefficient for SB samples. The p-value for dry sample is 0.001 which is a very good and satisfactory value. It indicates the data are significant with the percentage change of SB polymer in base binder. The Pearson product moment correlation coefficient is a dimensionless index that ranges from -1.0 to 1.0 inclusive and reflects the extent of a linear relationship between two data sets. We can see all the Pearson product moment correlation coefficients with $-NH_3$ are very close to 1 which indicates a strong relation among the data. Almost all the wet samples Pearson values are not very close to +1 or -1 which is an indication of the moisture effect on binders.

4.6.2 SBS Samples

Table 4.5 shows all the values of dry and wet adhesion forces as well as the p-value and Pearson product moment correlation coefficient for SBS samples. The p-values are very

good as falls below 0.1% for all dry and wet samples with all the AFM tips. The Pearson value with $–NH_3$ tip is very close to +1 which indicates the strong correlation among data.

4.6.3 Elvaloy Samples

Table 4.6 shows all the values of dry and wet adhesion forces as well as the p-value and Pearson product moment correlation coefficient for Elvaloy samples. P-value for all dry samples is well below 0.01%. Hence the data are significant from statistical point of view. The Pearson values are very close to +1/-1 with –OH, $-CH_3$ and $–Si_3N_4$ tips. Hence it can be said that Elvaloy modification of base binder is better than SB and SBS modification as it possesses a strong correlation coefficient with most of the AFM tips.

4.7 Conclusions

All the wet samples are vulnerable to moisture. The statistical significance test data are also good indication about the variation of percentage of the modifiers. The conclusions being made here are:

- The AFM test data are repeatable.
- The smaller pull-off force (adhesion) is related to strength of the material. The higher strength materials produce smaller adhesion force and vice versa.
- All base, SB, SBS and Elvaloy modified binders are vulnerable to moisture. Base binder is the weakest among all the binders. Polymer modification can reduce the damage due to moisture.
- The rate of damage in all binders is not same.

- The AFM data are significant from statistical point of view.
- The SB polymer modification of asphalt is good achieving higher adhesion force (resembles to asphalt-aggregate interaction), whereas the SBS polymer modification is good for achieving higher adhesion force (resembles to asphalt-asphalt interaction).
- The Elvaloy modification of base binder is better than modification with SB and SBS polymers as the output data are strongly correlated.

Table 4.1 Young's modulus values of hard samples

Sample	Young's Modulus (GPa)
Steel	200
Platinum	168
Gold	50-90

Table 4.2 Variation of adhesion force at 9-point tests per sample with – Si_3N_4 tip

Points	Pull-off or adhesion force (nN)				
	Base	1% SB	1% SBS	2% SB	2% SBS
1	152.02	37.11	22.96	25.16	24.18
2	154.08	37.58	24.89	23.88	29.63
3	157.15	35.68	26.31	23.87	29.14
4	157.31	38.12	25.4	23.27	27.88
5	154.77	40.19	21.87	22.86	28.75
6	146.36	38.8	19.36	23.19	18.21
7	125.01	38.86	18.91	28.42	20.4
8	165.57	38.33	22.44	30.12	16.1
9	160.52	37.58	20.07	28.76	17.89
Average	152.53	38.03	22.47	25.5	23.58
Standard deviation	11.63	1.27	2.69	2.81	5.48
% Variation	7.62	3.34	11.97	11.02	23.24

Table 4.3 Comparison of average adhesion force (nN) values

Tip type	Adhesion force or pull-off force (nN)								
	Base asphalt or unmodified asphalt			Styrene-Butadiene (SB) polymer modified asphalt			Styrene-Butadiene-Styrene (SBS) polymer modified asphalt		
	Dry	Wet	Ratio, wet/dry	Dry	Wet	Ratio, wet/dry	Dry	Wet	Ratio, wet/dry
Si_3N_4	104.4	62.5	0.60	48.9	173.0	3.54	41.4	118.0	2.85
-COOH	283.1	159.1	0.56	75.1	76.5	1.02	89.5	105.0	1.17
$-CH_3$	157.5	98.4	0.62	51.0	113.6	2.23	152.3	120.9	0.79
-OH	87.2	72.6	0.83	46.1	54.1	1.17	118.7	201.5	1.70

Table 4.4 All the test results with significance test results for SB

Tip	SB	Cond	Forces (nN)	P-value	Pearson value
-COOH	1%	Dry	56.00	0.0000033	0.222910874
	2%		67.87		
	3%		69.24		
	4%		88.00		
	5%		55.29		
	1%	Wet	76.00	0.0000006	-0.082779702
	2%		73.19		
	3%		85.11		
	4%		94.43		
	5%		62.18		
-OH	1%	Dry	57.18	0.0000654	0.234558821
	2%		31.78		
	3%		39.07		
	4%		38.80		
	5%		63.78		
	1%	Wet	28.58	0.0000585	0.890100277
	2%		51.87		
	3%		56.54		
	4%		69.09		
	5%		64.25		
$-NH_3$	1%	Dry	74.11	0.0003274	0.967640885
	2%		128.51		
	3%		124.37		
	4%		174.99		
	5%		214.56		
	1%	Wet	158.92	0.0005429	0.889526322
	2%		171.47		
	3%		163.71		
	4%		263.96		
	5%		368.02		
$-CH_3$	1%	Dry	64.00	0.0004340	-0.346968482
	2%		27.74		
	3%		25.06		
	4%		43.83		
	5%		38.91		
	1%	Wet	97.64	0.0000036	-

	2%		126.30		0.188767992
	3%		147.56		
	4%		97.99		
	5%		98.29		
-Si_3N_4	1%	Dry	38.03	0.0012616	0.577848878
	2%		25.50		
	3%		27.89		
	4%		29.71		
	5%		67.67		
	1%	Wet	119.38	0.0001702	0.355533594
	2%		181.20		
	3%		254.56		
	4%		271.62		
	5%		148.51		

Table 4.5 All the test results with significance test results for SBS

Tip	SBS	Cond	Forces (nN)	P-value	Pearson value
-COOH	1%	Dry	57.01	0.0001336	0.114665
	2%		87.00		
	3%		128.40		
	4%		92.97		
	5%		64.22		
	1%	Wet	84.85	0.0001063	0.203483
	2%		94.00		
	3%		142.00		
	4%		153.83		
	5%		77.44		
-OH	1%	Dry	49.93	0.0064277	0.104584
	2%		133.67		
	3%		166.87		
	4%		204.46		
	5%		38.53		
	1%	Wet	185.44	0.0000038	-0.401355
	2%		222.93		
	3%		252.11		
	4%		202.47		
	5%		144.31		
$-NH_3$	1%	Dry	45.59	0.0096901	0.972824
	2%		78.66		
	3%		213.41		
	4%		307.09		
	5%		327.42		
	1%	Wet	138.66	0.0033530	0.890637
	2%		126.55		
	3%		153.38		
	4%		359.94		
	5%		374.62		
$-CH_3$	1%	Dry	81.00	0.0001847	0.083882
	2%		145.98		
	3%		197.00		
	4%		113.00		
	5%		109.25		
	1%	Wet	105.00	0.0001208	-0.072165
	2%		151.60		
	3%		214.00		
	4%		117.00		

	5%		112.00		
$-Si_3N_4$	1%	Dry	22.47	0.0031243	0.695634
	2%		23.58		
	3%		9.31		
	4%		40.71		
	5%		47.82		
	1%	Wet	104.11	0.0000003	0.622192
	2%		128.83		
	3%		129.11		
	4%		156.42		
	5%		126.81		

Table 4.6 All the test results with significance test results for Elvaloy

Tip	Elvaloy %	Cond	Forces (nN)	P-value	Pearson value
-COOH	0.005	Dry	282.21	2.94E-05	-0.62336
	0.0075		197.94		
	0.015		214.98		
	0.02		199.72		
	0.005	Wet	542.37	2.56E-06	-0.92146
	0.0075		505.38		
	0.015		425.6		
	0.02		436.57		
-OH	0.005	Dry	165.07	0.000132	-0.94326
	0.0075		162.82		
	0.015		108.72		
	0.02		109.77		
	0.005	Wet	207.27	4.06E-05	-0.46628
	0.0075		285.8		
	0.015		238.1		
	0.02		186.58		
$-NH_3$	0.005	Dry	130.8	1.06E-05	-0.61679
	0.0075		98.37		
	0.015		97.72		
	0.02		101.07		
	0.005	Wet	292.67	0.011629	-0.697
	0.0075		444.91		
	0.015		352.21		
	0.02		65.87		
$-CH_3$	0.005	Dry	90.64	5.82E-05	-0.92142
	0.0075		81.21		
	0.015		59.87		
	0.02		62.87		
	0.005	Wet	272.38	3.65E-05	-0.63786
	0.0075		340.1		
	0.015		225.3		
	0.02		245.91		
$-Si_3N_4$	0.005	Dry	167.887	0.000256	-0.96082
	0.0075		135.54		
	0.015		108.187		
	0.02		93.12		
	0.005	Wet	237.58	4.99E-07	-0.95695
	0.0075		219.8		
	0.015		201.47		
	0.02		195.78		

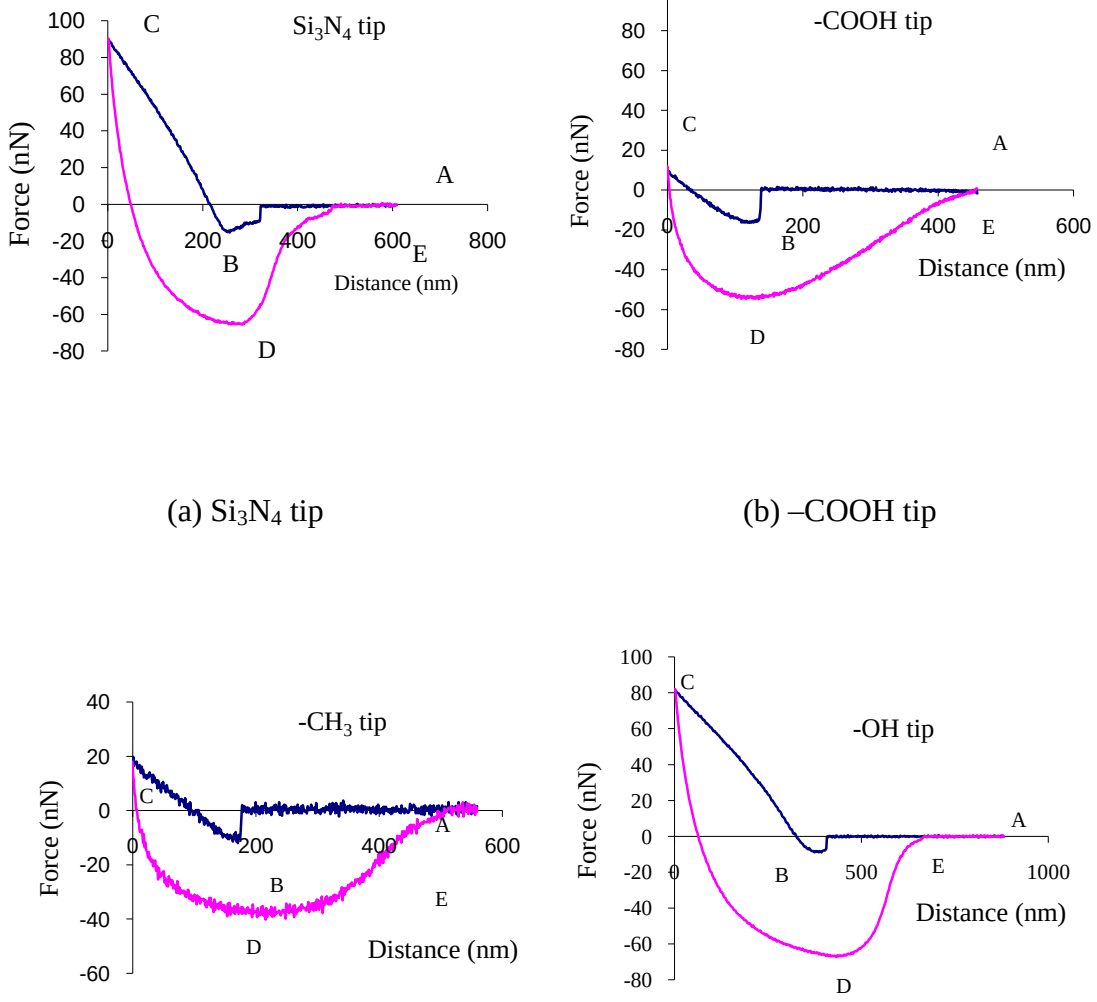

(a) Si_3N_4 tip

(b) –COOH tip

(c) $–CH_3$ tip

(d) –OH tip

Figure 4.1 Force-distance characteristics of asphalt samples (5% SBS, dry sample)

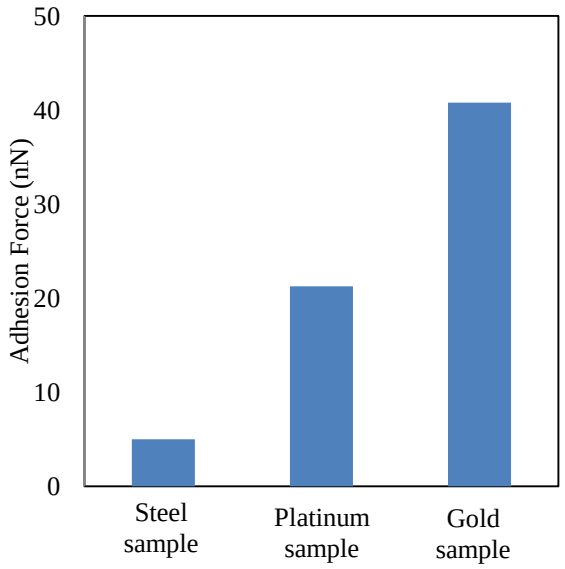

(a) $-Si_3N_4$

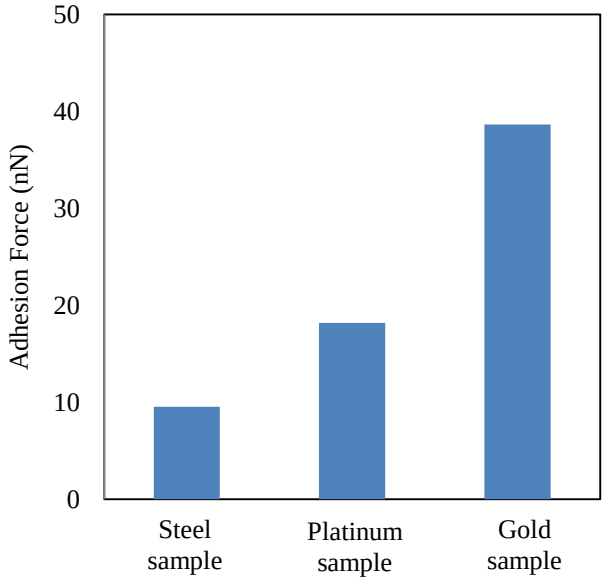

(b) $-CH_3$

Figure 4.2 Adhesion force results with $-Si_3N_4$ and $-CH_3$ tips

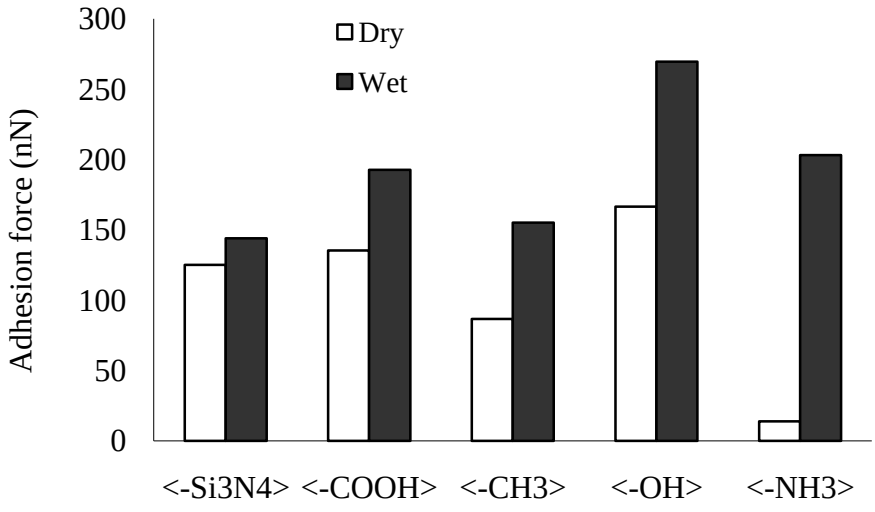

Figure 4.3 Dry vs. Wet: adhesion in base binder (0% polymer)

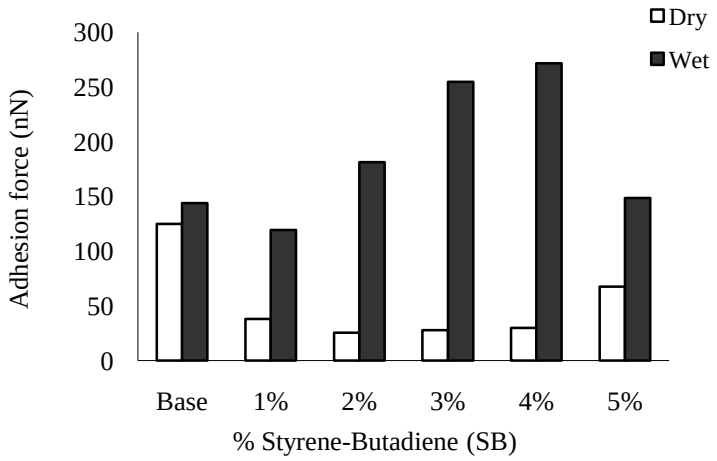

Figure 4.4 Dry vs. wet: adhesion forces in asphalt samples by -Si_3N_4 tip on SB polymer modified sample

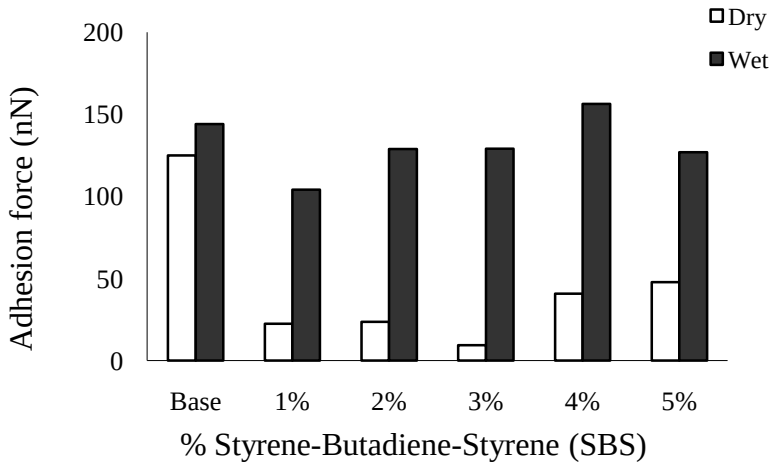

Figure 4.5 Dry vs. wet: adhesion forces in asphalt samples by -Si_3N_4 tip on SBS polymer modified sample

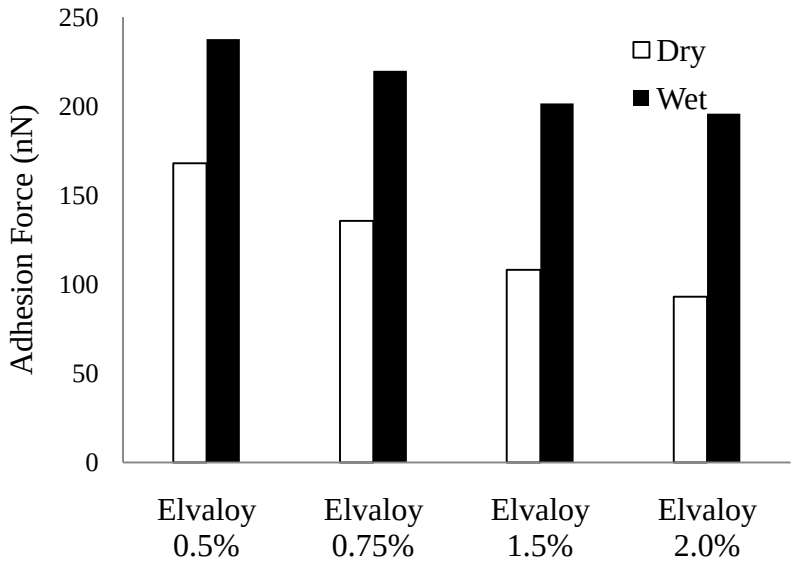

Figure 4.6 Dry vs. wet: adhesion forces in asphalt samples by -Si_3N_4 tip on Elvaloy modified sample

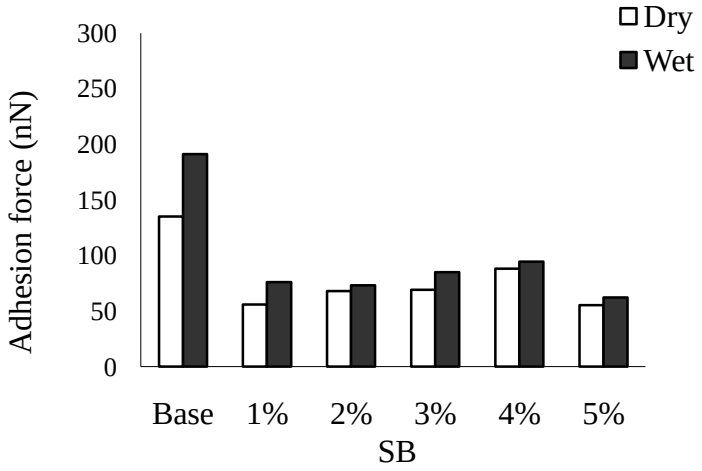

Figure 4.7 Dry vs. wet sample adhesion forces using –COOH tip on SB sample

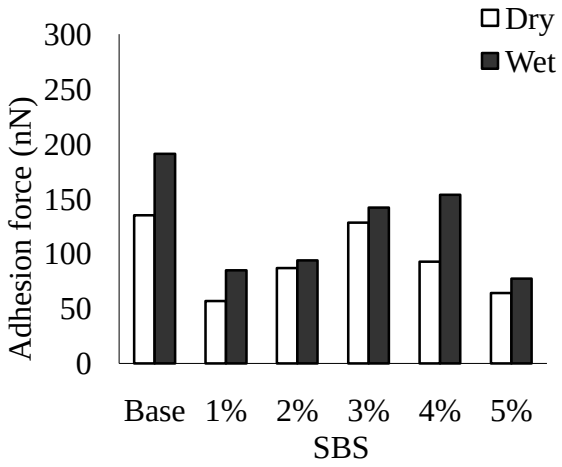

Figure 4.8 Dry vs. wet sample adhesion forces using –COOH tip on SBS sample

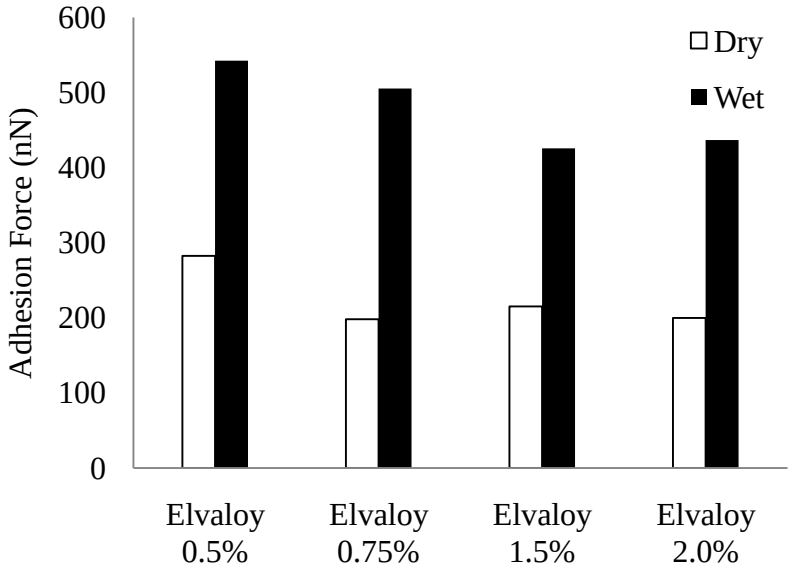

Figure 4.9 Dry vs. wet sample adhesion forces using –COOH tip on Elvaloy sample

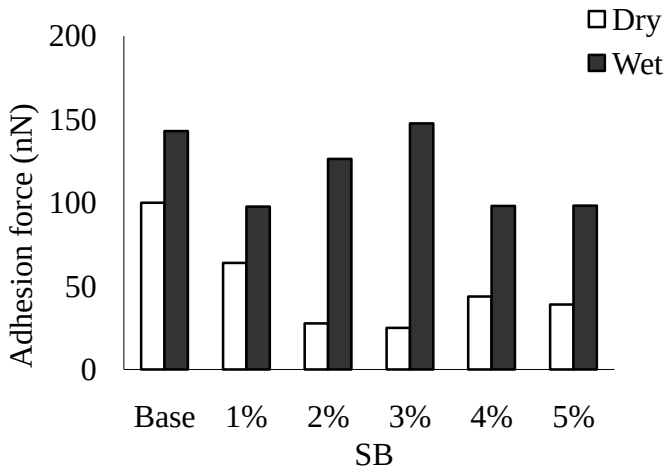

Figure 4.10 Dry vs. wet sample adhesion force using $-CH_3$ tip on SB modified asphalt

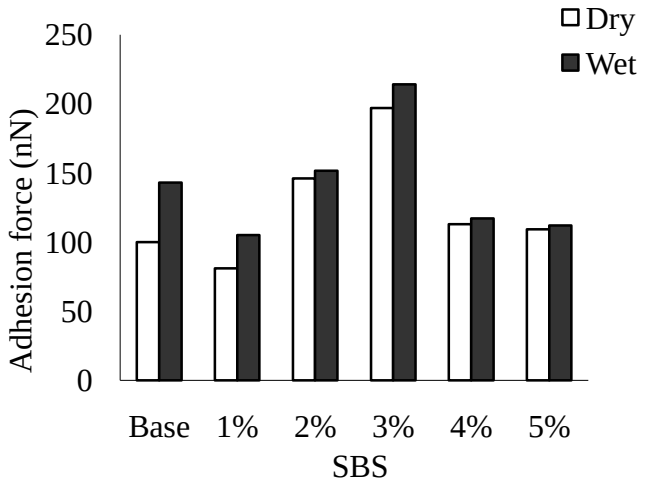

Figure 4.11 Dry vs. wet sample adhesion force using $–CH_3$ tip on SBS modified asphalt

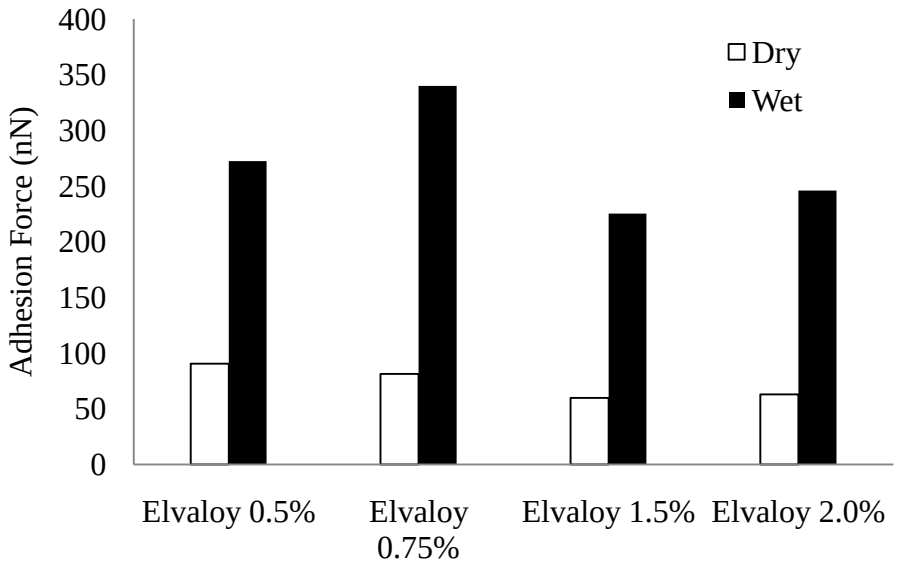

Figure 4.12 Dry vs. wet sample adhesion force using $-CH_3$ tip

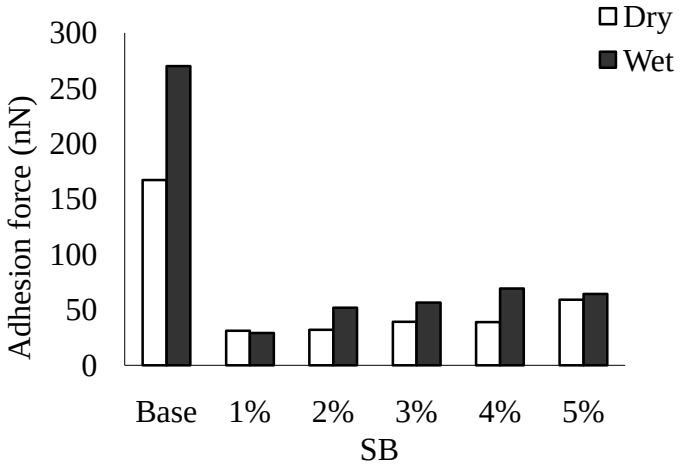

Figure 4.13 Dry vs. wet sample adhesion force using –OH tip on SB modified sample

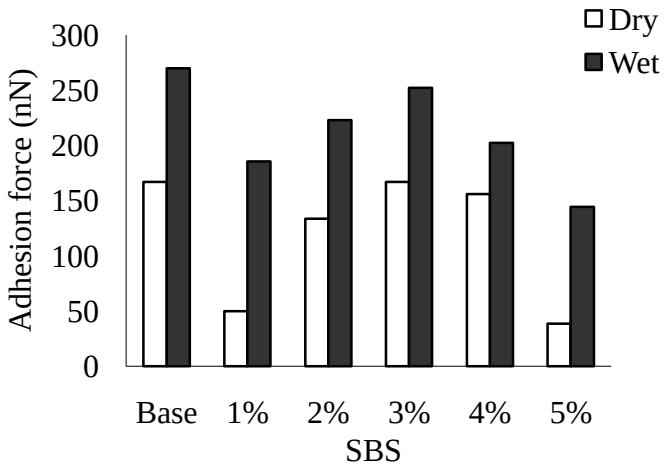

Figure 4.14 Dry vs. wet sample adhesion force using –OH tip on SBS modified sample

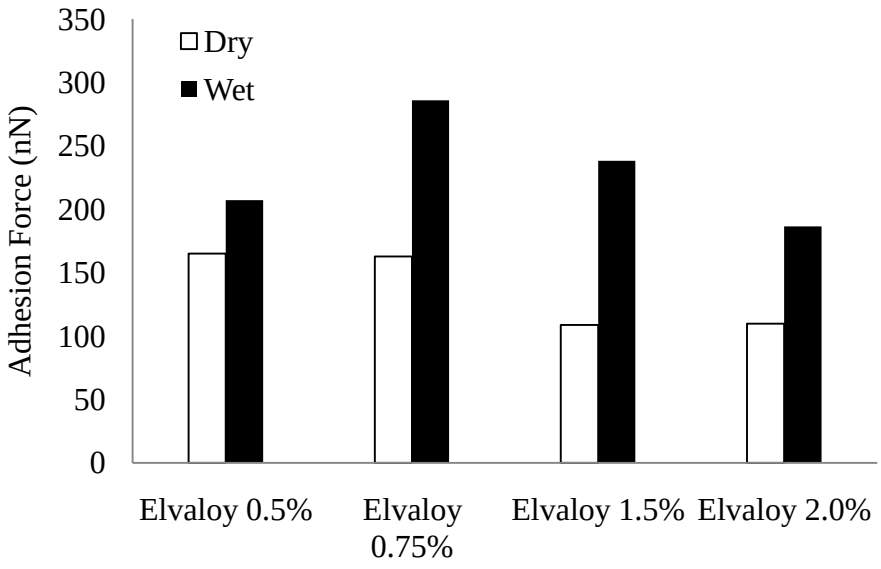

Figure 4.15 Dry vs. wet sample adhesion force using –OH tip

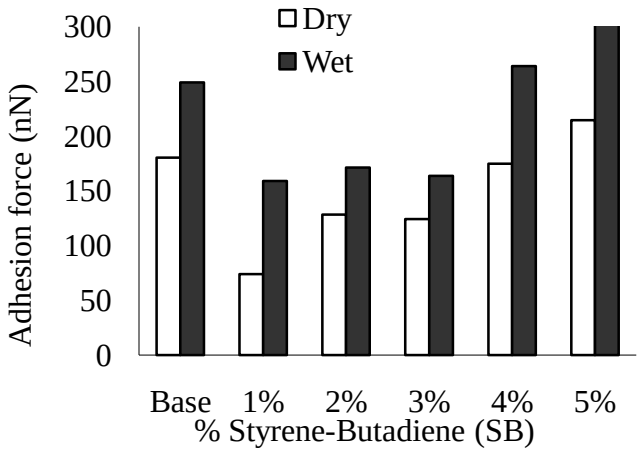

Figure 4.16 Dry vs. wet sample adhesion force using $-NH_3$ tip on SB modified sample

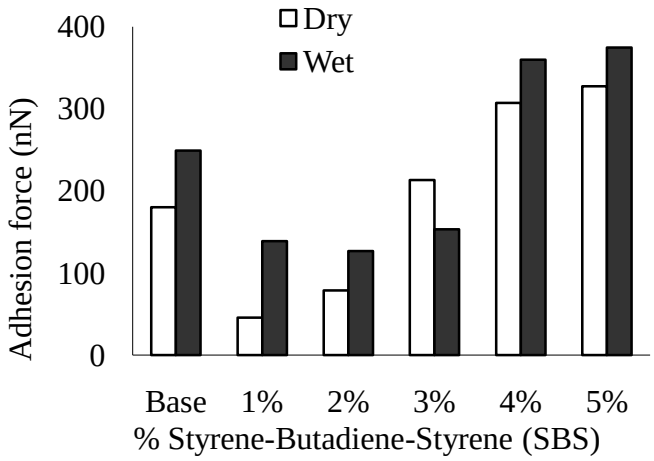

Figure 4.17 Dry vs. wet sample adhesion force using $-NH_3$ tip on SBS modified sample

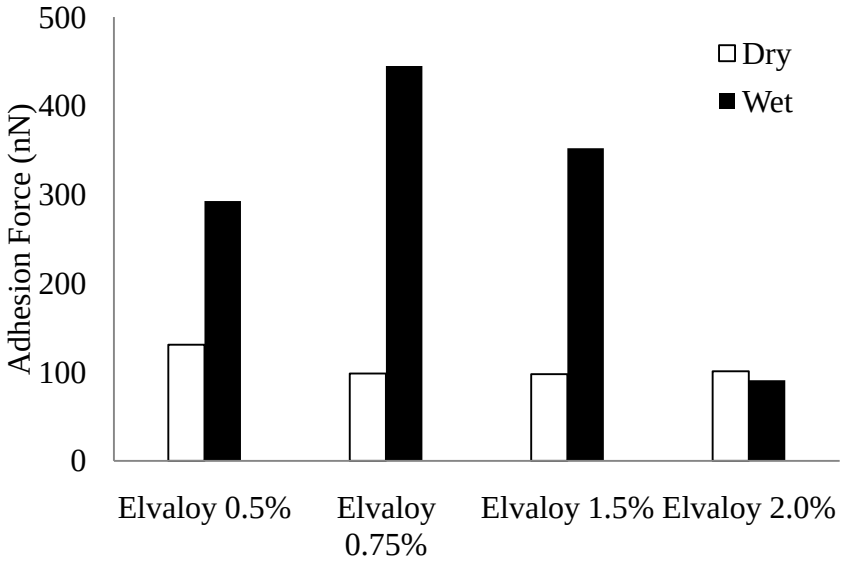

Figure 4.18 Dry vs. wet sample adhesion force using $-NH_3$ tip on Elvaloy modified sample

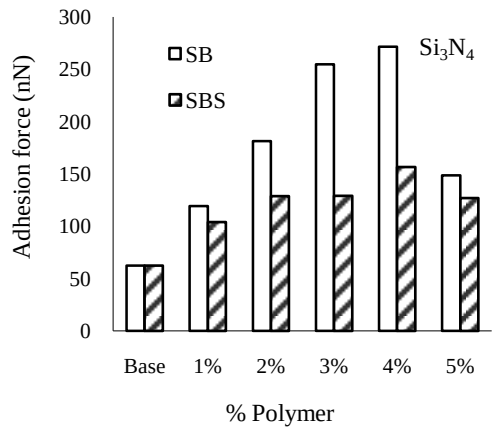

(a) Using Si_3N_4 tip

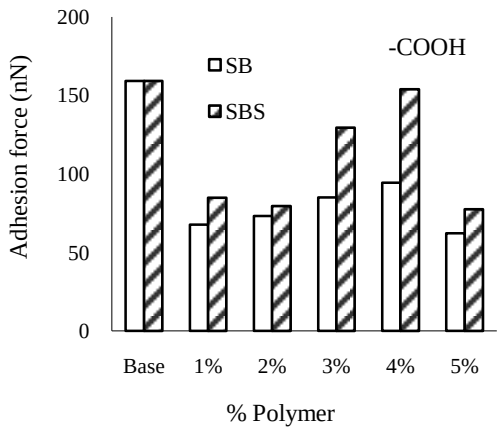

(b) Using –COOH tip

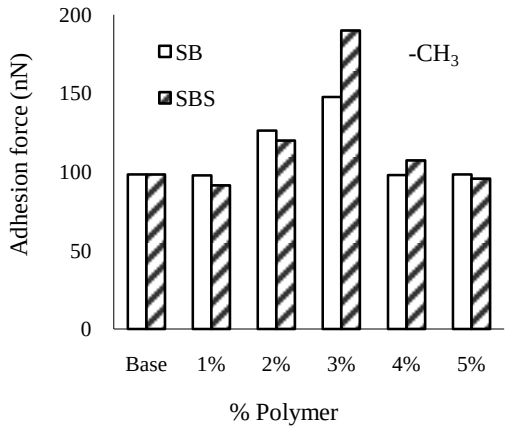

(c) Using $–CH_3$ tip

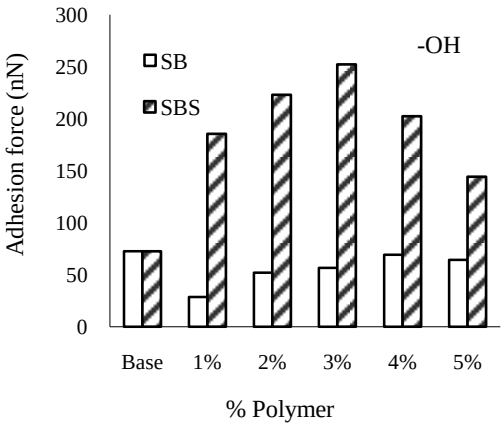

(d) Using –OH tip

Figure 4.19 Adhesion forces in wet SB vs. wet SBS polymer modified asphalt samples

CHAPTER 5

Adhesion Loss in Antistripping Treated Asphalt Binders Due to Moisture

5.1 Introduction

Antistripping agents are usually used with asphalt binder in very small quantity to prevent stripping (Hicks, 1991). Currently, two different types of antistripping agents are used to prevent the moisture damage. One is chemical antistripping agents and another is lime. Stripping is a kind of moisture damage where asphalt binder strips off the aggregate surface. Adding an antistripping agent to asphalt binder, the surface force or energy of the binder is reduced. Sometimes antistripping agents are used to change the surface charge of aggregate so as to stick to or adhere to binder. Among the chemical antistripping agents morlife, unichem, wetfix and kling beta are well known.

5.1.1 Past Study on Anstripping Agents and Moisture Damage

Usually two different types of additives or antistripping agents have been using to control moisture damage. They are chemical (liquid) and lime (non-liquid) types (Hicks 1991). The chemical or liquid types promote some uniform type of wetting of the aggregates hence reduce the surface tension of the asphalt binder. Lottman, et al. (1988) found that moisture damage of asphalt concrete pavements was a problem experienced by more than one-half of the State Highway Agencies (SHA) in the United States. In a seminar (TRB 2003), it was reported that 82 percent of highway agencies require the use of an antistrip additive in hot mix asphalt concrete or HMA.

In the pavement community, our group of researchers believes that antistripping agents are helpful to reduce moisture damage or stripping. As a result, most of agency uses 0.5 to 1.0% antistripping. However the fact is moisture damage or stripping is still a prevalent problem of our pavements. As a result, a group of researchers believe that antistrippingg agents do not help reduce moisture damage at all. So far, macro-scale strength test (e.g. AASHTO T283) has failed to resolve this conflict. Often time, a mixure with or without antistripping agents has shown failure in the field. In addition, laboratory macro-scale testing has shown false negative or positive with or without antistripping agents. The reason for this is that antistripping agent is very small (0.5 to 1.0%) in binder, which is even very small (5 to 6%) compared to the aggregate or total mix. Some believe that chemical antistripping agents evaporate or leave the binder surface during mixing and compaction, which requires to be done at a very high temperature (160ºC). No test procedure has been developed on binder to see whether antistripping agents work or not. There are State DOTs that rely on lime than chemical antistripping. For example, New Mexico DOT uses 1.0% lime in asphalt binder for all mixes. However, some contractors have shown interest in using morlife in New Mexico. Therefore, there is a need for studying whether antistripping agents have any effect on adhesion loss. If so, then what percentages is the most effective. Also, it is important to know which type of antistripping is most effective. Similarly, it will be interesting to know whether lime is more effective than chemical antistripping agents. All of these are done in this study based on AFM measured adhesion force or also known as pull-off force.

5.1.2 Objectives

The aim of this research is to present the consequences of using antistripping agents to resist the moisture damage problem in asphalt binder. A total of five different antistripping agents which has been using in the US for long time were chosen to evaluate the performance.

The main of objectives of this chapter are to:

1. Evaluate the effect of antistripping agents on asphalt binder.
2. Determine the type of antistripping agent that is more effective.
3. Determine where polymer or Elvaloy together with antistripping agents has any effect on moisture damage.

5.2 Test Matrix

Five types of antistripping agents are used in this study. They are lime, unichem, morlife, klingbeta and wetfix. All antistripping agents were used in three different percentages. Three types of polymers used to modify the base binder. The Styrene-Butadyne (SB) and Styrene-Butadyne-Styrene (SBS) were used at 3%, 4% and 5% by weight. Elvaloy was used in 0.5%, 0.75%, 1.5% and 2.0% by weight of the mix with the base binder. The test matrix is shown in Table 5.1. The test matrix consist of 11 (Base, 3 types of SB, 3 types of SBS and 4 types of Elvaloy) types of binder, 15 different types and percentages of antistripping agents (three different percentages of lime, kling beta, wetfix, morlife and unichem), 2 samples conditioning (wet and dry) and 5 types of tips (-CH_3, NH_3, -COOH,

-OH and $-Si_3N_4$). A total of 1650 AFM tests were conducted. Each test was done out 4 points. Average of those 4 is reported here.

5.3 Statistical Analysis of AFM Data

Statistical analysis is important in order to resolve issues involve the study of data analysis. Statistics has been described as the scientific and mathematical study of data. In a very large datasets or database, it is impossible and impractical to analyze every piece of data very quickly. Hence, a sample of the data is studied and the rest of the data results can be extrapolated from the sample data.

A test result from experiment will be called statistically significant if it is unlikely to have occurred by chance. But the word significant does not mean important or meaningful. It represents the true state of experimental data. The popular levels of significance are defined as 5% (0.05), 1% (0.01) and 0.1% (0.001). If a test of significance gives a p-value lower than the α-level, the null hypothesis is rejected. Typically a null hypothesis suggests a general position, such that there is no relationship between two measured occurrence or phenomena or that a potential treatment has no effect. Such results are informally referred to as 'statistically significant'.

5.3.1 Statistical Analysis with Pearson Value

Statistical analysis of adhesion values is performed to find product-moment correlation coefficient. It is a measure of the correlation (or linear dependence) between two different variables (Cohen et al, 2002). In this study, these two variables are adhesion and %

antistripping agents. The output is a value between -1 and +1. The value close to +1 indicates the strong linear proportional relations between the output and input data. The value close to -1 indicates the strong inverse proportional relation between input and output data. It is widely used in the engineering as a measure of the strength of linear dependence between two variables. Table 5.2 shows the Pearson values for lime modified 3%, 4% and 5% SB asphalt binders. The tests were accomplish with –COOH tip. The Pearson values for dry and wet samples of 3% SB are -0.997495 and -0.999980 which is very close to -1. This is shows a strong correlation between output and input data. The 4% SB dry samples Pearson values is -0.748231 which is also very close to -1. The wet samples Pearsons value is 0.487870 which is may be indication of the adverse water effect that took place on the wet samples. The 5% SB dry and wet samples Pearson values are -0.361816 and -0.460247. This is not a strong correlation value. The mixing of the lime may not be homogeneously happened on the 5% SB samples.

5.3.2 p- Value

In statistical significance testing, the p-value is the probability of obtaining a test statistic at least as extreme as the one that was actually observed, assuming that the null hypothesis is true. The lower the p-value, the less likely the result is if the null hypothesis is true, and consequently the more "significant" the result is, in the sense of statistical significance (Desrosières, 2004). One often accepts the alternative hypothesis, (i.e. rejects a null hypothesis) if the p-value is less than 0.05 or 0.01, corresponding respectively to a 5% or 1% chance of rejecting the null hypothesis when it is true. In this study we did analyze all the P value for the output data. Table 5.2 shows the p-values for lime

modified 3%, 4% and 5% SB asphalt binders mixined with three different percentages of lime. All the values are less than 0.01% which is the expected values. This suggests that the all test outputs are significant.

5.4 Antistripping Agents

In this study a total of five different antistripping agents were used.

5.4.1 Lime

Lime has been added to hot mix asphalt pavements for over 25 years. The growth of the demand has been significant, currently totaling over 400,000 tonnes per year (USGS, 2004). Lime contributes to both the mechanical and rheological properties of asphalt mixtures. Lime improves moisture sensitivity resistance and fracture toughness along with reducing the rate of oxidative aging of many asphalt binders. Considerable laboratory research has been performed to quantify the benefits of hydrated lime, and decades of field performance have validated the laboratory conclusions (Berger and Huege 2002).

Antistripping additives are used to increase physico-chemical bond between the bitumen and aggregate and to improve wetting by lowering the surface tension of the bitumen (Majidzahed and Brovold 1968, Hunter 2001). Stuart et al. (1990) tested (i) hydrated lime and quick lime, (ii) silane coupling agents, and (iii) silicone. Among them, hydrated lime and quicklime have shown to be the most effective antistripping agents (Zvejnicks 1958, Petersen 1987, Kennedy and Anagnos 1983). When lime is added to hot mix asphalt (HMA), it reacts with aggregate and strengthens the bond between the bitumen and the aggregate interface. Lime reacts with highly polar molecules to inhibit the formation of

water-soluble soaps that promote stripping. When polar molecules react with lime, they form insoluble salts that no longer attract water. Lime contains mostly silicium dioxide and surface moisture. Table 5.3 shows the properties of hydrated lime.

5.4.2 Kling Beta

Kling Beta is a brown color liquid (at 25 °C) consists of amines. It was supplied by Akzo Nobel Surface Chemistry, Texas. It does not have significant odor. A typical doge of 0.25-0.75% by weight of asphalt is recommended for use which should be determined in laboratory mix design tests. During plant mixing, Kling Beta is usually added to the asphalt binder by means of a specially designed injection system. Alternatively, it can be incorporated into the asphalt binder by mechanical agitation, pump circulation of the storage tank, or by injection into the asphalt loading line followed by recirculation through the truck bypass system until properly mixed. Usually flash point is 200°C. The viscosities of KlingBeta is 5500 mPa.s at 20 °C and 1000 mPa.s at 40 °C (Akzo Nobel Handbook 2006).

5.4.3 WetFix

Wetfix contains amines which is a dark brown liquid at 25°. For this study, it was collected from Akzo Nobel Surface Chemistry, Texas. The typical dozes are 0.25-1.0% by weight of asphalt binder. The percent is recommended by the manufacturers but not by laboratory mix design tests. Wetfix is usually added to the asphalt at the hot-mix plant by means of a specially designed injection system. Alternatively, the product can be incorporated into the asphalt binder by mechanical agitation, pump circulation of the

storage tank, or by injection into the asphalt loading line followed by recirculation through the truck bypass system until properly mixed. Its flash point is usually 200 °C. The viscosities are 1500 mPa.s at 20°C and 370 mPa.s at 40 °C. (Akzo Nobel Handbook 2006).

5.4.4 Unichem

Unichem is a dark brown color liquid with density 8.31 lb/gal, viscosity 236 mPa.s at 37.8 ^{o}C, viscosity 50 mPa.s at 60 ^{o}C, pour point <30^{o}C and flash point 100 ^{o}C. Unichem was collected from BJ chemicals, Wyoming. Unichem contains some heat stable ingredients that perform well in various heat stability evaluations. Unichem can be adsorbed directly onto the surface of the aggregate and which increase the wettability of aggregate surface (surface oil wet). This allows asphalt to easily coat the aggregate providing resistance to water stripping of the aggregate. Thus Unichem does not chemically alter the asphalt, as is the case with lime. Unichem is effective in concentrations ranging upward from 0.25 percent by weight of the asphalt (BJ Chemicals Laboratory Manual, 2008). In this study, Unichem is mixed with asphalt binder instead of precoating aggregate with Unichem and then mixing with asphalt binder.

5.4.5 Morlife

Antistripping agents Morlife-2200 was collected from MeadWestvaco Corporation. It is a high-performance product from different chemical alternatives for use in hot-mix asphalt pavements and it also improves the bond between asphalt and aggregates and overcome the problems that are associated with poor adhesion. HMA mixes treated with

MORLIFE-2200 exhibit improved resistance to moisture-related damage and stripping, resulting in longer lasting pavements. The low odor of MORLIFE-2200 is a dramatic improvement over other additives, resulting in undetectable odors at the paving site. Typical Properties of MORLIFE-2200 are dark brown liquid, specific gravity 1.1 (at 25 ^{o}C), pour point -5 ^{o}C, flash Point 180 ^{o}C (MeadWestvaco Manual 2008).

5.5 Wet vs. Dry: Base Asphalt with Lime

Figure 5.1 shows the adhesion forces for the dry and wet base asphalt binder samples modified with three different types of lime with the –COOH tip. We can see almost all wet samples adhesion forces are higher than that of dry samples. But the 1.5% lime modified samples seems to be more effective to resist the damage as compared to other samples. Figure 5.2 shows the dry and wet adhesion force comparison with –OH tip. All wet samples are suffered adhesion loss due to moisture here. Figure 5.3 shows the comparison with $–NH_3$ tip. The 1.0% lime modified samples is the worst effected by moisture here. Figure 5.4 shows the adhesion comparison with the $–CH_3$ tip. All the wet samples suffer damage due to moisture.

5.6 Wet vs. Dry: Elvaloy Modified Asphalt with Lime

The base binder (PG 58-28) was modified with four percentages (0.5%, 0.75%, 1.5% and 2.0% by weight) of Elvaloy. Each of the modified binders was then mixed with three different percentages of lime (0.5%, 1.0% and 1.5%). Two sets of AFM samples were prepared. One set was wet conditioned. Another set was tested as dry sample. The percentage in loss of adhesion has been calculated like:

$$\% \text{ adhesion loss} = \frac{(\text{Wet adhesion} - \text{Dry adhesion})}{\text{Dry adhesion}} X100 \text{---------- (5.1)}$$

5.6.1 On 0.5% Elvaloy Binder

Figure 5.5 shows the adhesion losses on 0.5% Elvaloy modified with 0.5%, 1.0% and 1.5% of lime. All the results with four different tips (i, e. –COOH, -OH, $-NH_3$ and $–CH_3$) are shown. The loss due to –COOH tips does not vary a lot and seems to steady. This is the lowest adhesion loss as compared to all of the tips. The loss measured with $–CH_3$ is the highest among all the tips for 0.5% and 1.0% lime modified samples. But this loss is less when we measure on 1.5% lime modified samples. This is the indication that losses are decreasing after modifying the 0.5% Elvaloy sample with 1.0% lime. With the –OH tip the losses show breakeven point after 1.0% lime modification. With the $–NH_3$ tip the losses seems to be proportional with percentage of lime.

For 0.5% Elvaloy modified binders with the three different percentages of lime's adhesion forces data from AFM testing are shown in Appendix A1. Some noticeable variation can be observed from the Elvaloy modified dry and wet samples. The raw data from testing are inserted in Appendix A1 for all the samples. All the dry samples adhesion forces are in between 390-400 nN range. But all the wet samples adhesion forces are much closer to 500 nN. So we observe that the adhesion losses are steady for all different types of sample irrespective of different percentages of lime. With –OH tip the adhesion forces of the dry samples adhesion forces are lower than that of wet samples. The average of the adhesion force is about 330 nN for the dry samples whereas the average value for the wet samples is about 600 nN. With $–NH_3$ tip the adhesion forces

loss comparison of all dry and wet samples. All the wet samples show considerable adhesion loss here. The change is constant with change of percentage of lime here. With $–CH_3$ tip the adhesion forces are higher than the dry samples in all cases.

5.6.2 On 0.75% Elvaloy Binder

Figure 5.6 shows the adhesion losses on the 0.75% Elvaloy modified binders. Here the losses with the –COOH tip is the lowest amount and again with the $–CH_3$ tip is the highest till some points. The losses with $–NH_3$ and –OH tips are in between. The losses in variation with –COOH tip is not much as compared to other tips measurements.

All the results are shown in Appendix A1. With –COOH tip the 0.75% Elvaloy modified binders with the three different percentages of lime's adhesion forces from AFM testing are shown in Appendix A1. Not much noticeable variation can be observed on the Elvaloy modified dry and wet samples. All the dry samples adhesion forces are in between 400 nN range. And all the wet samples adhesion forces are close to 450 nN. So we observe that the adhesion losses are not steady for all different types of sample irrespective of different percentages of lime. With –OH tip the adhesion forces on dry and wet samples of 0.75% Elvaloy are shown in Appendix A1. All of the dry samples adhesion forces are lower than that of wet samples. The average of the adhesion force is about 200 nN for the dry samples whereas the average value for the wet samples is about 500 nN. With $–NH_3$ tip in Appendix A1 shows the adhesion forces comparison of all dry and wets samples for the 0.75% Elvaloy. All wet samples show adhesion loss. With $–CH_3$ tip Appendix A1 shows the comparison of between dry and wet samples of 0.75%

Elvaloy and lime modified binders. The wet samples adhesion forces are higher than the dry samples. The 0.5% lime modified sample has the worst adhesion loss whereas the 1.5% lime modification is the best.

5.6.3 On 1.5% Elvaloy Binder

Figure 5.7 shows the adhesion losses on the 1.5% Elvaloy modified binders. The same trends with –COOH and $–CH_3$ are noticeable as before. Here the breakeven point is 1.0% lime for all the cases. All samples adhesion losses seem to be degrading after the 1.0% lime modification.

The results and raw data are shown in Appendix A1. With –COOH tip the 0.5% Elvaloy modified binders with the three different percentages of lime's adhesion forces from AFM testing are shown in Appendix A1. The adhesion forces for Elvaloy modified dry and wet samples are not similar in magnitude. All the dry samples adhesion forces are in between 340-380 nN range. But the average wet samples adhesion forces are close to 380 nN. So we observe that the adhesion losses are obvious for all different types of sample irrespective of different percentages of lime. With –OH tip the adhesion forces on dry and wet samples of 1.5% Elvaloy are shown in Appendix A1. All of the dry samples adhesion forces are lower than that of wet samples. The average of the adhesion force is about 350 nN for the dry samples whereas the average value for the wet samples is about 450 nN. With $–NH_3$ tip Appendix A1 shows the adhesion forces comparison of all dry and wet samples for the 1.5% Elvaloy. The 1.5% lime modified sample seems to be the best to prevent moisture damage here. For the other two samples the dry and wet samples

difference in adhesion is considerable. With $–CH_3$ tip Appendix A1 shows the comparison of between dry and wet samples of 1.5% Elvaloy and lime modified binders. The wet samples adhesion forces are much higher than that of dry samples.

5.6.4 On 2.0% Elvaloy Binder

Figure 5.8 shows the adhesion losses on the 2.0% Elvaloy modified binders. The losses are negligible and steady with the –COOH tip. But the losses are higher with the $–CH_3$ tip. Again the breakeven point with 2.0% Elvaloy for lime modification can be defined as 1.0%.

The results are shown in Appendix A1. With –COOH tip the 0.5% Elvaloy modified binders with the three different percentages of lime's adhesion forces from AFM testing are shown in Appendix A1. Not much variation can be observed on the Elvaloy modified dry and wet samples. All the dry samples adhesion forces are in between 350-400 nN range. And all the wet samples adhesion forces are close to 400 nN. With –OH tip the adhesion forces on dry and wet samples of 2.0% Elvaloy are shown in Appendix A1. All of the dry samples adhesion forces are lower than that of wet samples. With $–NH_3$ tip Appendix A1 shows the adhesion forces comparison of all dry and wets samples for the 2.0% Elvaloy. With $–CH_3$ tip Appendix A1 shows the comparison of between dry and wet samples of 2.0% Elvaloy and lime modified binders. The wet samples adhesion forces are higher than the dry samples.

Overall, the adhesion loss with lime modification is not much satisfactory with all the tips.

5.7 Wet vs. Dry: Elvaloy Modified Asphalt with Klingbeta (KB)

The Elvaloy modified with Kling Beta results are inserted in Appendix A2.

5.7.1 On 0.5% Elvaloy Modified KB

Figure 5.9 shows the adhesion losses on the 0.5% Elvaloy modified with KB antistripping agent binders. Here the losses are highest with the –COOH tip. The trends with $–NH_3$ tip and $–CH_3$ tips are very similar as both are considered as hydrophobic tip.

The adhesion forces for 0.5% Elvaloy mixed with three different percentages of KB with –COOH tip data are shown in Appendix A2. The 0.75% KB modified sample seems to be the most affected by the moisture action in this case. The 0.25% and 0.5% KB modified samples show lesser adhesion loss due to moisture. With –OH tip Appendix A2 shows the adhesion forces results from the 0.5% Elvaloy with KB modified binders with the –OH tip. Here the 0.75% KB modified sample is the least effected by moisture and the 0.25% and 0.5% KB modified samples are seems to not resist the water action as compared to other one. With $–NH_3$ tip Appendix A2 describes the adhesion force comparison for the 0.5% Elvaloy modified with KB with $–NH_3$ tip. All wet samples are evident of moisture damages. With $–CH_3$ tip the adhesion forces comparison of dry and wet samples for the 0.5% Elvaloy modified with the different percentages of KB with $–CH_3$ tip are shown in Appendix A2. All the wet samples damage due to moisture is consistent in this example.

5.7.2 On 0.75% Elvaloy Modified KB

Figure 5.10 shows the adhesion losses on the 0.75% Elvaloy modified with KB antistripping agent binders. The breakeven point for the loss is clearly defined as 0.5% KB here. After this point all the losses seem to be decreased.

The adhesion forces for 0.75% Elvaloy mixed with three different percentages of KB with –COOH tip are shown in Appendix A2. The 0.75% KB modified sample seems to be the most affected by the moisture action in this case. The 0.25% and 0.5% KB modified samples show lesser adhesion loss due to moisture. With –OH tip Appendix A2 shows the adhesion forces results from the 0.5% Elvaloy with KB modified binders with the –OH tip. Here the 0.75% KB modified sample is the least effected by moisture and the 0.25% and 0.5% KB modified samples are seems to not resist the water action as compared to other one. With $–NH_3$ tip Appendix A2 describes the adhesion force comparison for the 0.5% Elvaloy modified with KB with $–NH_3$ tip. All wet samples are evident of moisture damages. With $–CH_3$ tip the adhesion forces comparison of dry and wet samples for the 0.5% Elvaloy modified with the different percentages of KB with $–CH_3$ tip are shown in Appendix A2. All the wet samples damage due to moisture is consistent in this example.

5.7.3 On 1.5% Elvaloy Modified KB

Figure 5.11 shows the adhesion losses on the 1.5% Elvaloy modified with KB antistripping agent binders. The breakeven point for the loss is clearly defined as 0.5% KB here. After this point all the losses seem to be decreased.

The adhesion forces for 0.75% Elvaloy mixed with three different percentages of KB with –COOH tip are shown in Appendix A2. The 0.75% KB modified sample seems to be the most affected by the moisture action in this case with –COOH tip. The 0.25% and 0.5% KB modified samples show lesser adhesion loss due to moisture. With –OH tip Appendix A2 shows the adhesion forces results from the 0.5% Elvaloy with KB modified binders with the –OH tip. Here the 0.75% KB modified sample is the least effected by moisture and the 0.25% and 0.5% KB modified samples are seems to not resist the water action as compared to other one. With $–NH_3$ tip Appendix A2 describes the adhesion force comparison for the 0.5% Elvaloy modified with KB with $–NH_3$ tip. All wet samples are evident of moisture damages. With $–CH_3$ tip the adhesion forces comparison of dry and wet samples for the 0.5% Elvaloy modified with the different percentages of KB with $–CH_3$ tip are shown in Appendix A2. All the wet samples damage due to moisture is consistent in this example.

5.7.4 On 2.0% Elvaloy Modified KB

Figure 5.12 shows the adhesion losses on the 2.0% Elvaloy modified with klingbeta antistripping agent binders. The breakeven point for the loss for all most all cases is defined as 0.5% KB here. After this point all the losses seem to be decreased.

The adhesion forces for 2.0% Elvaloy mixed with three different percentages of KB with –COOH tip are shown in Appendix A2. The 0.75% KB modified sample seems to be the most affected by the moisture action in this case. The 0.25% and 0.5% KB modified

samples show lesser adhesion loss due to moisture. With –OH tip Appendix A2 shows the adhesion forces results from the 0.5% Elvaloy with KB modified binders with the –OH tip. Here the 0.75% KB modified sample is the least effected by moisture and the 0.25% and 0.5% KB modified samples are seems to not resist the water action as compared to other one. With $–NH_3$ tip Appendix A2 describes the adhesion force comparison for the 0.5% Elvaloy modified with KB with $–NH_3$ tip. All wet samples are evident of moisture damages. With $–CH_3$ tip the adhesion forces comparison of dry and wet samples for the 0.5% Elvaloy modified with the different percentages of KB with $–CH_3$ tip are shown in Appendix A2. All the wet samples damage due to moisture is consistent in this example.

5.8 Wet vs. Dry: Elvaloy Modified Asphalt with WetFix

Figure 5.13 shows the adhesion loss on 0.5% Elvaloy mixed with Wetfix antistripping agent. Here the losses with –COOH tip is the lowest as compared to others. Figure 5.14 shows the adhesion loss on 0.75% Elvaloy mixed with Wetfix antistripping agent. Here the losses with –COOH tip is the lowest and the $–NH_3$ is the highest as compared to others. Figure 5.15 shows the adhesion losses on the 1.5% Elvaloy modified with Wetfix antistripping agent binders. Losses with the $–CH_3$ tip is the highest here. The losses with –COOH tip is the minimum and steady with the percentage change of Wetfix. Figure 5.16 shows the adhesion losses on 2.0% Elvaloy modified with Wetfix. We could see that the losses with $–NH_3$ tip is the highest.

With –COOH tip Appendix A3 shows the adhesion force comparison for the 0.5% Elvaloy with –COOH tip. The least moisture damage is observed in the 0.65% Wf modified samples. With –OH tip the adhesion force comparison for the dry and wet samples of 2.0% Elvaloy modified with Wf and with –OH tip is shown in Appendix A3. The worst case is seen on the 0.25% Wf modified sample from the moisture damage point of view. With $–NH_3$ tip Appendix A3 shows the adhesion force comparison for the 0.75% Elvaloy and Wf modified samples with $–NH_3$ tip. All the wet samples adhesion forces are higher than the dry samples hence this certify the evidence of moisture damage. With $–CH_3$ tip the dry and wet adhesion forces comparison for the 0.75% Elvaloy with $–CH_3$ tip are shown in Appendix A3. The moisture dame in wet samples is consistent in all cases here. All the dry samples have almost similar or very close value of adhesion but the 0.65% WtFx modified wet sample looks the most damage due to moisture here.

5.9 Wet vs. Dry: Elvaloy Modified Asphalt with Morlife

Figure 5.17 shows the adhesion losses on 0.5% Elvaloy mixed with Morlife (Mf). Here the losses with –COOH tip is the lowest. The adhesion losses on 0.75% Elvaloy with all the tips are shown in Figure 5.18. The losses are the lowest with –COOH tip and higest with –OH tip here. Figure 5.19 shows the adhesion losses on 1.5% Elvaloy samples. The losses with –COOH tip is the lowest here. Figure 5.20 shows the adhesion losses on 2.0% Elvaloy samples mixed with Mf. Here the breakeven point is 1.0% Mf for all the cases. All samples adhesion losses seem to be changing trend after the 1.0% Mf modification.

With –COOH tip Appendix A4 shows the adhesion force comparison for the dry and wet samples of 1.5% Elvaloy modified by morlife with –COOH tip. A visible difference for the dry and wet samples can be seen here. The 0.6% morlife modified sample is the weakest to resist moisture action here. With –OH tip the adhesion force comparison for the dry and wet samples for 1.5% Elvaloy mixed with morlife are shown in Appendix A4. The 0.6% morlife mixed samples seems to be the highest in terms of dry and wet adhesion force measurement. All the wet samples adhesion forces are higher than that of dry samples here. With $–NH_3$ tip Appendix A4 shows the adhesion force comparison for the dry and wet samples of 1.5% Elvaloy mixed with morlife with $–NH_3$ tip. The 0.6% and 1.0% morlife mixed samples wet adhesion forces are higher than that of dry samples here. The adhesion force for the wet 0.25% morlife is lower than the dry sample due to some reasons. With $–CH_3$ tip adhesion force comparison for the 0.5% Elvaloy modified with morlife is shown in Appendix A4 with $–CH_3$ tip. The moisture damage seems to be consistent in all cases here. The 0.25% morlife mixed sample is the worst effects by the moisture here.

5.10 Wet vs. Dry: Elvaloy Modified Asphalt with Unichem

Figure 5.21 shows the adhesion losses with all the tips on 0.5% Elvaloy modified with Unichem (Um) agent. The losses with –COOH is the minimum here. The maximum losses are found with $–CH_3$ tip. Figure 5.22 shows the adhesion losses with all the tips on 0.75% Elvaloy samples. The maximum losses are found again with $–CH_3$ tip. Figure 5.23 shows the adhesion losses with all the tips. The minimum losses are with the –COOH tip

here. And maximum losses are with –OH and $–CH_3$ tips here. Figure 5.24 shows the adhesion losses with all the tips. The maximum losses are occurred with $–CH_3$ tip here.

With –COOH tip the dry and wet samples adhesion forces comparisons are shown in Appendix A5 for the 2.0% Elvaloy mixed unichem with –COOH tip. The 1.5% unichem modified sample seems to be worst affected by moisture here. The 0.25% unichem is the best to protect the moisture damage in this case. With –OH tip Appendix A5 shows the adhesion force comparison between dry and wet samples for the 0.5% Elvaloy modified with unichem samples tested with –OH tip. All the wet samples are prone to moisture damage here. The damage due to moisture is steady at this point. With $–NH_3$ tip the dry and wet adhesion force comparisons are shown in Appendix A5 for the 1.5% Elvaloy modified with unichem and tested with $–NH_3$ tip. All the wet samples are consistent for moisture damage perspective. With $–CH_3$ tip Appendix A5 depicts the dry and wet adhesion force comparison for the 0.75% Elvaloy modified by different percentages of unichem with $–CH_3$ tip. All the wet samples adhesion forces are consistently higher than that of dry samples. But the performance of 0.85% unichem modified samples is the best here.

5.11 Wet vs. Dry: SB Modified Asphalt with Lime

Table 5.4 and 5.5 shows all the results with four tips. For the –COOH tip we can see all the wet samples of 3%, 4% and 5% SB modified with lime modified samples experience adhesion loss. The Pearson value for the klingbeta modified 3% SB sample with-COOH tip is very close to -1, which indicates a very good correlation for the output data. Also,

the p-value shows a good agreement for the significance test for the 3%, 4% and 5% SB and lime modified samples.

5.12 Wet vs. Dry: SB Modified Asphalt with Kling Beta

Table 5.6 and 5.7 shows all the results for the 3%, 4% and 5% SB modified with klingBeta. The wet samples adhesion forces are higher than that of dry samples with all the tips. The Pearson values and p-values for the significance test are in good shape for the output results.

5.13 Wet vs. Dry: SB Modified Asphalt with WetFix (WF)

Table 5.8 and 5.9 shows all the results. With –COOH tip it seen that all wet samples has moisture damage as compared to dry samples. The Pearson value with the –COOH tip is in between +1 to -1 which indicated that the output results are correlated. The P-values are also significant as they are less than 0.05. With the –OH tip the adhesion loss for the wet samples are also obvious. The p-value and Pearson value for 4% and 5% SB modified samples are good. With $–NH_3$ tip all the wet samples show adhesion loss. The p-values for all the samples are less than 0.05. With the $–CH_3$ tip moisture damage is seen for all the wet samples. The p-value is less than 0.05 which indicates good correlation for the output data and the WF mixing.

5.14 Wet vs. Dry: SB Modified Asphalt with Unichem

Table 5.10 and 5.11 shows all the results. With the –COOH tip the all the wet samples adhesion forces are higher than that of dry samples which indicates moisture damage. All the P-values are less than 0.05. Some of the Pearson values are satisfactory. With the –---

-OH tip all the wet samples show moisture damage. All the p-values are less than 0.05. Hence the data are significant. With the $–NH_3$ tip all the wet samples adhesion forces are higher than the dry samples. The p-value is well below 0.05 for all tests. The Pearson values are also good. With $–CH_3$ tip all wet samples show moisture damage. p-values are less than 0.05. The Pearson values are good for 3% and 4% samples.

5.15 Wet vs. Dry: SB Modified Asphalt with Morlife

Table 5.12 and 5.13 shows all the results. With –COOH tip we can see all the wet samples experience loss in adhesion force due to moisture. The p-values are less than 0.05 for all the samples. With the –OH tip again the wet samples adhesion forces are higher than that of dry samples. The p-values are less than 0.05. With $–NH_3$ tip the wet samples adhesion forces are higher than dry samples.

5.16 Wet vs. Dry: SBS Modified Asphalt with Lime

Table 5.14 and 5.15 shows all the results. With –COOH tip we see all the wet samples are damaged by moisture as compared to dry samples. The p-values are satisfactory as well as the Pearson values. With –OH tip all the wet samples experienced damage due to moisture. The p-values are below 0.05. With $–NH_3$ tip the wet samples adhesion forces are less than that of dry samples. The p-values are below 0.05. The Pearson values are good. With $–CH_3$ tip the wet samples adhesion forces are higher than that of dry samples. The p-vales and Pearson values are good.

5.17 Wet vs. Dry: SBS Modified Asphalt with Kling Beta

Table 5.16 and 5.17 shows all the results. With –COOH tip all dry samples adhesion forces are lower than that of wet samples. The p-values are satisfactory as all are well below than 0.05. With –OH tip all the wet samples show damage due to moisture. The p-values are below 0.05. With $–NH_3$ tip the also all the wet samples experiences damage due to moisture. The p-values are below 0.05. The $–CH_3$ tip also shows moisture damage in all wet samples. The p-values are less than 0.05.

5.18 Wet vs. Dry: SBS Modified Asphalt with Wet Fix

Table 5.18 and 5.19 shows all the results. With –COOH, -OH, $-NH_3$ and CH_3 tip all the wet samples adhesion forces are higher than that of dry samples. The p-values are also well below than 0.05.

5.19 Wet vs. Dry: SBS Modified Asphalt with Unichem

Table 5.20 and 5.21 shows all the results. With –COOH tip all the dry samples adhesion forces are less than that of wet samples. p-values are less than 0.05. The Pearson values for 5% SBS modified samples are good. With the –OH tip again we see the moistyure damage in wet samples. The p-values are less than 0.05. With $–NH_3$ tips the wet samples show moisture damage. The p-values are satisfactory. With $–CH_3$ tip the moisture damage is happened for all the wet samples. The p-values are less than 0.05.

5.20 Wet vs. Dry: SBS Modified Asphalt with Morlife

Table 5.22 and 5.23 shows all the results. With –COOH tip all wet samples show damage due to moisture action. The p-values are less than 0.05 for all samples. The Pearson values for 3% and 5% SBS modified samples are good. With –OH tip moisture damage is vivid for all wet samples. The P-values are less than 0.05. The Pearson values are in between -1 to +1 here. With the $–NH_3$ tip all wet samples experienced damage due to moisture. The p-values are less than 0.05. With $–CH_3$ tip again moisture damage happened for all wet samples as compared to dry samples. The P-values are less than 0.05.

5.21 Lime vs. Liquid Antistripping Agents

5.21.1 Base Binder

The effect of adding lime and other antistripping agents to base binder is studied and the results are shown in Figure 5.25 and 5.26. The optimum dose was selected for all the antistripping agents which was 1.0% for lime, 0.65% morlife, 0.8% for unichem, 0.65% for wetfix and 0.5% for klingbeta. From the Figure 5.25 it is seen that the lime modified binder's dry/wet adhesion force variation is the least with –COOH tip when we compare it to the other antistripping modified binders. From Figure 5.25 (b) it can be concluded that the lime modified binder is the least affected by the moisture as compared to the other binders as tested with –OH tip. With the $–NH_3$ tip the conclusions is not decisive as shown in Figure 5.26(a). The ammines in liquid antistripping agents may be causing some action on $–NH_3$ chemical tip as both are from the same nitrogen origin. From Figure 5.26 (b) using $–CH_3$ tip it is apparent that the 1.0% lime modified base binder is

the best to resist the moisture related effect among the all antistripping agents. We can see the adhesion forces of dry and wet lime treated binders are the highest among all the samples.

5.22 Error Data for Lime Modified SB Binders

To get a general idea about accuracy of measurement error data are helpful tools. In analysis error data bars are used to represent graphs that indicate the error and uncertainty in a reported measurement. They give a general idea of how accurate a measurement is, or conversely, how far from the reported value the true (error free) value might be. Error bars often indicate one standard deviation of uncertainty, but may also indicate the standard error. These quantities are not the same and so the measure selected should be stated explicitly in the graph or supporting text (Wikipedia 2010). Figure 5.27 shows the error data plot for lime mixed 3% SB samples. Here the dry samples errors are less than that of wet samples. The errors in dry samples are about 5% and the same is 25% for the wet samples. Figure 5.28 shows the error data plot for lime mixed 4% SB samples and the similar trend is noticeable here. Figure 5.29 shows the error data plot for lime mixed 5% SB samples. The errors for the dry and wet samples are similar in magnitude here.

5.23 Effect of Antistripping Agent on SB Modified Asphalt

Figures 5.30 shows the comparison for 3%, 4% and 5% SB binder modified with lime antistripping agent. It is apparent that the lime modification causes less adhesion loss.

5.24 Effect of Antistripping Agent on SB Modified Asphalt

Figure 5.31 shows the adhesion loss comparison for 3%, 4% and 5% SB and KB. It can be concluded that the KB modification causes less adhesion loss.

5.25 Conclusions

This study reveals the moisture damage in asphalt binder with functionalized AFM tools. The research confirms the damage of moisture on asphalt binder even with the presence of antistripping agents. The performances of different agent are also different. The significance test results show good agreement with the change of modifier. All p-values for the tests are less than 0.05. The key features of this study found as:

- Damage due to moisture is possible in asphalt binder and can be proved from nano-scale testing. The adhesion loss in conditioned samples is observed as compared to original dry samples.
- This damage rate is not unique when we use different asphalt functional AFM tips like hydrophobic and hydrophilic tips.
- Hydrated lime antistripping agent performs better than the ammin based liquid antistripping agents (i, e morlife, unichem, klingbeta and wetfix). Hence it is the recommended additive to prevent damage due to moisture from nano-scale testing.
- The AFM testing on antistripping modified asphalt binder is significant from the statistical point of view but the correlation coefficient of the output data is not very straightforward.

Table 5.1 Test Matrix

Polymer	Additives (Three percentages)	Tips	Condition	No. of Tests	Total
3-5% SB	Lime Unichem Morlife Kling Beta Wet Fix	-COOH, -OH -CH_3, NH_3 -Si_3N_4	Dry	225	1650
			Wet	225	
3-5% SBS	Lime Unichem Morlife Kling Beta Wet Fix	-COOH, -OH -CH_3, NH_3 -Si_3N_4	Dry	225	
			Wet	225	
0.5%, 0.75%, 1.5% and 2.0% Elvaloy	Lime Unichem Morlife Kling Beta Wet Fix	-COOH, -OH -CH_3, NH_3 -Si_3N_4	Dry	300	
			Wet	300	
Base Binder	Lime Unichem Morlife Kling Beta Wet Fix	-COOH, -OH -CH_3, NH_3 -Si_3N_4	Dry	75	
			Wet	75	

Table 5.2 Statistical Analysis on AFM test results of SB and Lime modified asphalts with –COOH tip

Tip	SB%	Condition	Antistripping Agents	Forces (nN)	Pearson value	p-value
			Lime			
-COOH	3	Dry	0.25%	179.44	-0.997495	0.000058
			1.00%	162.42		
			1.50%	147.82		
		Wet	0.25%	262.06	-0.999980	0.000133
			1.00%	228.60		
			1.50%	206.80		
	4	Dry	0.25%	220.85	-0.748231	0.000140
			1.00%	174.57		
			1.50%	189.30		
		Wet	0.25%	225.91	0.487870	0.000265
			1.00%	199.00		
			1.50%	264.28		
	5	Dry	0.25%	224.58	-0.361816	0.000149
			1.00%	176.07		
			1.50%	211.88		
		Wet	0.25%	279.52	-0.460247	0.000002
			1.00%	289.09		
			1.50%	267.32		
			1.00%	198.26		
			1.50%	196.72		

Table 5.3 Properties of hydrated lime (Gorkem and Sengoz 2009)

Name	Formula	%
Silicium dioxide	SiO2	40%
Ferrous oxide+	Fe2O3+	12%
Aluminum oxide	Al2O3	10%
Calcium oxide	CaO	-
Magnesium oxide	MgO	-
Sulfur trioxide	SO3	-
Surface moisture	H2O	40%

Table 5.4 AFM test results of SB and Lime modified asphalts (with –COOH and –OH tip)

Tip	SB%	Condition	Antistripping Agents	Forces (nN)	Adhesion Loss (nN)	Pearson value	p-value
			Lime				
COOH	3	Dry	0.25%	179.44		-0.997495	0.000058
			1.00%	162.42			
			1.50%	147.82			
		Wet	0.25%	262.06	82.62	-0.999980	0.000133
			1.00%	228.60	66.18		
			1.50%	206.80	58.98		
	4	Dry	0.25%	220.85		-0.748231	0.000140
			1.00%	174.57			
			1.50%	189.30			
		Wet	0.25%	225.91	5.06	0.487870	0.000265
			1.00%	199.00	24.43		
			1.50%	264.28	74.98		
	5	Dry	0.25%	224.58		-0.361816	0.000149
			1.00%	176.07			
			1.50%	211.88			
		Wet	0.25%	279.52	54.94	-0.460247	0.000002
			1.00%	289.09	113.02		
			1.50%	267.32	55.44		
OH	3	Dry	0.25%	104.96		0.212974	0.002190
			1.00%	161.76			
			1.50%	111.16			
		Wet	0.25%	152.83	47.87	0.990186	0.000078
			1.00%	169.88	8.12		
			1.50%	188.49	77.33		
	4	Dry	0.25%	128.94		0.930814	0.000137
			1.00%	137.97			
			1.50%	162.34			
		Wet	0.25%	172.53	43.59	0.649913	0.000030
			1.00%	166.00	28.03		
			1.50%	194.00	31.66		
	5	Dry	0.25%	122.48		0.894259	0.000169
			1.00%	128.46			
			1.50%	154.84			
		Wet	0.25%	211.31	88.83	-0.951589	0.000002
			1.00%	198.26	69.80		
			1.50%	196.72	41.88		

Table 5.5 AFM test results of SB and Lime modified asphalts (with $-NH_3$ and $-CH_3$ tip)

Tip	SB%	Condition	Antistripping Agents	Forces (nN)	Adhesion Loss (nN)	Pearson value	p-value
			Lime				
$-NH_3$	3	Dry	0.25%	89.91		0.999968	0.000008
			1.00%	96.80			
			1.50%	101.26			
		Wet	0.25%	127.45	37.54	0.235993	0.000078
			1.00%	153.91	57.11		
			1.50%	130.98	29.72		
	4	Dry	0.25%	121.00		-0.930911	0.000289
			1.00%	95.36			
			1.50%	94.31			
		Wet	0.25%	154.45	33.45	-0.999494	0.000301
			1.00%	130.02	34.66		
			1.50%	115.55	21.24		
	5	Dry	0.25%	145.70		-0.801023	0.000472
			1.00%	106.72			
			1.50%	116.12			
		Wet	0.25%	156.00	10.30	0.371522	0.000984
			1.00%	123.46	16.74		
			1.50%	185.53	69.41		
$-CH_3$	3	Dry	0.25%	121.70		0.894710	0.000176
			1.00%	127.74			
			1.50%	154.24			
		Wet	0.25%	136.04	14.34	0.940897	0.000109
			1.00%	165.75	38.01		
			1.50%	168.00	13.76		
	4	Dry	0.25%	137.99		0.439989	0.003483
			1.00%	101.96			
			1.50%	180.41			
		Wet	0.25%	144.40	6.41	0.718381	0.004899
			1.00%	130.99	29.03		
			1.50%	226.00	45.59		
	5	Dry	0.25%	106.48		-0.013055	0.004771
			1.00%	166.33			
			1.50%	96.87			
		Wet	0.25%	153.93	47.45	0.991014	0.001021
			1.00%	210.00	43.67		
			1.50%	231.77	134.90		

Table 5.6 AFM test results of SB and Kling Beta modified asphalts (with –COOH and –OH tip)

Tip	SB%	Condition	Antistripping Agents	Forces (nN)	Adhesion Loss (nN)	Pearson value	p-value
			KlingBeta				
-COOH	3	Dry	0.25%	224.46		-0.998532	0.001475
			0.50%	187.25			
			0.75%	142.32			
		Wet	0.25%	463.06	238.60	0.911700	0.000050
			0.50%	541.94	354.69		
			0.75%	551.66	409.35		
	4	Dry	0.25%	293.85		-0.400318	0.006929
			0.50%	143.34			
			0.75%	233.22			
		Wet	0.25%	339.94	46.09	0.973224	0.001494
			0.50%	478.36	335.02		
			0.75%	536.41	303.19		
	5	Dry	0.25%	173.26		0.848720	0.002594
			0.50%	169.75			
			0.75%	261.84			
		Wet	0.25%	523.81	350.55	0.781252	0.000051
			0.50%	508.41	338.66		
			0.75%	604.04	342.20		
-OH	3	Dry	0.25%	212.05		0.094265	0.001771
			0.50%	139.41			
			0.75%	220.46			
		Wet	0.25%	897.67	685.62	-0.443554	0.005446
			0.50%	235.03	95.62		
			0.75%	603.15	382.70		
	4	Dry	0.25%	208.53		0.960866	0.000006
			0.50%	225.69			
			0.75%	231.42			
		Wet	0.25%	216.81	8.28	0.882083	0.000011
			0.50%	245.54	19.85		
			0.75%	983.30	751.88		
	5	Dry	0.25%	296.84		0.812306	0.000164
			0.50%	288.94			
			0.75%	361.70			
		Wet	0.25%	700.81	403.97	0.529643	0.001845
			0.50%	450.26	161.32		
			0.75%	983.30	621.60		

Table 5.7 AFM test results of SB and Kling Beta modified asphalts (with $-NH_3$ and $-CH_3$ tip)

Tip	SB%	Condition	Antistripping Agents	Forces (nN)	Adhesion Loss (nN)	Pearson value	p-value
			KlingBeta				
-NH_3	3	Dry	0.25%	63.32		0.699067	0.002598
			0.50%	107.93			
			0.75%	95.51			
		Wet	0.25%	272.71	209.39	-0.889543	0.000469
			0.50%	209.07	101.14		
			0.75%	205.35	109.84		
	4	Dry	0.25%	40.54		0.990893	0.033189
			0.50%	104.68			
			0.75%	144.38			
		Wet	0.25%	261.83	221.29	0.969305	0.001136
			0.50%	360.64	255.96		
			0.75%	399.13	254.75		
	5	Dry	0.25%	143.02		-0.868710	0.016712
			0.50%	142.48			
			0.75%	56.37			
		Wet	0.25%	299.62	156.60	-0.943568	0.000089
			0.50%	288.54	146.06		
			0.75%	243.10	186.73		
-CH_3	3	Dry	0.25%	244.74		-0.487264	0.000000
			0.50%	248.58			
			0.75%	241.09			
		Wet	0.25%	295.62	50.88	-0.919096	0.000016
			0.50%	290.97	42.39		
			0.75%	259.50	18.41		
	4	Dry	0.25%	184.42		0.999711	0.000013
			0.50%	211.00			
			0.75%	239.89			
		Wet	0.25%	203.71	19.29	0.996786	0.000950
			0.50%	261.61	50.61		
			0.75%	305.36	65.47		
	5	Dry	0.25%	213.00		-0.248448	0.000058
			0.50%	252.58			
			0.75%	199.24			
		Wet	0.25%	249.00	36.00	-0.031448	0.000131
			0.50%	303.05	50.47		
			0.75%	247.00	47.76		

Table 5.8 AFM test results of SB and WetFix modified asphalts (with –COOH and –OH tip)

Tip	SB%	Condition	Antistripping Agents	Forces (nN)	Adhesion Loss (nN)	Pearson value	p-value
			WetFix				
-COOH	3	Dry	0.25%	156.57		0.991260	0.000862
			0.65%	205.63			
			1.00%	232.13			
		Wet	0.25%	494.54	337.98	0.864174	0.000005
			0.65%	496.41	290.78		
			1.00%	542.02	309.89		
	4	Dry	0.25%	266.33		-0.864686	0.000099
			0.65%	219.81			
			1.00%	221.97			
		Wet	0.25%	591.10	324.77	0.141074	0.000091
			0.65%	497.02	277.21		
			1.00%	613.19	391.22		
	5	Dry	0.25%	367.85		-0.986811	0.015488
			0.65%	225.79			
			1.00%	157.86			
		Wet	0.25%	377.12	9.27	0.998869	0.000087
			0.65%	421.79	196.00		
			1.00%	467.89	310.03		
-OH	3	Dry	0.25%	194.13		0.111724	0.000146
			0.65%	240.72			
			1.00%	197.93			
		Wet	0.25%	918.04	723.91	-0.895769	0.106984
			0.65%	844.00	603.28		
			1.00%	251.03	53.10		
	4	Dry	0.25%	248.74		0.748661	0.000175
			0.65%	320.41			
			1.00%	302.69			
		Wet	0.25%	927.00	678.26	0.909555	0.000003
			0.65%	1001.00	680.59		
			1.00%	1006.00	703.31		
	5	Dry	0.25%	331.37		0.569001	0.000013
			0.65%	313.71			
			1.00%	358.37			
		Wet	0.25%	838.00	506.63	0.995964	0.000004
			0.65%	890.00	576.29		
			1.00%	923.00	564.63		

Table 5.9 AFM test results of SB and WetFix modified asphalts (with $-NH_3$ and $-CH_3$ tip)

Tip	SB%	Condition	Antistripping Agents	Forces (nN)	Adhesion Loss (nN)	Pearson value	p-value
			WetFix				
$-NH_3$	3	Dry	0.25%	111.61		0.407940	0.001163
			0.65%	86.08			
			1.00%	131.97			
		Wet	0.25%	251.18	139.57	0.694315	0.001904
			0.65%	220.20	134.12		
			1.00%	344.73	212.76		
	4	Dry	0.25%	63.27		-0.141322	0.018873
			0.65%	116.46			
			1.00%	50.76			
		Wet	0.25%	226.80	163.53	0.996036	0.000220
			0.65%	259.20	142.74		
			1.00%	297.83	247.07		
	5	Dry	0.25%	88.20		0.991771	0.002108
			0.65%	111.81			
			1.00%	144.16			
		Wet	0.25%	134.75	46.55	0.999526	0.022944
			0.65%	280.14	168.33		
			1.00%	394.34	250.18		
$-CH_3$	3	Dry	0.25%	237.14		0.573060	0.000231
			0.65%	196.87			
			1.00%	299.84			
		Wet	0.25%	290.75	53.61	0.246869	0.000563
			0.65%	224.48	27.61		
			1.00%	318.08	18.24		
	4	Dry	0.25%	248.55		-0.969237	0.000167
			0.65%	208.51			
			1.00%	195.57			
		Wet	0.25%	295.58	47.03	-0.358730	0.000011
			0.65%	318.25	109.74		
			1.00%	280.65	85.08		
	5	Dry	0.25%	259.99		-0.185526	0.000003
			0.65%	239.00			
			1.00%	256.66			
		Wet	0.25%	266.00	6.01	0.818383	0.000045
			0.65%	263.45	24.45		
			1.00%	308.77	52.11		

Table 5.10 AFM test results of SB and Unichem modified asphalts (with –COOH and –OH tip)

Tip	SB%	Condition	Antistripping Agents	Forces (nN)	Adhesion Loss (nN)	Pearson value	p-value
			Unichem				
-COOH	3	Dry	0.25%	350.99		0.563799	0.000072
			0.80%	430.87			
			1.50%	401.00			
		Wet	0.25%	428.42	77.43	0.283622	0.000016
			0.80%	492.18	61.31		
			1.50%	451.00	50.00		
	4	Dry	0.25%	412.24		0.925357	0.001467
			0.80%	595.20			
			1.50%	644.82			
		Wet	0.25%	414.00	1.76	0.612152	0.000001
			0.80%	402.09	-193.11		
			1.50%	428.99	-215.83		
	5	Dry	0.25%	559.63		-0.369727	0.000458
			0.80%	688.50			
			1.50%	501.26			
		Wet	0.25%	572.00	12.37	-0.995933	0.001102
			0.80%	470.82	-217.68		
			1.50%	376.76	-124.50		
-OH	3	Dry	0.25%	312.60		0.999997	0.000150
			0.80%	350.82			
			1.50%	399.89			
		Wet	0.25%	751.00	438.40	-0.799368	0.001343
			0.80%	808.00	457.18		
			1.50%	523.00	123.11		
	4	Dry	0.25%	350.89		0.572866	0.000168
			0.80%	307.49			
			1.50%	396.96			
		Wet	0.25%	599.00	248.11	0.804393	0.000525
			0.80%	824.00	516.51		
			1.50%	813.00	416.04		
	5	Dry	0.25%	402.16		-0.219903	0.001314
			0.80%	259.02			
			1.50%	359.97			
		Wet	0.25%	720.00	317.84	0.362304	0.016551
			0.80%	336.26	77.24		
			1.50%	888.00	528.03		

Table 5.11 AFM test results of SB and Unichem modified asphalts (with $-NH_3$ and $-CH_3$ tip)

Tip	SB%	Condition	Antistripping Agents	Forces (nN)	Adhesion Loss (nN)	Pearson value	p-value
			Unichem				
$-NH_3$	3	Dry	0.25%	182.01		0.646319	0.001849
			0.80%	295.20			
			1.50%	263.46			
		Wet	0.25%	317.14	135.13	0.828867	0.000001
			0.80%	314.29	19.09		
			1.50%	333.32	69.86		
	4	Dry	0.25%	166.21		0.111262	0.000041
			0.80%	137.88			
			1.50%	167.63			
		Wet	0.25%	282.00	115.79	-0.738041	0.000525
			0.80%	207.24	69.36		
			1.50%	219.08	51.45		
	5	Dry	0.25%	211.70		0.876584	0.000026
			0.80%	241.93			
			1.50%	245.28			
		Wet	0.25%	330.71	119.01	-0.320250	0.000218
			0.80%	251.47	9.54		
			1.50%	299.96	54.67		
$-CH_3$	3	Dry	0.25%	186.06		-0.890616	0.007142
			0.80%	113.00			
			1.50%	102.00			
		Wet	0.25%	196.49	10.43	-0.922601	0.000104
			0.80%	167.00	54.00		
			1.50%	159.33	57.33		
	4	Dry	0.25%	104.00		-0.639852	0.000494
			0.80%	118.00			
			1.50%	84.00			
		Wet	0.25%	238.45	134.45	-0.738336	0.000900
			0.80%	263.43	145.43		
			1.50%	177.31	93.31		
	5	Dry	0.25%	85.00		0.023793	0.035916
			0.80%	222.04			
			1.50%	99.00			
		Wet	0.25%	163.38	78.38	0.112291	0.003541
			0.80%	273.18	51.14		
			1.50%	184.44	85.44		

Table 5.12 AFM test results of SB and Morlife modified asphalts (with –COOH and –OH tip)

Tip	SB%	Condition	Antistripping Agents	Forces (nN)	Adhesion Loss (nN)	Pearson value	p-value
			Morlife				
-COOH	3	Dry	0.25%	387.00		0.179217	0.000340
			0.60%	514.52			
			1.00%	416.00			
		Wet	0.25%	434.25	47.25	-0.008059	0.000723
			0.60%	593.57	79.05		
			1.00%	439.75	23.75		
	4	Dry	0.25%	329.59		0.402464	0.000023
			0.60%	383.96			
			1.00%	353.43			
		Wet	0.25%	442.32	112.73	-0.539455	0.000011
			0.60%	469.99	86.03		
			1.00%	413.90	60.47		
	5	Dry	0.25%	356.77		0.925327	0.007064
			0.60%	661.21			
			1.00%	729.61			
		Wet	0.25%	494.51	137.74	-0.752001	0.000020
			0.60%	431.22	-229.99		
			1.00%	441.86	-287.75		
-OH	3	Dry	0.25%	359.52		0.898625	0.000004
			0.60%	389.80			
			1.00%	393.84			
		Wet	0.25%	684.00	324.48	-0.467893	0.000013
			0.60%	736.00	346.20		
			1.00%	644.00	250.16		
	4	Dry	0.25%	421.92		-0.283308	0.000001
			0.60%	392.36			
			1.00%	412.27			
		Wet	0.25%	808.00	386.08	-0.995790	0.000027
			0.60%	743.00	350.64		
			1.00%	689.00	276.73		
	5	Dry	0.25%	333.41		0.936354	0.000029
			0.60%	378.10			
			1.00%	390.18			
		Wet	0.25%	645.00	311.59	0.994871	0.000246
			0.60%	762.00	383.90		
			1.00%	856.00	465.82		

Table 5.13 AFM test results of SB and Morlife modified asphalts (with $-NH_3$ and $-CH_3$ tip)

Tip	SB%	Condition	Antistripping Agents	Forces (nN)	Adhesion Loss (nN)	Pearson value	p-value
			Morlife				
$-NH_3$	3	Dry	0.25%	280.33		0.897463	0.000034
			0.60%	323.11			
			1.00%	328.67			
		Wet	0.25%	354.76	74.43	0.587712	0.000164
			0.60%	457.42	134.31		
			1.00%	418.90	90.23		
	4	Dry	0.25%	113.34		0.992719	0.000067
			0.60%	211.00			
			1.00%	284.25			
		Wet	0.25%	278.00	164.66	0.634165	0.000002
			0.60%	269.00	58.00		
			1.00%	292.00	7.75		
	5	Dry	0.25%	257.35		-0.252392	0.000011
			0.60%	282.29			
			1.00%	250.09			
		Wet	0.25%	298.90	41.55	0.272233	0.000059
			0.60%	361.16	78.87		
			1.00%	318.57	68.48		
$-CH_3$	3	Dry	0.25%	94.97		0.997002	0.000009
			0.60%	120.41			
			1.00%	142.63			
		Wet	0.25%	159.47	64.50	0.740683	0.000620
			0.60%	144.54	24.13		
			1.00%	202.31	59.68		
	4	Dry	0.25%	121.94		-0.355253	0.000137
			0.60%	142.77			
			1.00%	111.89			
		Wet	0.25%	147.13	25.19	0.651920	0.005264
			0.60%	284.87	142.10		
			1.00%	243.30	131.41		
	5	Dry	0.25%	84.00		0.884615	0.000013
			0.60%	84.00			
			1.00%	94.00			
		Wet	0.25%	153.92	69.92	0.972899	0.001733
			0.60%	175.87	91.87		
			1.00%	238.79	144.79		

Table 5.14 AFM test results of SBS and Lime modified asphalts (with –COOH and –OH tip)

Tip	SBS%	Condition	Antistripping Agents	Forces (nN)	Adhesion Loss (nN)	Pearson value	p-value
			Lime				
-COOH	3	Dry	0.25%	200.55		-0.852196	0.001130
			1.00%	194.12			
			1.50%	134.17			
		Wet	0.25%	214.37	13.82	-0.273253	0.000018
			1.00%	233.48	39.36		
			1.50%	202.40	68.23		
	4	Dry	0.25%	189.39		0.997503	0.000171
			1.00%	225.97			
			1.50%	244.59			
		Wet	0.25%	250.43	61.04	-0.295838	0.000004
			1.00%	228.00	2.03		
			1.50%	246.05	1.46		
	5	Dry	0.25%	253.02		-0.887494	0.000023
			1.00%	247.17			
			1.50%	218.63			
		Wet	0.25%	330.65	77.63	-0.981895	0.000786
			1.00%	284.80	37.63		
			1.50%	225.10	6.47		
-OH	3	Dry	0.25%	108.40		0.987377	0.001505
			1.00%	137.04			
			1.50%	170.42			
		Wet	0.25%	204.52	96.12	-0.652694	0.000061
			1.00%	168.07	31.03		
			1.50%	184.00	13.58		
	4	Dry	0.25%	178.74		-0.082268	0.000059
			1.00%	150.60			
			1.50%	179.82			
		Wet	0.25%	207.00	28.26	0.509968	0.000009
			1.00%	197.32	46.72		
			1.50%	222.15	42.33		
	5	Dry	0.25%	148.93		0.883716	0.000764
			1.00%	213.22			
			1.50%	207.64			
		Wet	0.25%	257.08	108.15	0.329390	0.000036
			1.00%	232.48	19.26		
			1.50%	276.15	68.51		

Table 5.15 AFM test results of SBS and Lime modified asphalts (with $-NH_3$ and $-CH_3$ tip)

Tip	SBS%	Condition	Antistripping Agents	Forces (nN)	Adhesion Loss (nN)	Pearson value	p-value
			Lime				
$-NH_3$	3	Dry	0.25%	117.40		-0.898649	0.001438
			1.00%	109.23			
			1.50%	75.39			
		Wet	0.25%	141.14	23.74	0.858763	0.000034
			1.00%	143.69	34.46		
			1.50%	164.29	88.90		
	4	Dry	0.25%	140.41		-0.991256	0.000066
			1.00%	127.97			
			1.50%	114.76			
		Wet	0.25%	148.56	8.15	-0.475412	0.000002
			1.00%	153.49	25.52		
			1.50%	141.88	27.12		
	5	Dry	0.25%	109.37		0.995961	0.000123
			1.00%	129.00			
			1.50%	138.24			
		Wet	0.25%	166.67	57.30	0.984569	0.000029
			1.00%	188.43	59.43		
			1.50%	195.33	57.09		
$-CH_3$	3	Dry	0.25%	106.91		0.644640	0.000029
			1.00%	102.78			
			1.50%	120.00			
		Wet	0.25%	136.74	29.83	0.454923	0.000003
			1.00%	131.26	28.48		
			1.50%	143.58	23.58		
	4	Dry	0.25%	114.00		0.968617	0.001575
			1.00%	138.61			
			1.50%	178.54			
		Wet	0.25%	137.00	23.00	0.955878	0.000265
			1.00%	151.94	13.33		
			1.50%	181.00	2.46		
	5	Dry	0.25%	131.72		0.768927	0.000010
			1.00%	149.00			
			1.50%	144.00			
		Wet	0.25%	137.99	6.27	0.905217	0.000032
			1.00%	160.40	11.40		
			1.50%	159.63	15.63		

Table 5.16 AFM test results of SBS and KlingBeta modified asphalts (with –COOH and –OH tip)

Tip	SBS%	Condition	Antistripping Agents	Forces (nN)	Adhesion Loss (nN)	Pearson value	p-value
			KlingBeta				
-COOH	3	Dry	0.25%	208.86		0.672462	0.008041
			0.50%	159.60			
			0.75%	317.56			
		Wet	0.25%	540.44	331.58	0.255487	0.000041
			0.50%	640.23	480.63		
			0.75%	566.86	249.30		
	4	Dry	0.25%	404.76		-0.463905	0.000793
			0.50%	275.47			
			0.75%	344.73			
		Wet	0.25%	471.28	66.52	0.657145	0.001384
			0.50%	737.62	462.15		
			0.75%	649.63	304.90		
	5	Dry	0.25%	211.29		0.948903	0.000370
			0.50%	270.95			
			0.75%	287.00			
		Wet	0.25%	451.92	240.63	0.546854	0.000468
			0.50%	631.61	360.66		
			0.75%	550.33	263.33		
-OH	3	Dry	0.25%	505.61		0.001105	0.009341
			0.50%	239.36			
			0.75%	505.95			
		Wet	0.25%	701.21	195.60	0.390678	0.002004
			0.50%	511.29	271.93		
			0.75%	824.49	318.54		
	4	Dry	0.25%	201.20		0.141232	0.000238
			0.50%	159.70			
			0.75%	208.65			
		Wet	0.25%	250.43	49.23	-0.982682	0.000015
			0.50%	229.41	69.71		
			0.75%	218.74	10.09		
	5	Dry	0.25%	279.36		0.281278	0.000116
			0.50%	348.97			
			0.75%	299.51			
		Wet	0.25%	716.01	436.65	-0.268382	0.000748
			0.50%	813.54	464.57		
			0.75%	678.62	379.11		

Table 5.17 AFM test results of SBS and KlingBeta modified asphalts (with –NH3 and –CH3 tip)

Tip	SBS%	Condition	Antistripping Agents	Forces (nN)	Adhesion Loss (nN)	Pearson value	p-value
			KlingBeta				
-NH_3	3	Dry	0.25%	106.49		0.234081	0.000033
			0.50%	124.97			
			0.75%	111.00			
		Wet	0.25%	309.80	203.31	0.303927	0.001022
			0.50%	229.43	104.46		
			0.75%	346.09	235.09		
	4	Dry	0.25%	154.07		0.936443	0.000003
			0.50%	156.57			
			0.75%	168.31			
		Wet	0.25%	391.71	237.64	0.816452	0.011288
			0.50%	357.18	200.61		
			0.75%	698.72	530.41		
	5	Dry	0.25%	175.88		-0.982863	0.001441
			0.50%	154.24			
			0.75%	111.78			
		Wet	0.25%	222.26	46.38	0.121752	0.012399
			0.50%	449.29	295.05		
			0.75%	252.29	140.51		
-CH_3	3	Dry	0.25%	316.22		-0.992225	0.000385
			0.50%	241.00			
			0.75%	192.63			
		Wet	0.25%	333.80	17.58	-0.328896	0.000061
			0.50%	274.33	33.33		
			0.75%	313.89	121.26		
	4	Dry	0.25%	307.00		0.927424	0.000010
			0.50%	312.54			
			0.75%	343.75			
		Wet	0.25%	307.00	0.00	0.998696	0.000161
			0.50%	347.05	34.51		
			0.75%	394.87	51.12		
	5	Dry	0.25%	88.86		0.952321	0.000006
			0.50%	140.30			
			0.75%	320.00			
		Wet	0.25%	230.95	142.09	0.949678	0.000971
			0.50%	253.12	112.82		
			0.75%	334.39	14.39		

Table 5.18 AFM test results of SBS and WetFix modified asphalts (with –COOH and –OH tip)

Tip	SBS%	Condition	Antistripping Agents	Forces (nN)	Adhesion Loss (nN)	Pearson value	p-value
			WetFix				
-COOH	3	Dry	0.25%	377.39		-0.999939	0.000978
			0.65%	309.48			
			1.00%	252.31			
		Wet	0.25%	612.42	235.03	-0.947005	0.000115
			0.65%	515.44	205.96		
			1.00%	495.78	243.47		
	4	Dry	0.25%	319.48		-0.670297	0.001828
			0.65%	357.69			
			1.00%	220.91			
		Wet	0.25%	503.00	183.52	0.084079	0.000367
			0.65%	656.45	298.76		
			1.00%	510.90	289.99		
	5	Dry	0.25%	325.72		-0.046654	0.000415
			0.65%	418.62			
			1.00%	316.09			
		Wet	0.25%	539.33	213.61	0.222787	0.000022
			0.65%	621.19	202.57		
			1.00%	555.39	239.30		
-OH	3	Dry	0.25%	461.61		0.297142	0.000003
			0.65%	435.21			
			1.00%	475.17			
		Wet	0.25%	1009.00	547.39	0.251612	0.000042
			0.65%	888.00	452.79		
			1.00%	1060.00	584.83		
	4	Dry	0.25%	319.79		-0.290942	0.000983
			0.65%	213.54			
			1.00%	291.82			
		Wet	0.25%	1144.00	824.21	-0.873298	0.116811
			0.65%	273.23	59.69		
			1.00%	296.78	4.96		
	5	Dry	0.25%	272.44		-0.667679	0.000001
			0.65%	256.20			
			1.00%	261.92			
		Wet	0.25%	922.00	649.56	0.032663	0.027051
			0.65%	304.39	48.19		
			1.00%	975.00	713.08		

Table 5.19 AFM test results of SBS and WetFix modified asphalts (with $-NH_3$ and $-CH_3$ tip)

Tip	SBS%	Condition	Antistripping Agents	Forces (nN)	Adhesion Loss (nN)	Pearson value	p-value
			WetFix				
$-NH_3$	3	Dry	0.25%	78.43		0.749421	0.002301
			0.65%	130.91			
			1.00%	117.99			
		Wet	0.25%	275.40	196.98	0.055989	0.000002
			0.65%	295.34	164.43		
			1.00%	275.80	157.81		
	4	Dry	0.25%	99.82		0.518296	0.000763
			0.65%	145.77			
			1.00%	122.11			
		Wet	0.25%	410.14	310.32	-0.936499	0.002347
			0.65%	375.09	229.32		
			1.00%	245.73	123.62		
	5	Dry	0.25%	220.16		-0.817116	0.006058
			0.65%	226.58			
			1.00%	117.25			
		Wet	0.25%	309.03	88.87	0.729548	0.000661
			0.65%	444.25	217.67		
			1.00%	407.24	289.99		
$-CH_3$	3	Dry	0.25%	119.36		0.894285	0.000000
			0.65%	285.88			
			1.00%	290.00			
		Wet	0.25%	232.12	112.76	0.987240	0.000583
			0.65%	298.44	12.56		
			1.00%	330.50	40.50		
	4	Dry	0.25%	249.88		0.444098	0.000072
			0.65%	306.29			
			1.00%	273.09			
		Wet	0.25%	325.22	75.34	0.997471	0.000013
			0.65%	346.89	40.60		
			1.00%	371.16	98.07		
	5	Dry	0.25%	417.06		-0.307035	0.000069
			0.65%	230.38			
			1.00%	365.00			
		Wet	0.25%	457.55	40.49	-0.681169	0.000704
			0.65%	320.00	89.62		
			1.00%	366.20	1.20		

Table 5.20 AFM test results of SBS and Unichem modified asphalts (with –COOH and –OH tip)

Tip	SBS%	Condition	Antistripping Agents	Forces (nN)	Adhesion Loss (nN)	Pearson value	p-value
			Unichem				
-COOH	3	Dry	0.25%	341.00		0.075938	0.000018
			0.80%	389.00			
			1.50%	348.47			
		Wet	0.25%	423.00	82.00	0.310855	0.000003
			0.80%	395.14	6.14		
			1.50%	432.49	84.02		
	4	Dry	0.25%	293.76		-0.202986	0.001882
			0.80%	416.92			
			1.50%	272.76			
		Wet	0.25%	532.66	238.90	0.214953	0.000040
			0.80%	461.40	44.48		
			1.50%	546.03	273.27		
	5	Dry	0.25%	409.62		0.828408	0.000109
			0.80%	502.87			
			1.50%	502.68			
		Wet	0.25%	571.53	161.91	-0.967486	0.000488
			0.80%	538.11	35.24		
			1.50%	411.10	-91.58		
-OH	3	Dry	0.25%	174.23		0.837495	0.000000
			0.80%	363.45			
			1.50%	366.68			
		Wet	0.25%	203.99	29.76	0.886329	0.000490
			0.80%	470.96	107.52		
			1.50%	507.80	141.13		
	4	Dry	0.25%	304.51		-0.851468	0.000209
			0.80%	312.00			
			1.50%	242.00			
		Wet	0.25%	616.62	312.11	-0.418438	0.036033
			0.80%	357.49	45.49		
			1.50%	492.15	250.15		
	5	Dry	0.25%	194.62		0.698604	0.004427
			0.80%	361.76			
			1.50%	326.00			
		Wet	0.25%	256.54	61.92	0.991600	0.001447
			0.80%	388.70	26.94		
			1.50%	662.61	336.61		

Table 5.21 AFM test results of SBS and Unichem modified asphalts (with $-NH_3$ and $-CH_3$ tip)

Tip	SBS%	Condition	Antistripping Agents	Forces (nN)	Adhesion Loss (nN)	Pearson value	p-value
			Unichem				
$-NH_3$	3	Dry	0.25%	291.24		-0.789052	0.000001
			0.80%	310.56			
			1.50%	221.27			
		Wet	0.25%	323.49	32.24	-0.438878	0.000181
			0.80%	376.06	65.50		
			1.50%	291.35	70.08		
	4	Dry	0.25%	304.46		-0.770586	0.000109
			0.80%	357.85			
			1.50%	139.40			
		Wet	0.25%	417.85	113.39	-0.926649	0.001160
			0.80%	407.23	49.38		
			1.50%	279.49	140.09		
	5	Dry	0.25%	276.21		0.191457	0.000814
			0.80%	396.71			
			1.50%	308.50			
		Wet	0.25%	412.04	135.83	0.720302	0.000000
			0.80%	431.49	34.78		
			1.50%	427.91	119.41		
$-CH_3$	3	Dry	0.25%	269.02		0.456111	0.000934
			0.80%	206.98			
			1.50%	309.75			
		Wet	0.25%	347.68	78.66	0.912632	0.000155
			0.80%	425.23	218.25		
			1.50%	442.48	132.73		
	4	Dry	0.25%	92.69		0.899411	0.000100
			0.80%	93.18			
			1.50%	299.86			
		Wet	0.25%	174.02	81.33	0.806201	0.035091
			0.80%	130.41	37.23		
			1.50%	361.34	61.48		
	5	Dry	0.25%	220.85		0.825836	0.000285
			0.80%	288.00			
			1.50%	287.51			
		Wet	0.25%	244.29	23.44	0.501318	0.000356
			0.80%	333.65	45.65		
			1.50%	294.45	6.94		

Table 5.22 AFM test results of SBS and Morlife modified asphalts (with –COOH and –OH tip)

Tip	SBS%	Condition	Antistripping Agents	Forces (nN)	Adhesion Loss (nN)	Pearson value	p-value
			Morlife				
-COOH	3	Dry	0.25%	326.00		0.956628	0.000408
			0.60%	415.00			
			1.00%	448.30			
		Wet	0.25%	378.70	52.70	0.999815	0.000501
			0.60%	447.00	32.00		
			1.00%	530.49	82.19		
	4	Dry	0.25%	405.56		0.252018	0.000024
			0.60%	471.24			
			1.00%	425.06			
		Wet	0.25%	490.41	84.85	0.624795	0.000003
			0.60%	538.75	67.51		
			1.00%	522.62	97.56		
	5	Dry	0.25%	840.71		-0.978654	0.000383
			0.60%	776.63			
			1.00%	614.32			
		Wet	0.25%	437.43	-403.28	0.629638	0.000242
			0.60%	388.45	-388.18		
			1.00%	512.00	-102.32		
-OH	3	Dry	0.25%	364.09		0.845769	0.000298
			0.60%	355.12			
			1.00%	459.40			
		Wet	0.25%	433.75	69.66	0.742875	0.002002
			0.60%	616.70	261.58		
			1.00%	583.46	124.07		
	4	Dry	0.25%	419.91		-0.992166	0.000050
			0.60%	394.40			
			1.00%	348.44			
		Wet	0.25%	621.51	201.60	0.962144	0.000031
			0.60%	699.76	305.36		
			1.00%	731.76	383.32		
	5	Dry	0.25%	307.00		0.968118	0.000026
			0.60%	319.00			
			1.00%	357.00			
		Wet	0.25%	638.51	331.51	-0.996204	0.003000
			0.60%	558.28	239.28		
			1.00%	433.12	76.12		

Table 5.23 AFM test results of SBS and Morlife modified asphalts (with $-NH_3$ and $-CH_3$ tip)

Tip	SBS%	Condition	Antistripping Agents	Forces (nN)	Adhesion Loss (nN)	Pearson value	p-value
			Morlife				
$-NH_3$	3	Dry	0.25%	250.00		0.552417	0.001061
			0.60%	379.47			
			1.00%	326.00			
		Wet	0.25%	298.48	48.48	0.624828	0.000171
			0.60%	385.39	5.92		
			1.00%	356.39	30.39		
	4	Dry	0.25%	354.00		-0.702808	0.000067
			0.60%	375.00			
			1.00%	307.00			
		Wet	0.25%	360.00	6.00	-0.255413	0.000238
			0.60%	498.43	123.43		
			1.00%	319.00	12.00		
	5	Dry	0.25%	268.58		0.635038	0.000109
			0.60%	337.13			
			1.00%	315.07			
		Wet	0.25%	309.12	40.54	0.999821	0.001828
			0.60%	400.90	63.77		
			1.00%	499.12	184.05		
$-CH_3$	3	Dry	0.25%	271.75		0.807265	0.000063
			0.60%	326.44			
			1.00%	322.23			
		Wet	0.25%	361.70	89.95	0.131646	0.001514
			0.60%	544.19	217.75		
			1.00%	394.70	72.47		
	4	Dry	0.25%	158.57		-0.225748	0.000064
			0.60%	164.16			
			1.00%	157.18			
		Wet	0.25%	180.29	21.72	0.022350	0.000950
			0.60%	253.60	89.44		
			1.00%	185.27	28.09		
	5	Dry	0.25%	102.20		0.957583	0.000080
			0.60%	172.87			
			1.00%	199.72			
		Wet	0.25%	223.37	121.17	0.972716	0.000506
			0.60%	245.01	72.14		
			1.00%	307.30	107.58		

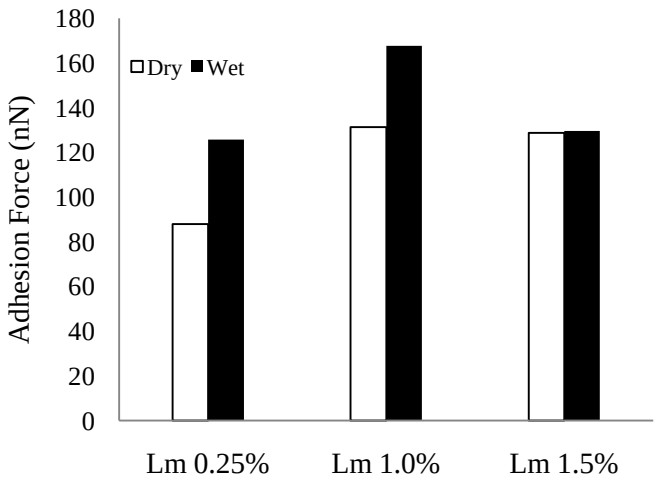

Figure 5.1 Adhesion force comparison with –COOH tip on base binder

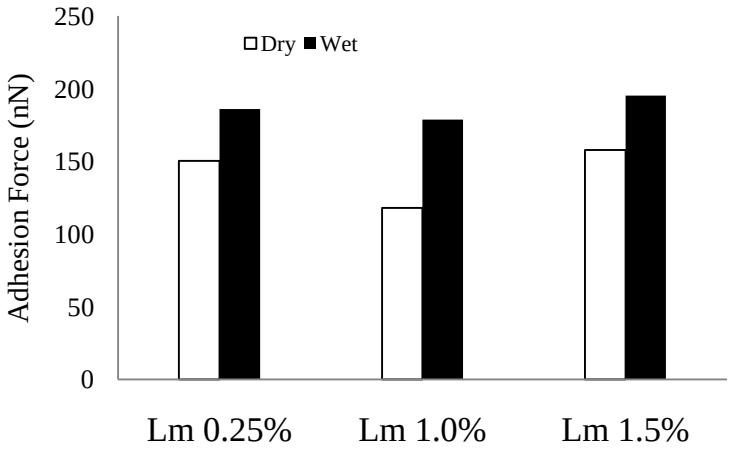

Figure 5.2 Adhesion force comparison with –OH tip on base binder

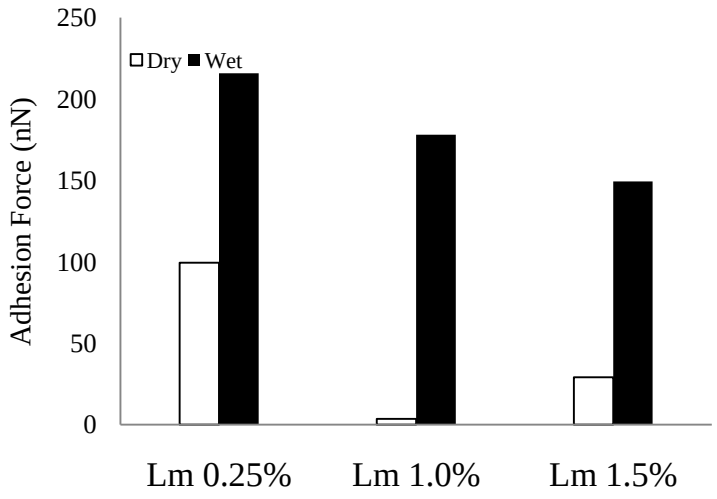

Figure 5.3 Adhesion force comparison with $-NH_3$ tip on base binder

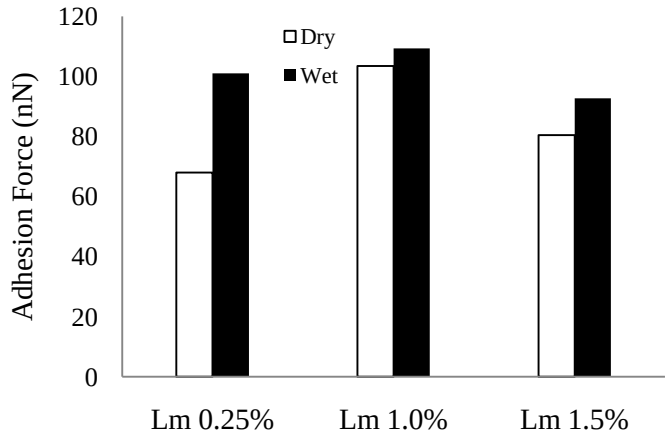

Figure 5.4 Adhesion force comparison with $-CH_3$ tip on base binder

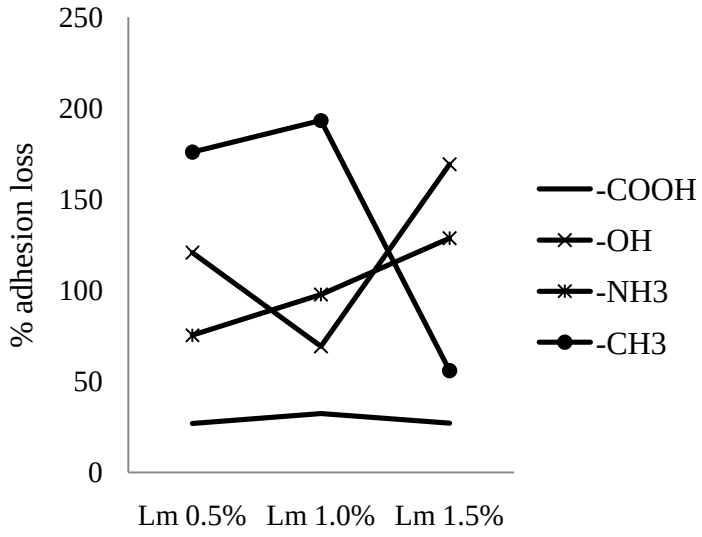

Figure 5.5 Adhesion forces loss in 0.5% Elvaloy samples

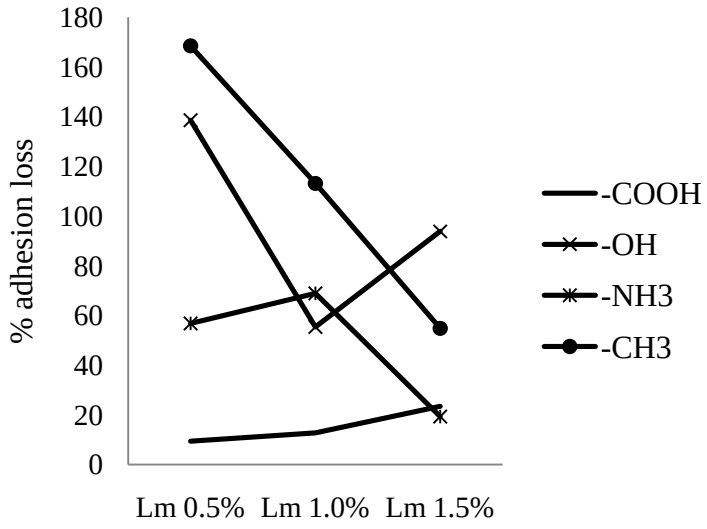

Figure 5.6 Adhesion forces loss in 0.75% Elvaloy samples

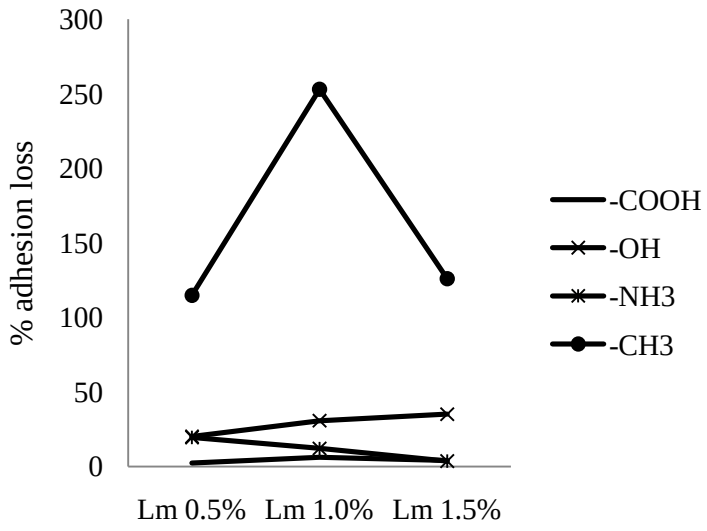

Figure 5.7 Adhesion forces loss in 1.5% Elvaloy samples

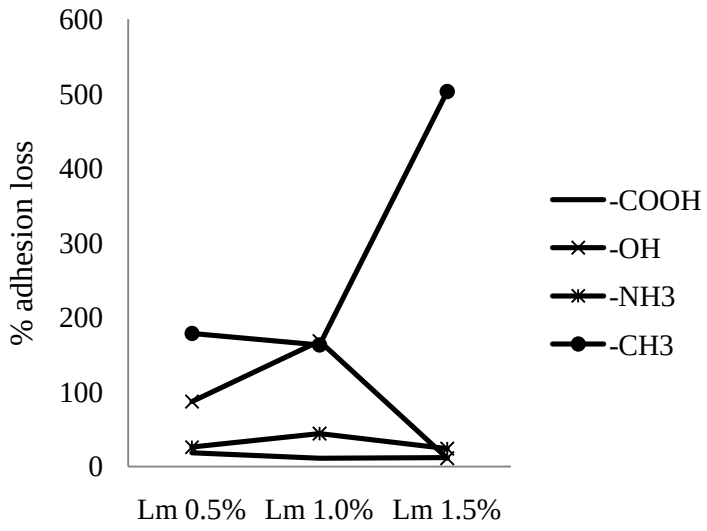

Figure 5.8 Adhesion forces loss in 2.0% Elvaloy samples

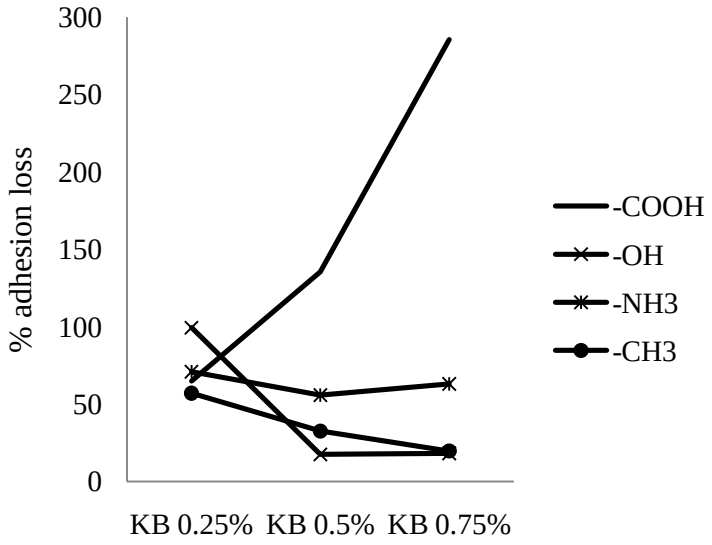

Figure 5.9 Adhesion forces loss in 0.5% Elvaloy samples

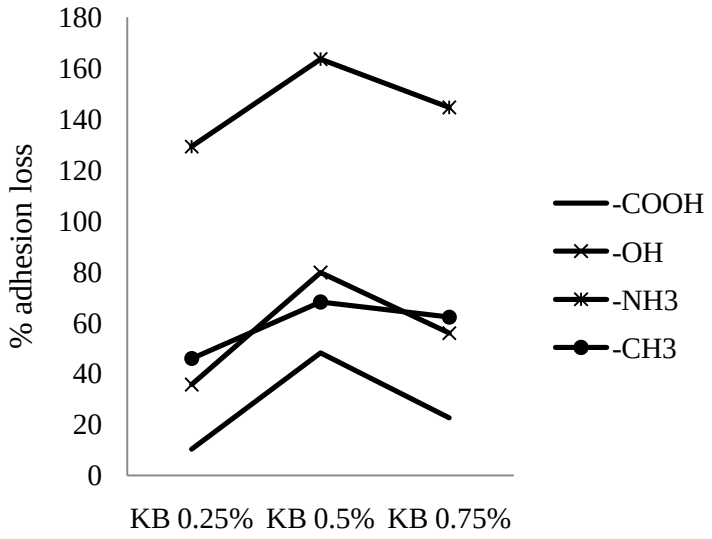

Figure 5.10 Adhesion forces loss in 0.75% Elvaloy samples

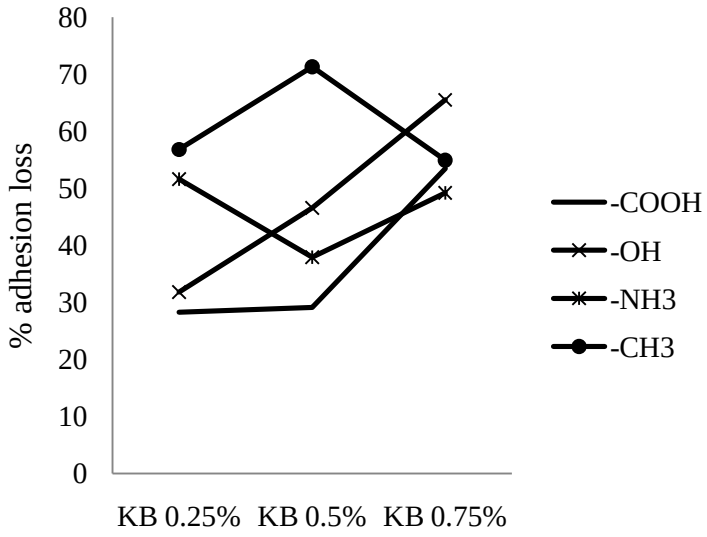

Figure 5.11 Adhesion forces loss in 1.5% Elvaloy samples

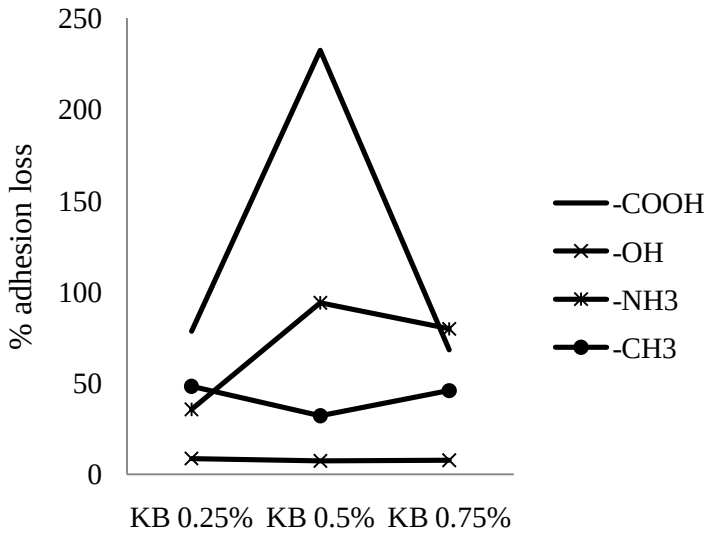

Figure 5.12 Adhesion forces loss in 2.0% Elvaloy samples

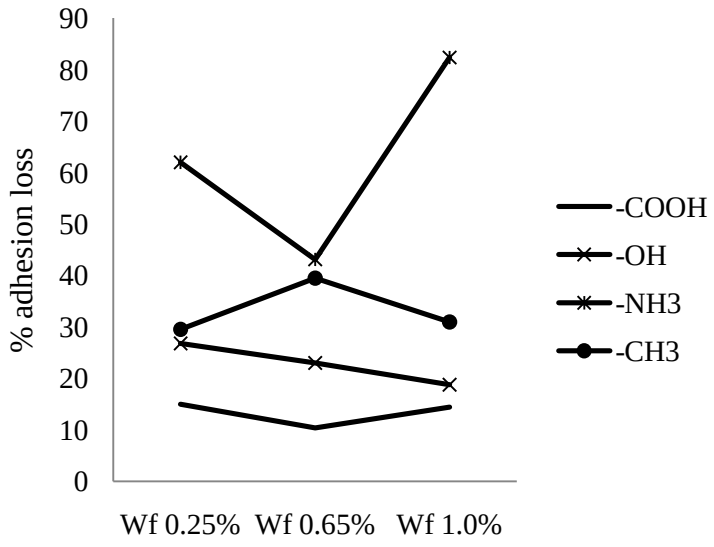

Figure 5.13 Adhesion forces loss in 0.5% Elvaloy samples

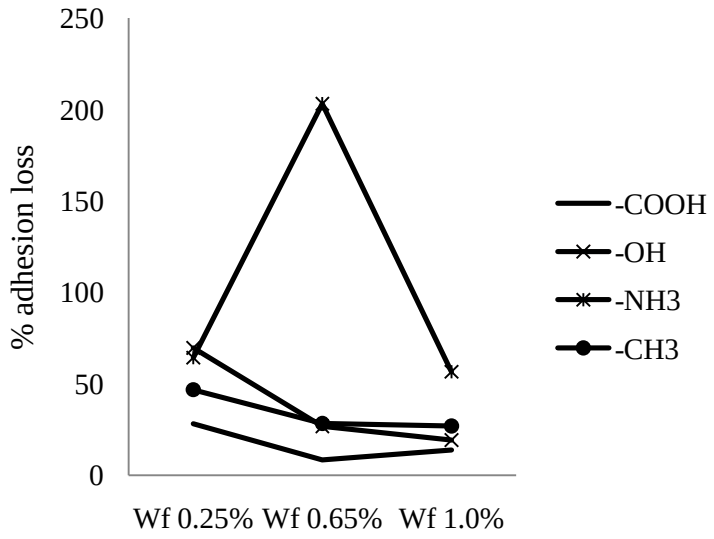

Figure 5.14 Adhesion forces loss in 0.75% Elvaloy samples

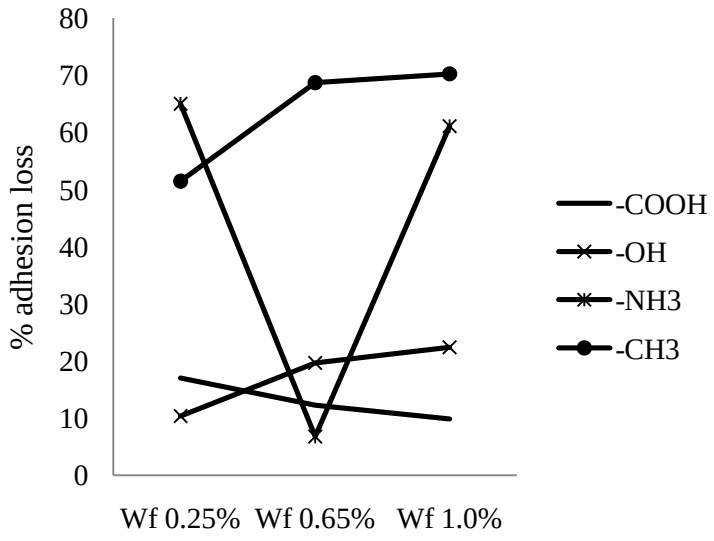

Figure 5.15 Adhesion forces loss in 1.5% Elvaloy samples

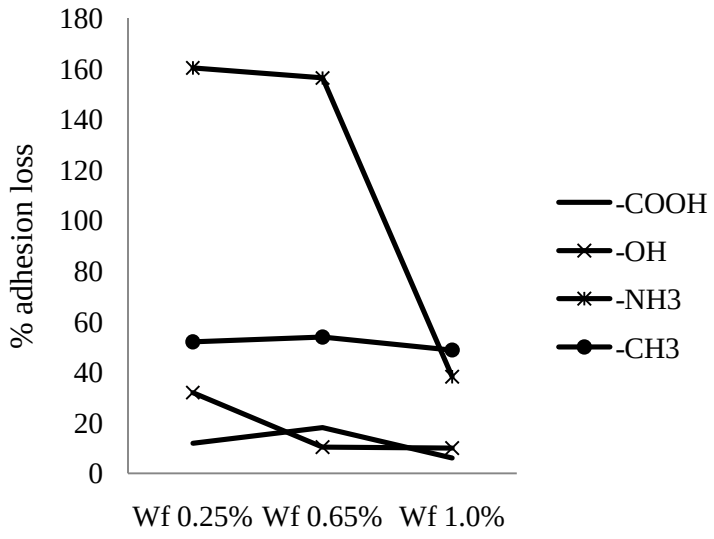

Figure 5.16 Adhesion forces loss in 2.0% Elvaloy samples

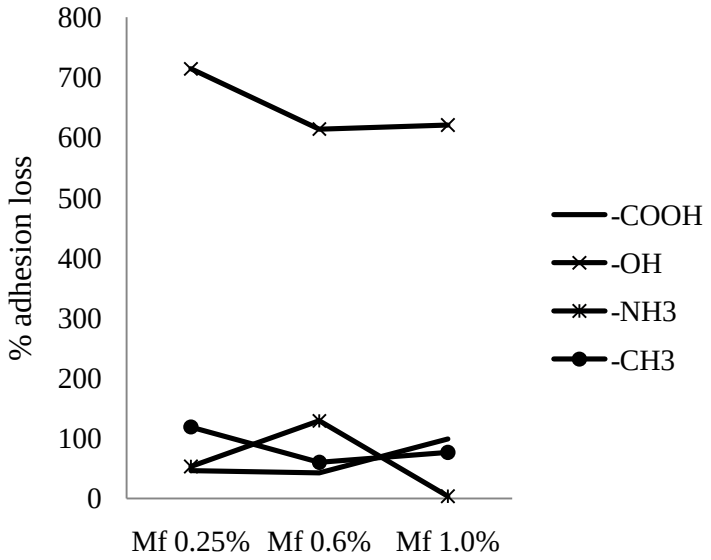

Figure 5.17 Adhesion forces loss in 0.5% Elvaloy samples

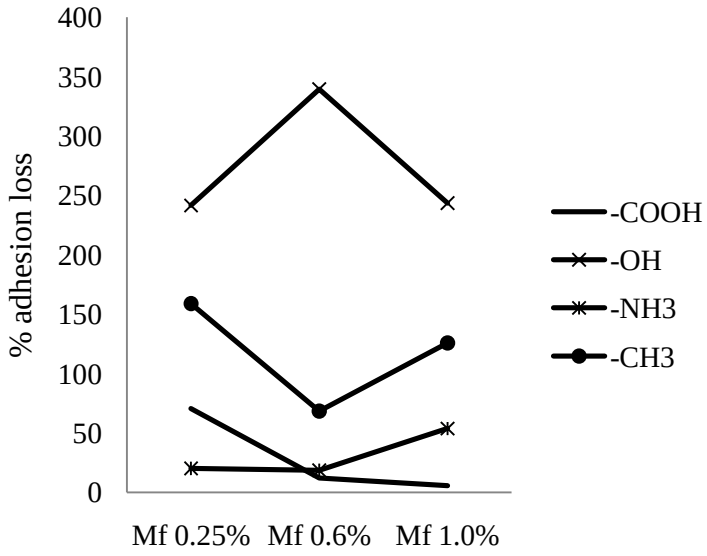

Figure 5.18 Adhesion forces loss in 0.75% Elvaloy samples

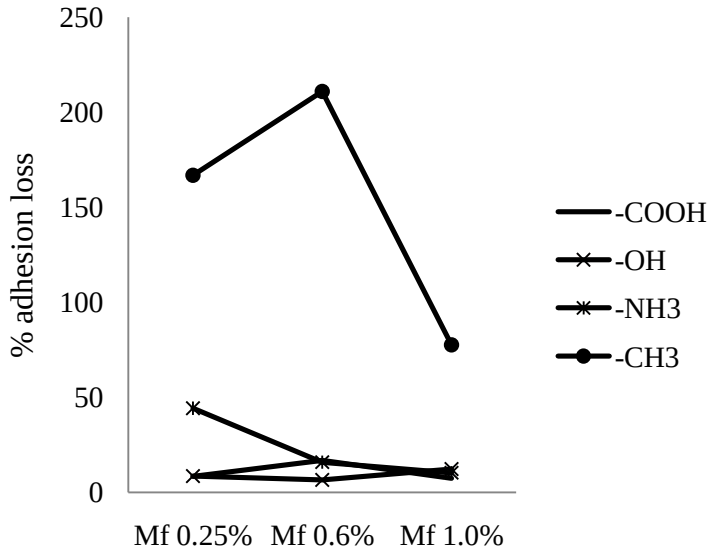

Figure 5.19 Adhesion forces loss in 1.5% Elvaloy samples

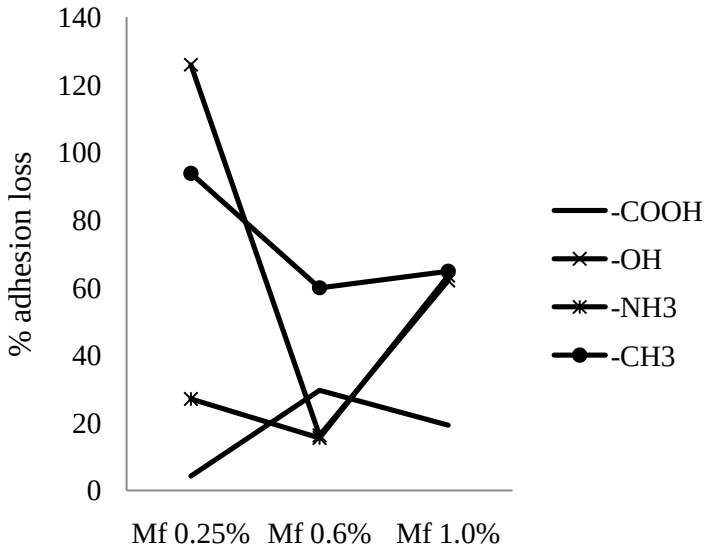

Figure 5.20 Adhesion forces loss in 2.0% Elvaloy samples

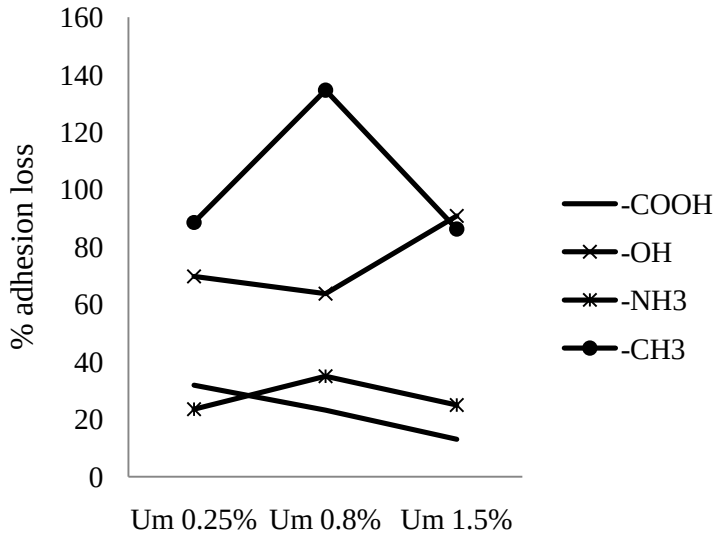

Figure 5.21 Adhesion forces loss in 0.5% Elvaloy samples

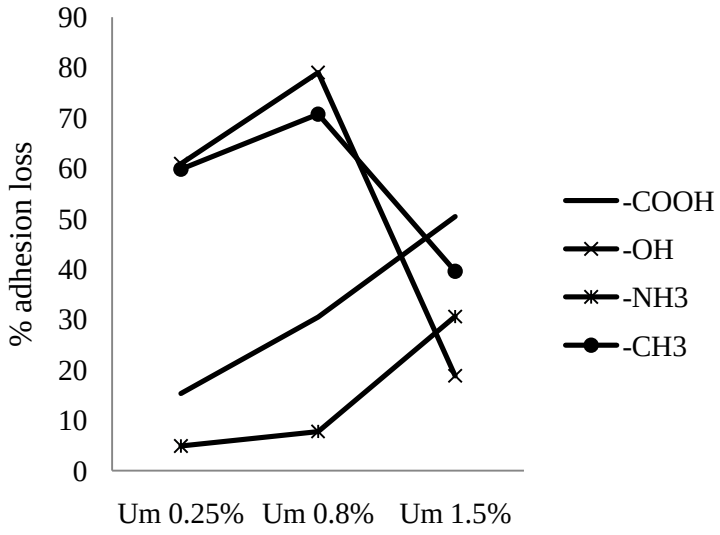

Figure 5.22 Adhesion forces loss in 0.75% Elvaloy samples

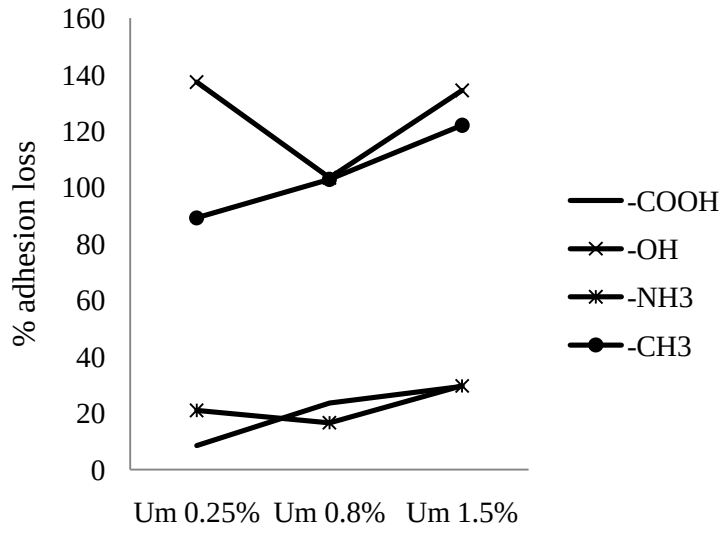

Figure 5.23 Adhesion forces loss in 1.5% Elvaloy samples

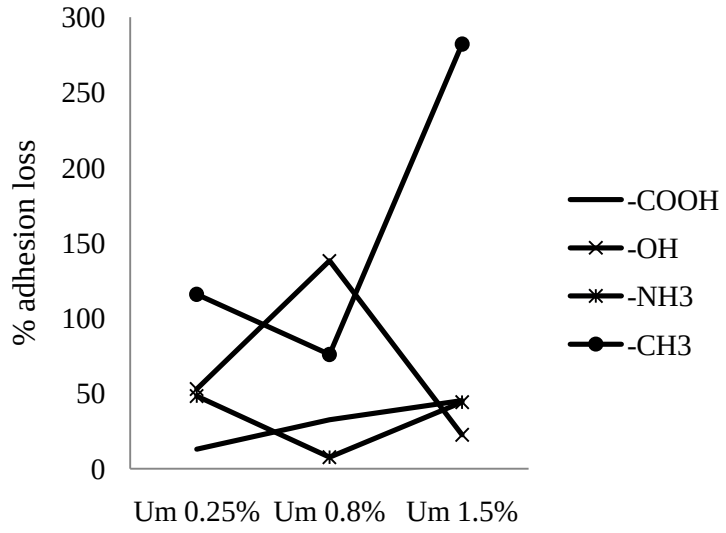

Figure 5.24 Adhesion forces loss in 2.0% Elvaloy samples

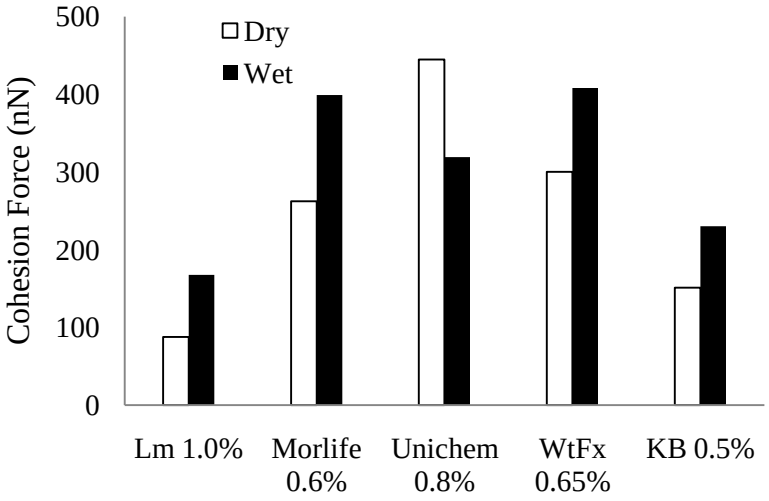

(a) COOH

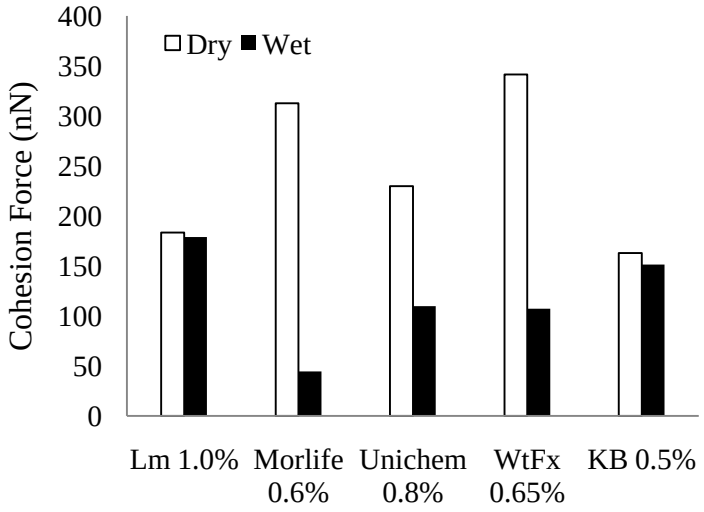

(b) -OH

Figure 5.25 Adhesion force comparison for the base binder with –COOH and –OH tips

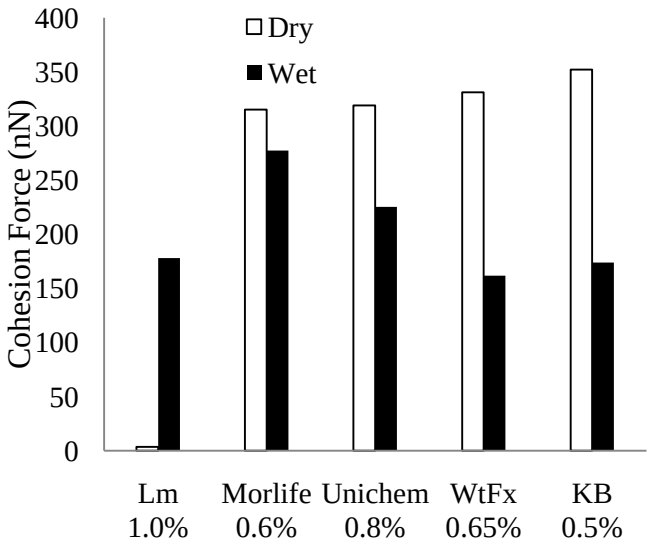

(a)–NH_3

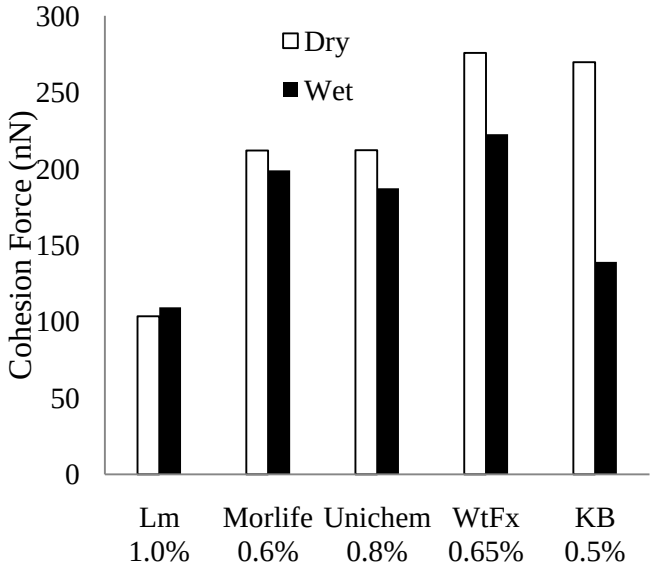

(b)–CH_3

Figure 5.26 Adhesion force comparison for the base binder with – NH_3 and – CH_3 tips

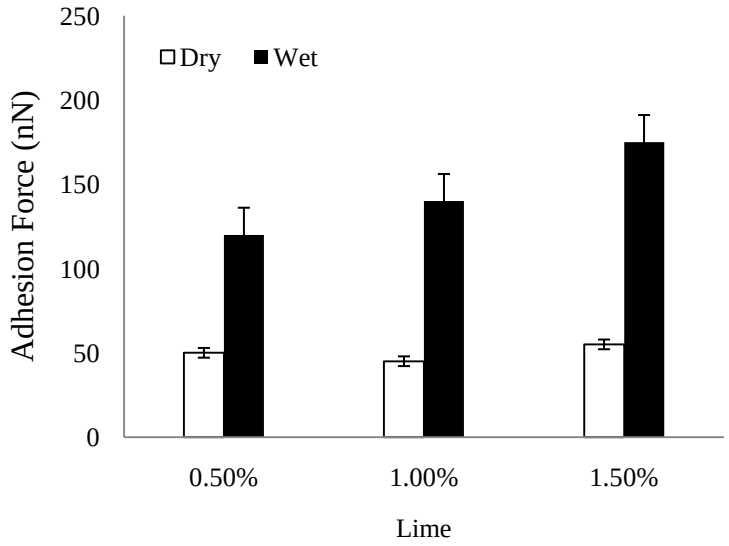

Figure 5.27 Error bar plot for lime mixed 3% SB samples

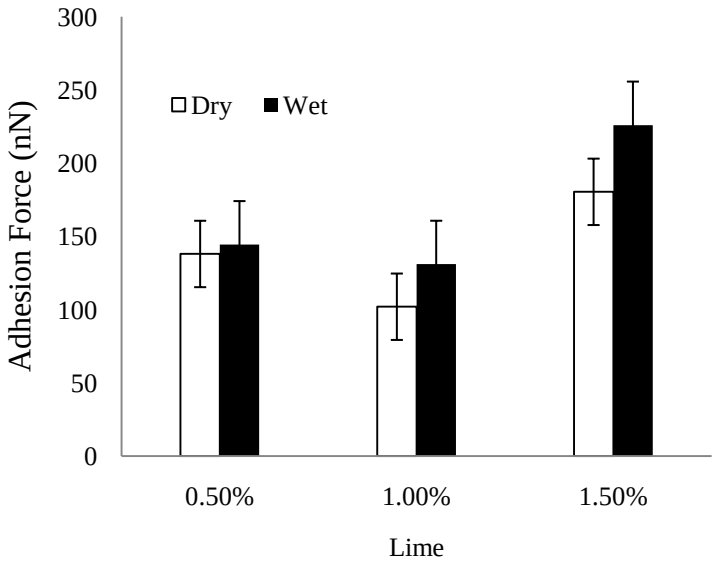

Figure 5.28 Error bar plot for lime mixed 4% SB samples

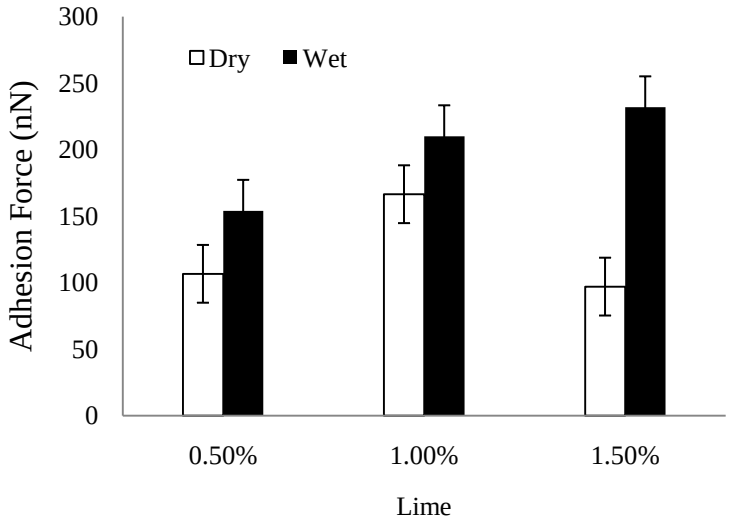

Figure 5.29 Error bar plot for lime mixed 5% SB samples

-CH_3

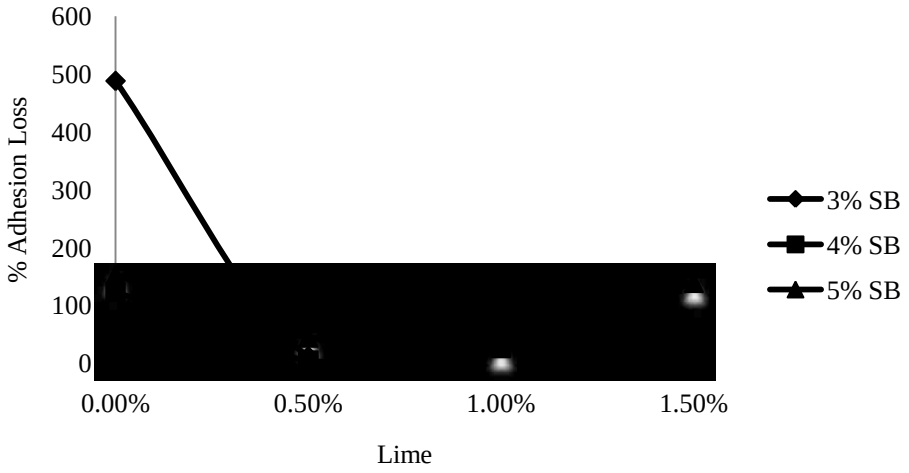

Figure 5.30 Adhesion losses comparison for the 4% SB binder modified with lime using –CH_3 tips

-CH_3

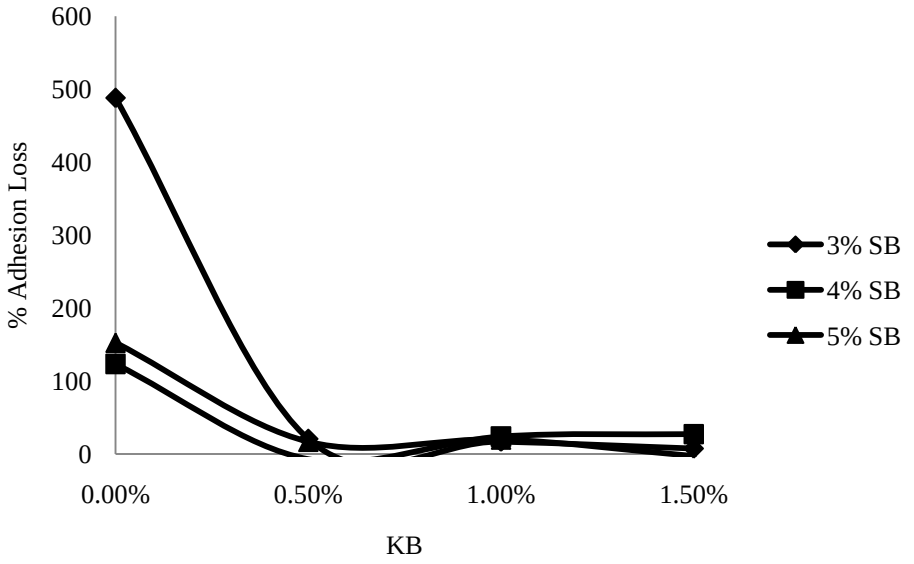

Figure 5.31 Adhesion losses comparison for the 5% SB binder modified with KB using –CH_3 tips

CHAPTER 6

Relation between AFM Results to Mechanical Testing Results

6.1 Introduction

The durability of asphalt concrete (AC) is mainly depends on the bonding between asphalt binder and aggregates. The bond may be weakened due to water action. This type of moisture damage in AC is a major problem in the US and all over the world in the arena of asphalt concrete pavement. Although other factors like traffic volume and intensity, construction method, local weather are responsible but water is the major concern and cause for the damage in AC. Kandhal (1989) and Forsyth (1987) showed that moisture held within the pavement can clearly lead to the damage in AC. According to Yoon and Tarrer (1988) the chemical and electrochemical interaction between water and the aggregate surface plays a major role in stripping than the physical characteristics of the aggregate. In this particular study asphalt concrete cylinder samples were prepared and tested under dry and wet conditions to investigate the moisture damage. Later on the test results were compared to the adhesion losses on asphalt binder from the AFM data. Hence, this chapter is a rational approach to relate the macro-scale moisture damage to the nano-scale moisture damage in AC.

6.2 Objectives

The objectives of this chapter were:

i. To determine the indirect tensile strength (IDT) of dry and wet asphalt concrete sample.

ii. To correlate indirect tensile strength of asphalt concrete with the adhesion value of corresponding asphalt binder.

6.3 Description of Test and Materials

The asphalt concrete mix was prepared from the 4% and 5% SB and SBS modified binders. Several trials were needed to keep the maximum air void within 7 ± 0.5%. The total mix design materials was something like: 0.293 kg of binder, RAP materials of 1.242 kg, #56 passing aggregate 1.552 kg, #7 passing aggregate 0.621 kg, coarse fine 1.862 kg, natural fines 0.931 kg. The asphalt concrete cylinder was made from the HMA using superpave gyratory compactor in the laboratory. The gyration number, sample height etc. were reached after several trials.

6.4 Test Matrix

A total of 24 cylinders samples were prepared from the loose mix AC using superpave gyratory compactor. The test matrix is as follows: 12 cylinders of 4% and 5% SB and SBS (3 cylinders each) X 2 conditions (dry and wet) = 24 samples.

6.5 Superpave Gyratory Compactor and Sample Preparation

The manufacturer of the superpave gyratory machine is Pine Instrument Inc., Pennsylvania. The Superpave Gyratory Compactor's (SGC) main function is to compact and prepare Hot Mix Asphalt (HMA) specimens at a constant consolidation pressure, at a constant angle of gyration, and at a fixed speed of gyration. As shown in Figure 6.1 it is featured with an integrated control system with display and an extruder function for removing compacted HMA specimens from the molds. The SGC imparts a constant vertical pressure of 600 ± 5 kPa to the sample, the sample is tilted 1.25 ± 0.02^{o} from the vertical axis and the angle of the mold is gyrated at a speed of 30 ± 0.5 rpm. All of our samples were compacted to produce the final specimen size of 150 mm in diameter and 115 mm tall. The compaction effort is controlled by the number of gyrations. This method of compaction results in a material that more closely resembles that on the road in terms of particle alignment and density (Coree and VanDerHorst 1998). Mixtures are compacted at the temperature where the viscosity of the binder is 0.28 Pa.s. The required number of gyrations is based on traffic level. Mixtures that are exposed to higher traffic levels in the field are compacted in the laboratory to a higher density. This higher density is obtained in the laboratory by increasing the number of gyrations (Kandhal et al. 1998). The numbers of gyrations for specified traffic levels are shown in Table 6.1 (Roberts et al. 1996). The term N_i is N-initial and is a measure of mixture compactibility. The N_d, or N-design is number of gyrations required to produce a density in the mix that is equivalent to the expected density in the field after the indicated amount of traffic. In the mix design process, an asphalt content is selected that will provide 4 percent air voids when the mix is compacted to N_d gyrations. Nm provides an estimate of the ultimate field

density. The N_m is the N-maximum and is the number of gyrations required to produce a density in the laboratory that should absolutely never be exceeded in the field.

6.6 Moisture Damage Determination using AASHTO T 283 Method

AASHTO T 283 has been used to determine moisture susceptible pavements through the determination of a factor called tensile strength ratio (TSR). It is a test method that can be used to determine if the materials may be subject to stripping. And this test can also measure the effectiveness of additives or antistripping agents. The test is performed by compacting specimens to an air void level of about six to eight percent. For quality assurance and field representative results, three specimens are selected as a control and tested without moisture conditioning, and three more specimens are selected to be conditioned by saturating with water undergoing a freeze cycle, and subsequently having a warm-water soaking cycle. The specimens are then tested for indirect tensile strength by loading the specimens at a constant rate and measuring the force required to break the specimen. The tensile strength of the conditioned specimens is compared to the control specimens to determine the tensile strength ratio (TSR). This test may also be performed on cores taken from the finished pavement. (AASHTO T 283). This is a standard method for determining the AC for moisture susceptibility or stripping. Separation and removal of asphalt binder from aggregate surface due primarily to the action of moisture and/or moisture vapor is generally termed as stripping (Kandhal and Richards 2001).

6.7 Summary of Test

The water bath which is capable of maintaining a temperature of 140 ± 2°F (60 ± 1°C) is shown in Figure 6.2. Vacuum container for saturating asphalt concrete cylinder specimens according to AASHTO T283 is as shown in Figure 6.3. The balance, general purpose class G2 (AASHTO M 231) was used for measurement purpose. The pans with surface area of 75-200 in^2 (48,400 – 129,000) mm^2 in the bottom and a depth of approximately 1 in. (25 mm) were used. Loading strips with a curved face to match the side of the specimen was used to test samples. Forced-draft oven, capable of maintaining a temperature from room temperature to 350 ± 15°F (176 ± 3°C) and freezer, capable of maintaining a temperature of 0 ± 5°F (-18 ± 3°C) were used to condition AC samples. In order to avoid losing any moisture plastic wrap and heavy-duty leak proof plastic bags were used.

6.8 Sample Preparation

In indirect tensile strength test (IDT), sample should be 6 in. (150 mm) diameter and 2.5 in. (63.5 mm). We prepared eight specimens at the optimum binder content for the mixture. In sample preparation, mixture is placed in the pans and spread to about 1 in. (25 mm) thick. The mix is then cooled to room temperature for 2 ± 0.5 hours. The mixture is placed in the oven for 2 hours at 275 ± 5°F (135 ± 3°C) for short term aging and stirred every 60 ± 5 minutes to maintain conditioning. Several trials were needed that to reach the air void ratio to 7 ± 0.5 percent. The specimens were compacted in accordance with AASHTO T 312. The final sample is shown in Figure 6.4. After the specimens were removed from the molds and stored at room temperature for 24 ± 3 hours. At the end of

the curing period, the dry subset was wrapped with plastic in a heavy duty and leak proof plastic bag. The specimens were then placed in a 77 ± 1°F (25 ± 0.5°C) water bath for 2 hours ± 10 minutes with a minimum of 1 in. (25 mm) of water above their surface.

6.9 Determination of Bulk Specific Gravity (Gmb)

Bulk Specific Gravity of the Compacted Asphalt Mixture (G*mb*) is defines as the ratio of the mass in air of a unit volume of a permeable material (including both permeable and impermeable voids normal to the material) at a stated temperature to the mass in air (of equal density) of an equal volume of gas-free distilled water at a stated temperature. This value is used to determine weight per unit volume of the compacted mixture. It is very important to measure G*mb* as accurately as possible. Since it is used to convert weight measurements to volumes, any small errors in G*mb* will be reflected in significant volume errors, which may go undetected. The test is according to AASHTO T 166 designation. The procedure to determine G*mb* as follows: Dry the specimen (as shown in Figure 6.4) to a constant mass so that further drying at 125 ± 5 °F (52 ±3 °C) does not alter the mass by more than 0.05 percent. Samples saturated with water shall initially be dried overnight at 125 ± 5 °F (52 + 3°C) and then weighed at two-hour drying intervals. Recently molded laboratory samples which have not been exposed to moisture do not require drying. Cool the specimen to room temperature at 77 ± 9 °F (25 ± 5 °C), and record the dry mass A. With the setup shown in Figure 6.5, immerse each specimen in water at 77 ± 3 °F (25 ± 1 °C) for 4 ± 1 minutes and record the immersed mass, C. Remove the specimen from the water, quickly damp dry the specimen by blotting with a damp towel as quickly as possible, and determine the surface-dry mass, B. (Any water

that seeps from the specimen during weighing operation is considered part of the saturated specimen). Calculate the Bulk Specific Gravity of each specimen using the following equation:

Bulk Specific Gravity (G*mb*) of Core = $G_{mb} = \frac{A}{B-C}$----------(6.1)

Where:
A = Weight of Core in Air
B = SSD Weight of Core in Air
C = Weight of Core in Water
All the results of G*mb* in our experiments were in between the value of 2.30-2.32.

6.10 Maximum Specific Gravity (G*mm*)

The ratio of the mass of a given volume of voidless (V*a* = 0) HMA at a stated temperature (usually 25°C) to a mass of an equal volume of gas-free distilled water at the same temperature. It is also called Rice Specific Gravity (after James Rice who developed the test procedure). The maximum specific gravity (G*mm*) is determined by AASHTO T 209 in which vacuuming are used to extract all the air from the mixture. This represents 100% density (no air voids) for a particular asphalt mixture. This value is used in conjunction with the bulk specific gravity to determine the density of the compacted specimens for that mixture. Determining the maximum specific gravity (G*mm*) is performed as follows: After quartering or splitting a mixture to obtain the sample weight needed for the particular mixture, spread the mix out on a table to cool (as shown in Figure 6.6), Separate the mix particles so that there are no particles larger than 1/4 inch. The procedures were as followed: Weigh the Rice bucket in air and record the weight

(A), Place the sample in the Rice bucket, Weigh the sample and the bucket together in air. (C), Add water to the sample in the bucket until the sample is completely covered with water. The temperature of the water must be 77°F (25°C). Place the top on the Rice bucket and pull the vacuum to 27.75 + 2.25 mm HG. Maintain the vacuum for 15 ± 2 minutes, shaking the bucket at 2 minute intervals or place the bucket on a slow continuous shaker. The vacuum is removing the air voids in the mix. After the 15 minutes are up, release the vacuum, remove the top and place the bucket suspended in the bath for 10 ±1 minute. (The water in this bath must also be 77°F (25°C). After 10 minutes are up, record the weight of the sample and bucket in water (D). After recording this weight, gently pour water from bucket back into water bath, dispose of sample in bucket (you no longer need the sample). Then place empty bucket back into water bath, leaving it immersed for 10 ± 1 minute. Record this weight (B) (this will be the weight in water of the empty bucket). Calculate the Maximum Specific Gravity (G*mm*) using the following equation:

Maximum Specific Gravity (Gmm) of Core = $Gmm = \frac{C-A}{(C-A)-(D-B)}$ ----------(6.2)

Where,
A = Weight of Container in air
B = Weight of Container in water
C = Weight of Container and Sample in air
D = Weight of Container and Sample in water

The Superpave Indirect Tensile Test (IDT) is used to determine the creep compliances and indirect tensile strengths of asphalt mixtures at low and intermediate pavement temperatures. These measurements can be used in performance prediction models, such as Superpave, to predict the low-temperature thermal cracking potential and intermediate-

temperature fatigue cracking potential of asphalt pavements. The setup of the IDT is shown in Figure 6.7.

The IDT formula (SI units) is:

$$St = \frac{2000P}{\pi tD} \text{----------(6.3)}$$

where:
St = tensile strength, kPa
P = maximum load, Newtons
t = specimen thickness, mm
D = specimen diameter, mm

6.11 Results of the Tests on AC

The results are shown in Table 6.2 for 4% and 5% SB modified asphalt concrete cylinders and Table 6.3 for 4% and 5% SBS modified asphalt concrete cylinders. The diameters, height, maximum applied load (N) and indirect tensile test stress (MPa) are shown in the Tables 6.2 and 6.3. The percentage of loss has been calculated as:

$$\text{Loss} = \frac{(\text{Dry IDT} - \text{Wet IDT})}{\text{Dry IDT}} X100 \text{----------(6.4)}$$

It can be seen that almost all the wet samples are damaged due to the water and conditioning action. The wet samples IDT are less than that of dry samples. The average value of loss for the 4% SB AC cylinders is 36.82%, for 5% SB is 24.81%, for 4% SBS is 24.22% and for 5% SBS is 45.37%. The test no. 1 for 5% SBS sample has little higher wet IDT value than the dry sample. This can be happened due to the material variation in AC mix, non homogeneous compaction, uneven temperature control etc (Zaniewski and Viswanathan 2006).

This test confirms the moisture damage in asphalt concrete cylinder sample by macro-level laboratory testing.

6.12 Moisture Damage Correlations between Binders and AC

Table 6.4 shows the adhesion loss with all the five AFM tips (-COOH, -OH, $-NH_3$, $-CH_3$ and $-Si_3N_4$) on 4% and 5% dry and wet SB and SBS samples. It is observed from the Table 6.4 that all the functional AFM tips adhesion losses are within reasonable ranges and are comparable to AC cylinder test results as shown in Tables 6.2 and 6.3. The results are compared and showed in graphical form in Figures.

6.12.1 On 4% SB Binder and AC

Figure 6.8 shows the comparison for adhesion losses in 4% SB modified AC cylinder and binders. It is noted that the loss in AC is very similar as to the losses measured with all functional (i, e. –COOH, -OH, $-NH_3$ and $–CH_3$) tips. Only the nonfunctionalized tip ($-Si_3N_4$) shows very high percentage of adhesion loss here.

6.12.2 On 5% SB Binder and AC

Figure 6.9 shows the comparison for adhesion losses in 5% SB modified AC cylinder and binders. There is not much variation with the AC cylinder to the functionalized tips in this case.

6.12.3 On 4% SBS Binder and AC

Figure 6.10 shows the comparison for adhesion losses in 4% SBS modified AC cylinder and binders. The loss in adhesion on AC cylinder is very close to that tested with –COOH, -OH and $–NH_3$ tip. The $–CH_3$ tip shows a little loss in adhesion on 4% SBS binder.

6.12.4 On 5% SBS Binder and AC

Figure 6.11 shows the comparison for adhesion losses in 5% SBS modified AC cylinder and binders. The adhesion loss in AC cylinder is very close to that measured with –COOH and $–NH_3$ tip here.

So it can be concluded that the moisture damage are closely related to AC cylinder and SB and SBS modified asphalt binders measured with different functional tips. The $–Si_3N_4$ tip shows very high adhesion losses as compared to other tips. This may be due to the absence of functional chemical on its surface here.

6.13 Conclusions

In this chapter mechanical laboratory testing was done to understand the damage due to moisture in AC. The asphalt base binder was modified with SB and SBS polymers of two different percentages (4% and 5%) of were used to prepare and test the asphalt concrete samples. The wet samples indirect tensile strength was found to be less than that of dry samples. The average value of loss for the 4% SB AC cylinders is 36.82%, for 5% SB is 24.81%, for 4% SBS is 24.22% and for 5% SBS is 45.37%. The test results show that the

damage due to moisture in AC is possible from the macro-scale laboratory testing. The SB and SBS modified binders are both susceptible to moisture. The 4% SB samples IDT loss is about 36.82% which is similar to adhesion loss with –COOH (loss 30.68%), -OH (loss 34.21%), -NH_3 (loss 36.06%) AFM tips. The 5% SB samples IDT loss is found to be 24.81% which is similar to adhesion loss with -OH (loss 17.59%) and -NH_3 (loss 240.14%) AFM tips. The IDT average loss of 4% SBS samples is about 24.22% which is similar to loss with –COOH (loss 36.13%) and -NH_3 (loss 17.21%) AFM tips. The 5% SBS samples IDT loss is about 45.37% which is closer to loss with –COOH (loss 20.59%) and -NH_3 (loss 14.41%) AFM tips. The overall loss found with –Si_3N_3 is higher and is not conclusive.

Table 6.1 Selection of number of gyrations for Superpave Gyratory Compactor

Design ESALs (millions)	Number of Gyrations		
	N_i	N_d	N_m
<0.3 Light traffic	7	78	121
0.3 to <3 Medium traffic	8	100	158
3 to <30 Heavy traffic	9	128	208
≥30 Extra heavy traffic	9	146	240

Table 6.2 Dry and wet SB modified AC cylinder samples results

AC Sample	Cond	Test	Dia (mm)	Ht. (mm)	Max. load (N)	IDT (MPa)	Loss %	Avg. Loss %
4% SB	Dry	1	150	74	15781.50	904.75	47.69	36.82
	Wet	1	150	73	8144.29	473.31		
	Dry	2	150	74	19148.64	1097.79	38.00	
	Wet	2	150	74	11871.71	680.61		
	Dry	3	150	75	16626.62	940.50	24.77	
	Wet	3	150	73	12174.18	707.51		
5% SB	Dry	1	150	73	14095.71	819.18	17.13	24.81
	Wet	1	150	75	12000.70	678.83		
	Dry	2	150	75	19464.45	1101.02	40.13	
	Wet	2	150	75	11653.76	659.20		
	Dry	3	150	74	15923.84	912.91	17.18	
	Wet	3	150	73	13010.40	756.10		

Table 6.3 Dry and wet SBS modified AC cylinder samples results

Sample	Cond	Test	Dia (mm)	Ht. (mm)	Max. load (N)	IDT (MPa)	Ratio	Avg. Loss %
4% SBS	Dry	1	150	74	17725.28	1016.19	17.34	24.22
	Wet	1	150	74	14651.71	839.98		
	Dry	2	150	75	14620.58	827.02	36.11	
	Wet	2	150	75	9340.80	528.37		
	Dry	3	150	74	17160.38	983.81	19.21	
	Wet	3	150	76	14238.05	794.79		
5% SBS	Dry	1	150	75	11933.98	675.05	-11.82	45.37
	Wet	1	150	73	12988.16	754.81		
	Dry	2	150	75	16746.72	947.29	44.14	
	Wet	2	150	74	9229.60	529.13		
	Dry	3	150	74	16595.49	951.42	46.61	
	Wet	3	150	75	8980.51	507.99		

Table 6.4 Adhesion loss of dry/wet SB and SBS samples

Tip	Sample	Adhesion Force (nN)		Adhesion Loss %
		Dry	Wet	(Wet-Dry)/Dry X 100
-COOH	4% SB	88.00	115.00	30.68
	5% SB	55.29	62.18	12.46
	4% SBS	113.00	153.83	36.13
	5% SBS	64.22	77.44	20.59
-OH	4% SB	76.00	102.00	34.21
	5% SB	63.78	75.00	17.59
	4% SBS	204.46	235.00	14.94
	5% SBS	38.53	137.00	255.57
$-NH_3$	4% SB	194.00	263.96	36.06
	5% SB	145.00	180.00	24.14
	4% SBS	307.09	359.94	17.21
	5% SBS	327.42	374.62	14.41
$-CH_3$	4% SB	50.16	86.38	72.20
	5% SB	42.70	89.91	110.56
	4% SBS	113.00	117.00	3.54
	5% SBS	109.25	112.00	2.52
$-Si_3N_4$	4% SB	29.71	271.62	814.24
	5% SB	67.67	148.51	119.46
	4% SBS	40.71	156.42	284.23
	5% SBS	47.82	126.81	165.18

Figure 6.1 Superpave Gyratory Compactor

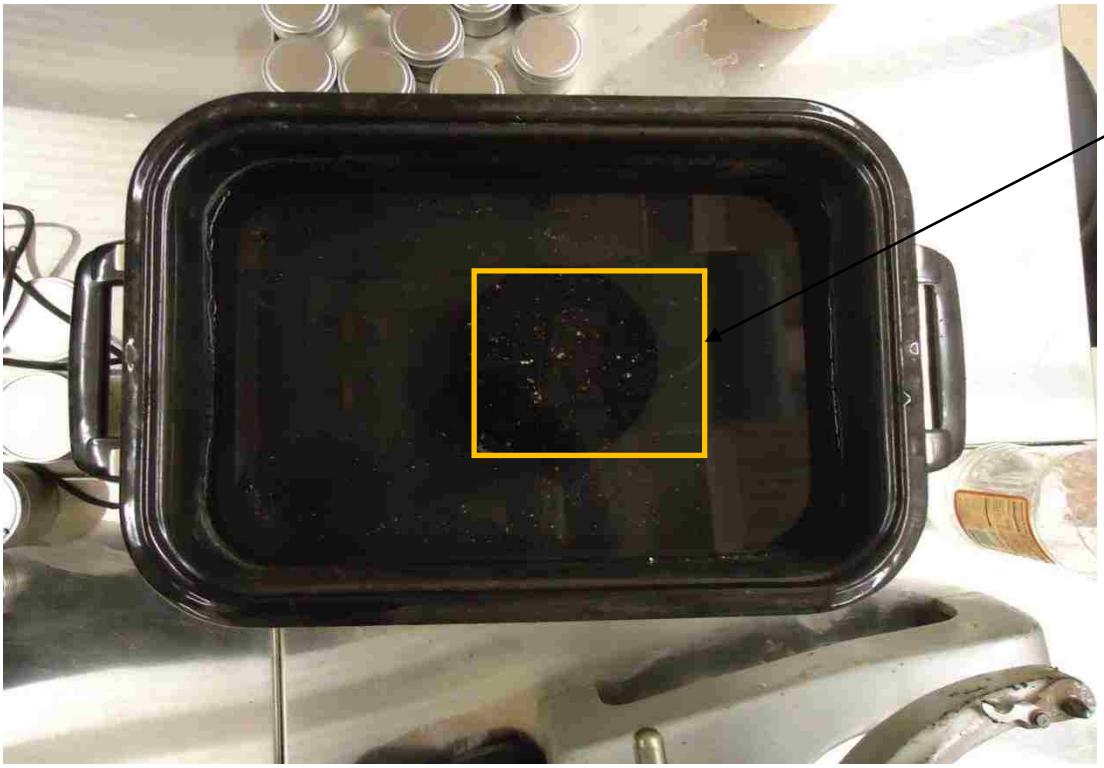

Figure 6.2 Top view of water bath

Figure 6.3 Vacuum machine setup

Figure 6.4 Gyratory compacted cylinder sample

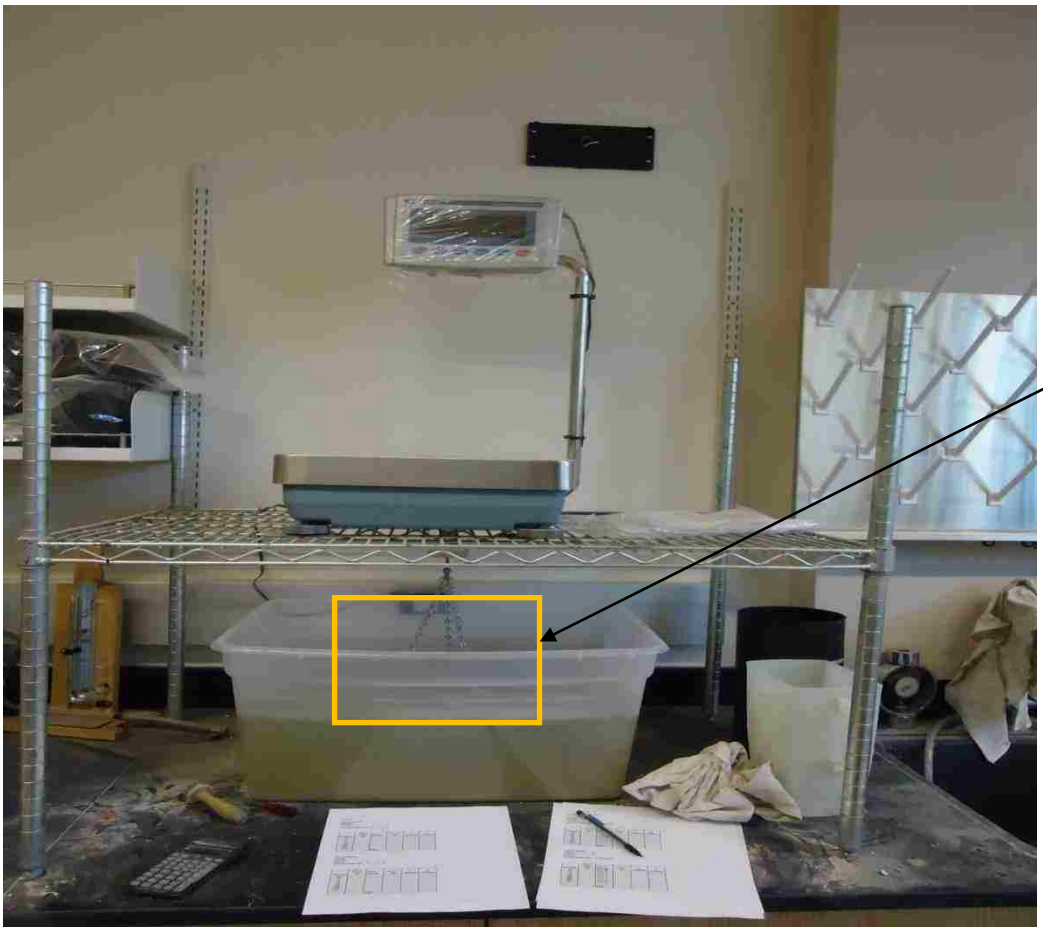

Figure 6.5 A part of laboratory setup for measuring G*mb*

Figure 6.6 Loose mix sample

Figure 6.7 IDT setup

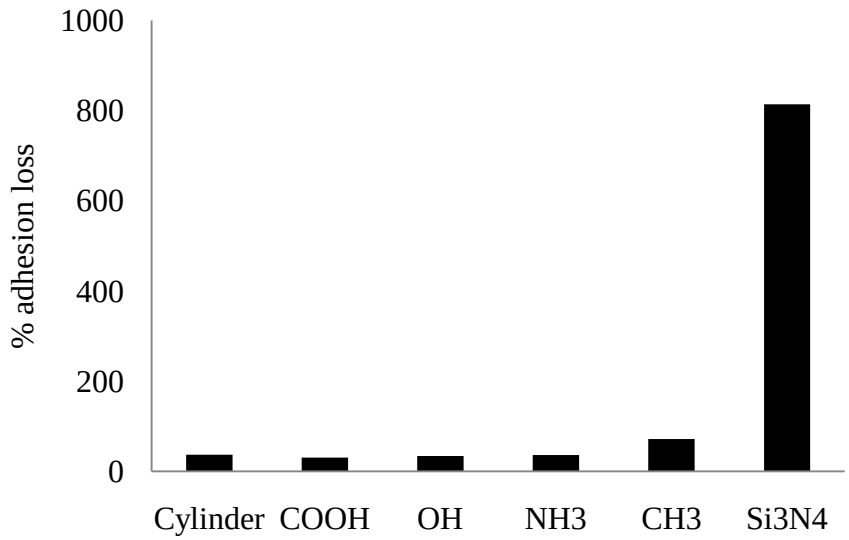

Figure 6.8 Adhesion loss comparison on 4% SB binder and AC sample

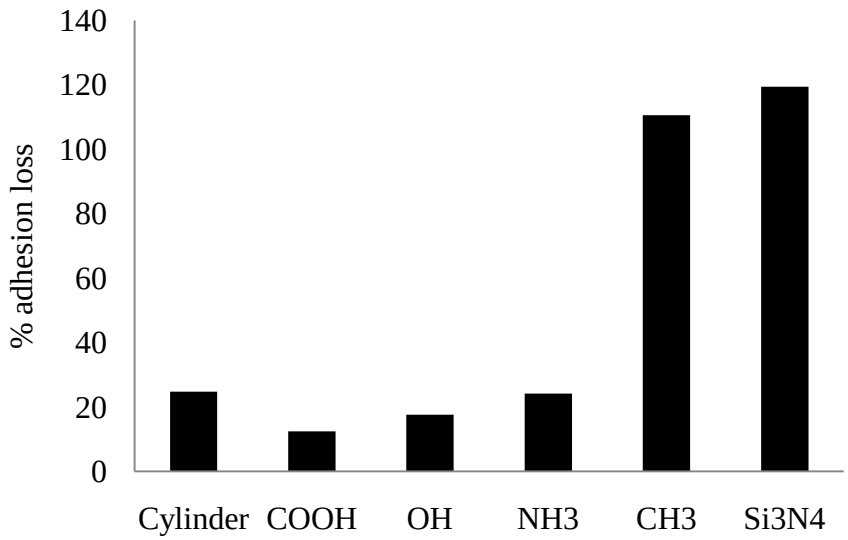

Figure 6.9 Adhesion loss comparison on 5% SB binder and AC sample

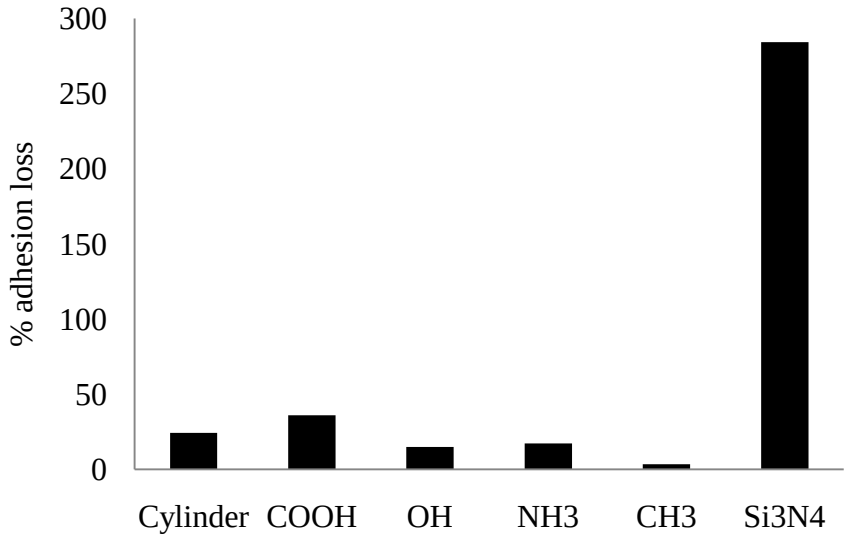

Figure 6.10 Adhesion loss comparison on 4% SBS binder and AC sample

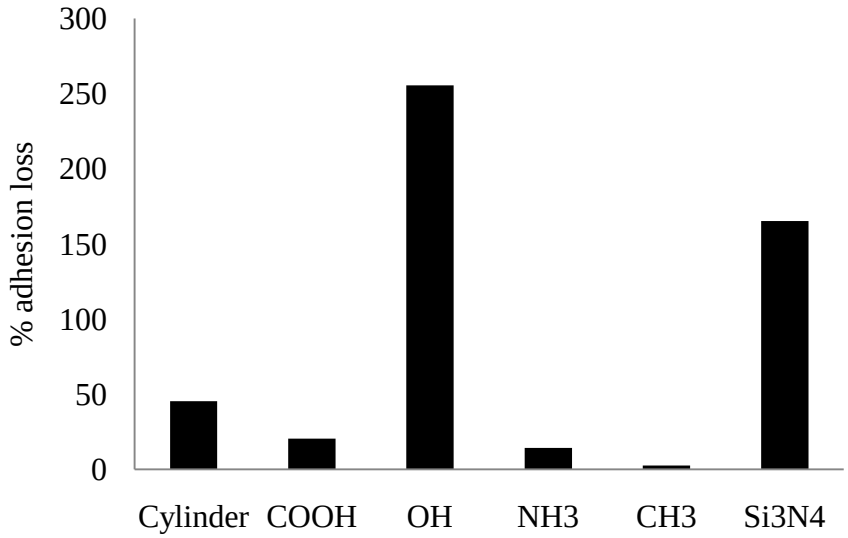

Figure 6.11 Adhesion loss comparison on 5% SBS binder and AC sample

CHAPTER 7

Conclusions and Recommendations

7.1 Summary

This thesis documents a comprehensive laboratory investigation of nano-scale moisture damage in asphalt concrete, in particular, the effect of asphalt chemistry, polymers, antistripping agents on moisture damage. Moisture damage is defined by the increase in adhesion or pull-off force measured using an AFM. Although most of study focuses on asphalt binder, attempts are made to relate the findings on asphalt binder with the macro-scale asphalt concrete strength, which is also measured in the laboratory.

Moisture damage is a poorly understood problem. The main problem with the past studies on moisture damage is that those studies involve mostly asphalt concrete strength at macro-scale. However, moisture damage occurs mainly through adhesion loss, which occurs at nano-scale.

Chapter 2 covers previous studies done to investigate the moisture damage as well as their limitations. A number of equipments and methods developed in the past to study moisture damage are described. In the past, moisture damage was not address from nano-scale point of view. Hence the nano-scale testing is recommended addressing the current problem in AC for moisture damage.

Chapter 3 covers whether asphalt chemistry is sensible to adhesion. In order to facilitate, for the first time this study has coated AFM tips with chemical functional that are present in asphalt binder. Four functional such as carboxyl (-COOH), hydroxyl (-OH), ammin (-NH_3) and methyl (-CH_3) are used to determine adhesion force or loss within an asphalt binder. In addition, a –Si_3N_4 tip is used to facilitate measurement of adhesion loss between an aggregate molecule and asphalt molecule (i, e. interface or failure weakening). AFM is not a trivial test as AFM testing has traditionally been done on hard samples in materials and polymer science. On contrary, AFM testing on asphalt is very challenging because asphalt is a sticky material. Contact mode AFM and in many cases uncareful non-contact mode AFM on asphalt is subjected to tip failure. It is the first time this study has discovered a set of laboratory AFM testing parameters and laboratory asphalt sample preparation procedure for AFM measurement of asphalt. Laboratory binder sample preparation is confirmed by the minimum surface roughness measured by AFM. Each of the functionalized tips was calibrated to find the tip spring constant, which was not supplied by manufacturers.

Starting from last one and half decades, polymer has been a part of asphalt binder. An asphalt binder without polymer modification is virtually non-existence, although there is still some use of base asphalt binder (unmodified) due to geographical locations (moderate climate). Therefore this study includes moisture damage characteristics of polymer modified binders which are described in chapter 4. Two polymers SB and SBS as well as Elvaloy are examined for their role in adhesion loss. Each polymer are mixed with 1%, 2%, 3%, 4% and 5% and Elvaloy is mixed with 0.5%, 0.75%, 1.5% and 2%

with a base binder. Thus the effect of percentages of polymer is also investigated in this thesis.

Moisture damage is a problem which is not considered during pavement thickness design, which is unlikely fatigue and pavement damage problem. Many states use 0.5% to 1% antistripping agents. The benefits of antistripping agents cannot be quantified using macro-scale AASHTO T 283 strength test. These state agencies often rely on false belief or doubt about whether antistripping agents are working or not. One of the main problems with macro-scale testing is that it is not enough to understand whether such small quantity contributes to the strength of overall mixure. Antistripping agent is only 0.5-1% of the binder, which is only 4-6% of the asphalt concrete (aggregate = 95%). Therefore a study of adhesion loss of binder which is done in chapter 5, is very appropriate to examine effectiveness of antistripping agents. Five antistyripping agents Lime, Klingbeta, Wetfix, Morlife and Unichem are examined. Each mixed ranges about 0.5% to 1.5% with base and modified binders, which were tested using five tips. As a result, the test matrix grows very high. In fact, 1600 tests results are reported only in this chapter.

It would have been interesting to know whether the finding on binder study reflects in asphalt concrete. Chapter 6 describes the mechanical laboratory testing in order to show the moisture damage in AC from macro-scale point of view. The test results show good agreements with the nano-scale strength values. A co-relation is also described between the adhesion losses for nano to macro scale testing.

7.2 Conclusions

Chemical functional groups of asphalt influence the intermolecular adhesion force in wet and dry asphalt binders. Therefore the technique of AFM can be considered as nano-scale tool measure moisture damage in AC. Based on the finding of this study, the following conclusions are made:

1. The technique of AFM can be considered as nano-scale tool measure moisture damage in AC.
2. Image analysis through AFM indicates that the wet sample exhibits rougher surface than the dry samples which shows the damage due to moisture. That means wet sample has some damages.
3. Appropriate scanning rate is important for capturing a good quality image and the scan rate between 1 and 3 Hz is found to produce high quality AFM images. The gain value is found to be 0.1 for all the successful tests which controls the error signal to generate a feedback output.
4. The AFM test data are repeatable. The smaller pull-off force (adhesion) is related to strength of the material. The higher strength materials produce smaller adhesion force and vice versa. All base, SB, SBS and Elvaloy modified binders are vulnerable to moisture. Base binder is the weakest among all the binders. The SB polymer modification of asphalt is good achieving higher adhesion force (resembles to asphalt-aggregate interaction), whereas the SBS polymer modification is good for achieving higher adhesion force (resembles to asphalt-asphalt interaction).

5. Polymers modification of asphalt binders are unable to resist moisture from nano-scale point of view. This damage rate is not unique when we use different asphalt functional AFM tips like hydrophobic and hydrophilic tips.

6. Based on the ratio of wet to dry adhesion forces, it is shown that overall the SB polymer modified binders are less susceptible to moisture damage compared to the SBS polymer modified asphalt binders.

7. Using Si_3N_4 tips, the adhesion force in wet SB modified asphalt samples is found to be larger than that in the wet SBS modified asphalt samples. In contrast, using –OH tips, the adhesion force in wet SBS modified asphalt samples is found to be larger than that in the wet SBS modified asphalt samples. Using of –COOH (hydrophilic) and $–CH_3$ (hydrophobic) tips, no significant difference is found between the wet SB and SBS polymer modified asphalt samples.

8. For both SB and SB polymer modifications, approximately 3% polymer is shown to be optimum to maximize the adhesion forces in wet asphalts, and thereby reducing the moisture-induced damage in the SB and SBS modified asphalt binder system.

9. Lime is the better antistripping agent to be effective to fight against moisture as compared to other agents. The performance of Klingbeta, Wetfix, Morlife and Unichem are not good and inconsistent.

10. The damage in AC from macro-scale testing can be correlated with the –COOH, –OH, $-NH_3$ and $-CH_3$ tips.

7.3 Recommendations for future study

1. To use sulfate (-SO) functionalized tip is recommended. That will explore a broader area to investigate moisture damage in AC. However, this was not included in this study. Because, the tip modification company Novascan was unable to do (-SO) functionalization. It is possible that in future a company from Europe or Asia can do such functionalization. A researcher may develop his own functionalization scheme, instead of customization by a company.
2. AFM testing on asphalt concrete (solid) sample has not been done in this study. Because cutting an AC sample with geological saw shows very rough surface, which was not suitable for AFM testing. Of course, a saw cut surface can be smoothed/polished using fine grade sand papers or mechanical polishing device.
3. This study focuses only on laboratory testing and used raw adhesion loss to understand asphalt factors for moisture damage. Lifshitz van der Waals and/or acid-base components of the microscopic work of adhesion can be quantified in future. Simply, Johnson-Kandall-Roberts (JKR) and Derjaguin-Muller-Toporov (DMT) models can be used to calculate surface force or energy representative of whole asphalt samples. Construction of Neural Network Classifier could be helpful for such quantification.
4. Full factorial analysis should be done to decide the best antistripping agent.

REFERENCES

AASHTO T 283. "Resistance of Compacted Bituminous Mixture to Moisture Induced Damage for Superpave." *American Association of State Highway and Transportation Officials* (AASHTO), Washington D. C., (2000).

AASHTO T 312. "Standard Method of Test for Preparing and Determining the Density of Hot Mix Asphalt (HMA) Specimens by Means of the Superpave Gyratory Compactor." *American Association of State Highway and Transportation Officials* (AASHTO), Washington D. C.

AASHTO T 166. "Bulk Specific Gravity of Compacted Bituminous Mixtures using Saturated Surface – Dry Specimens." *American Association of State Highway and Transportation Officials (AASHTO),* Washington D. C., (2000).

Abraham, T., Christendat, D., Karan, K., Xu, Z., and Masliyah, J. (2002). "Asphaltene-Silica Interactions in Aqueous Solutions: Direct Force Measurements Combined with Electrokinetic Studies." *Industrial and Engineering Chemistry Research,* 41 (9), pp 2170-2177.

Adhikari, R., Godehardt, R., Lebek, W., Weidisch, R., Michler, G.H., and Knoll, K. (2001). "Correlation between Morphology and Mechanical Properties of Different Styrene/Butadiene Triblock copolymers: A Scanning Force Microscopy Study." J. *Macromol. Sci.* B 40(5), pp 833-847.

Airey, G.D. (2004). "Styrene Butadiene Styrene Polymer Medication of Road Bitumens." *J Mater Sci.,* 99, pp 951–99.

ASTM-Road and Paving Material; Vehicle-Pavement Systems. *Annual Book of ASTM Standards*, V 4.03, 1998.

Becker, Y, Me´ndez, M.P., and Rodrı´guez Y. (2001). "Polymer modified asphalt." *Vision Technolgica*, 9(1), 39–50.

Berger and Huege (2005), <www.international**lime**.org/doc/BERGER%20Eric.doc)> (September, 2010)

Biggs, S. and Mulvaney, P. (1994). "Measurement of the Forces Between Gold Surfaces in Water by Atomic Force Microscopy." *J. Chem. Phys*., 100(11), 501-505.

Biggs, S. and Mulvaney, P. (1994). "Measurement of the Forces Between Gold Surfaces in Water by Atomic Force Microscopy." *J. Chem. Phys.*, 100(11), 501-505.

Burnham, N. A., and Kulik, A. J., (1997). "Surface Force and Adhesion." in Handbook of Mico/Nanotribiology, Edited by Bhushan, B., *CRC Press*, Boca Raton, FL.

Chen, J.S., Liao, M.C., and Shiah, M.S. (2002). "Asphalt Modified by Styrene–Butadiene–Styrene Triblock Copolymer: Morphology and Model." *J Mater Civil Eng*, 14 (3), 224–9.

Cheng, D., Little, D., Lytton, R., and Holste, J. (2002). "Use of Surface Free Energy Properties of the Asphalt- Aggregate System to Predict Moisture Damage Potential". *Journal of the Association of Asphalt Paving Technologists*, Vol.71, pp. 59-88.

Cohen, J., Cohen P., West, S.G., & Aiken, L.S. (2002). *"Applied multiple regression/correlation analysis for the behavioral sciences."* (3rd ed.) Psychology Press.

Coree, B. J., and VanDerHorst, K. (1998). Superpave Compaction, Transportation Conference Proceedings. Center for Transportation Research and Education, Ames, Iowa, 1998.

Curtis,C.W., Ensley, K., and Epps, J. (1993). "Fundamental Properties of Asphalt – Aggregate Interactions Including Adhesion and Absorption." *Transportation Research Board,* Final Report SHRP A-003B.

Desrosières, Alain (2004). "The Politics of Large Numbers: A History of Statistical Reasoning." *Trans. Camille Naish*. Harvard University Press.

Drelich, J. (2006). "Adhesion Forces Measured Between Particles and Substrate with Nano-Roughness." Minerals & Metallurgical Processing, Vol. 23, No. 4, pp. 226-232.

Ecopath website, <http://www.ecopathindustries.com/index.php?option=com_content&view=article&id=87&Itemid=94> (September, 2010)

Forsyth, R. A., Wells, G., and Woodstrom, J. (1987) "Economic Impact of Pavement Subsurface Drainage" Transportation Research Record No. 1121, Transportation Research Board, 77-85.

Fromm, J.H. "The Mechanisms of Asphalt Stripping From Aggregate Surfaces." *Proceedings of the Association of Asphalt Paving Technologists,* Vol. 43, 1974.

Gorkem, C. and Sengoz, B. (2009). "Predicting stripping and moisture induced damage of asphalt concrete prepared with polymer modified bitumen and hydrated lime." Construction and Building Materials, 23, 2227–2236.

Hicks, R. (1991). "Moisture damage in asphalt concrete." NCHRP synthesis of highway practice 175, Washington (DC): Transportation Research Board, National Research Council.

Hicks, R.G., Leahy, R.B., Cook, M., Moulthrop, J.S, and Button, J. (2004). "Road Map for Mitigating National Moisture Sensitivity Concern in Hot Mix Pavements."

Horacos, I., Fernandez, R., Gomez-Rodriguez, J., Colchero, J., Gomez-Herrero, J. and Baro, A. (2007). "WSXM: A Software for Scanning Probe Microscopy and a Tool for Nanotechnology." *Review of Sci. Instruments*, Vol. 78, Issue 1, pp. 013705-013708.

Huang, S.C., Turner, T.F., Pauli, A.T., Miknis, F.P., Branthaver, J.F., and Robertson, R.E. (2005). "Evaluation of Different Techniques for Adhesive Properties of Asphalt-Filler Systems at Interfacial Region." *Journal of ASTM International*, vol. 2, no. 5, pp. 1-15.

Huang, B., Shu, X., Dong, Q., and and Shen, J. (2010) "Laboratory Evaluation of Moisture Susceptibility of Hot-Mix Asphalt Containing Cementitious Fillers." Journal of Materials in Civil Engineering, *ASCE*, 667.

Hunter, E.R. (2001). "Evaluating moisture susceptibility of asphalt mixes." MPC report. University of Wyoming, WY, 2001.

Isacsson., U., and Lu, X. (1995). "Testing and appraisal of polymer modified road bitumen." *Material structure*, Volume 28, pp. 139–159.

Isacsson, U., and Lu, X. (1999). "Characterization of Bitumens Modified with SEBS, EVA and EBA Polymers." *J Mater Sci*, 34, pp 3737–45.

Jo, M.C., Tarrer, A.R., Jeon, Y.W., Park, S.J. and Yoon, H.H. (1997). "Investigation of The Effect of Aggregate Pretreatment With Anti-Stripping Agents on the Asphalt-Aggregate Bond*." Petroleum Science and Technology*, 15(3)(4), 245-271.

Kanitpong, K. and Bahia, H. (2005). "Relating Adhesion and Cohesion of Asphalt to Effect of Moisture on Asphalt Mixtures' Laboratory Performance." *The 84th Annual Meeting of Transportation Research Board*, CD-ROM paper, Washington, D.C.

Kandhal, P.S. (1992). "Moisture Susceptibility of HMA Mixes: Identification of Problem and Recommended Solutions." *National Center for Asphalt Technology*, NCAT Report 92-1.

Kandhal, P.S., Lubold, C.W., and Roberts, F.L. (1989). "Water Damage to Asphalt Overlays: Case Histories", *Proceedings*, Association of Asphalt Paving Technologists, Volume 58, pp 40-76.

Kandhal P. and Rickards, I. (2001) "Premature Failure of Asphalt Overlays from Stripping: Case Histories." NCAT Report 01-01, Paper presented at the annual

meeting of the Association of Asphalt Paving Technologists held in Clear Water, Florida (March 19-21, 2001).

Kandhal P. S. (1998). "Intersection rutting Rectified, Roads and Bridges." *Des Plaines*, IL, May 1998.

Kennedy, T.W, and Anagnos, N.J. (1983). "Lime Treatment of Asphalt Mixtures." *Center for Transportation Research*, The University of Texas at Austin, pp 20–8.

Kim, M.G., Button, J.W., and Park D.W. (1999). "Coatings to improve low-quality local aggregates for hot mix asphalt pavements." Report SWUTC/ 99/167405-1, Texas Transportation Institute, Texas A&M University, College Station, TX.

Kim, S., and Coree, B. (2005). "Evaluation of Hot Mix Asphalt Moisture Sensitivity Using the Nottingham Asphalt Test Equipment." *Center for Transportation Research and Education (CTRE)*, CTRE Project 02-117.

King, G. (1999). "Additives in asphalt." *J Assoc Asphalt Paving Technol A*, 68, 32–69.

Kiridena, W., Jain, V., Kuo, P., and Liu, G.Y. (1998). "Nanometer Scale Elasticity Measurements on Organic Monolayers Using Scanning Force Microscopy." *Surface Interface Anal*., Vol. 25, pp. 383-389.

Knoell, T., Safarik, J., Cormack, T., Riley, R., Lin, S. W., and Ridgway, H. (1999). "Biofouling Potentials of Microporous Polysulfone Membranes Containing A Sulfonated Polyether-Ethersulfone: Correlation of Membrane Surface Properties with Bacterial Attachment." *J. Memb. Sci*., 157, 17-138.

Little, D.N. and Jones, D.R. (2003). "Chemical and Mechanical Mechanisms of Moisture Damage in Hot Mix Asphalt Pavements." *National Seminar in Moisture Sensitivity*, San Diego, California.

Loeber, L., Sutton, O., Morel, J., Valleton, J.M. & Muller, G. (1996). "New direct observations of asphalts and asphalts binders by scanning electron microscopy and atomic force microscopy." *J. Microsc.* 182(1), 32–39.

Lottman, R.P. "Predicting Moisture-Induced Damage to Asphalt Concrete." *Transportation Research Board*, NCHRP Report 192.

Lottman, R.P. (1982). "Predicting Moisture-Induced Damage to Asphalt Concrete – Field Evaluation." *Transportation Research Board*, NCHRP Report 246.

Long, J., Zhang, L., Xu, Z. and Masliyah, J. (2006). "Colloidal Interaction between Langmuir-Blodgett Bitumen Films and Fine Solid Particles." *Langmuir*, Vol 22, No 21, pp. 8831-8839.

Liu, J., Zhang, L., Xu, Z., Masliyah, J. (2006). "Colloidal Interactions between Asphaltene Surfaces in Aqueous Solutions." *Langmuir*, Vol 22, No. 4, 1485-1492.

Mahabir P., and Mazumdar, M. (1999). "Engineering properties of EVA modified bitumen binder for paving mixes." *J Mater Civil Eng*, 11(2), 131–137.

Majidzahed, K., and Brovold, F.N. (1968). "Effect of Water on Bitumen–aggregate Mixtures." *Highway research board special report*, 98, 1968.

Masson, J-F., Leblond, V. and Margeson, J. (2006). "Bitumen morphologies by phase-detection atomic force microscopy." *J. Microsc.* 221, 17–29.

Masad, E., Castelblanco, A, and Birgisson, B. (2006). "Effects of Air Void Size Distribution, Pore Pressure, and Bond Energy on Moisture Damage." *ASTM Journal of Testing and Evaluation*, Vol 34, Issue 1, pp. 9-16.

Moraes, M.B., Pereira, R.B., Simao, R.A. and Leite, L.F.M. (2009). "High Temperature AFM Study of CAP 30/45 Pen Grade Bitumen." *Journal of Microscopy*, 239(1), 46 – 53.

Ohler, B. (2007). "Cantilever spring constant calibration using laser Doppler vibrometry." *Rev. Sci. Instrum*. Vol. 78, No. 06370, pp 1-5.

Park, S., Jo, M.C., and Park, J.B. (2000). "Adsorption and Thermal Desorption Behavior of Asphalt-Like Functionalities on Silica." *Adsorption Science & Technology*, 18, 675-684.

Pauli, A. T., Grimes, W., Huang, S. C., and Robertson, R. E. (2003). "Surface Energy Studies of SHRP Asphalts by AFM." *Petroleum Chemistry Division Preprints*, 48(1), 14-18.

Pauli, A.T., Branthaver, J.F., Robertson, R.E. and Grimes, W. (2001). "Atomic Force microscopy investigation of SHRP asphalts." Symposium on Heavy Oil and Resid. Compatibility and Stability, 110–114. Petroleum Chemistry Division American Chemical Society, San Diego, CA.

Petersen, C. J., Plancher, H., and Harnsbergen M. (1987). "Lime Treatment of Asphalt to Reduce Age Hardening and Improve Flow Properties. In: Proceedings, AAPT, vol. 56.

Petersen, C. J. and Plancher, H., (1998). "Model Studies and Interpretive Review and The Competitive Adsorption and Water Displacement of Petroleum Asphalt Chemical Functionalities on Mineral Aggregate Surfaces." *Petroleum Sci. & Technology*, 16, 89-131.

Putman, B., and Amirkhanian, S. (2006). "Laboratory Evaluation of Anti-Strip Additivesin Hot Mix Asphalt." *Report No. FHWA-SC-06-07*, South Carolina Department of Transportation, November 10, 2006.

Ren, S., Zhao, H., Long, J., and Masliyah, J. (2009). "Understanding Weathering of Oil Sands Ores by Atomic Force Microscopy." *AIChE Journal*, Volume 55, Issue 12, 3277-3285.

Robertson, R. E. (2000). "Chemical Properties of Asphalts and Their Effects on Pavement Performance." *Transportation Research Circular Number 499*, Transportation Research Board, National Research Council.

Roberts, F. L., Kandhal, P. S., Brown, E. R., Lee, D. and Kennedy, T. W. (1996). "Hot Mix Asphalt Materials, Mixture Design and Construction." *NAPA Education Foundation*, Lanham, MD.

Roque, R., Birgisson, B., Tia, M., Kim, B., and Cui, Z. (2004). "Guidelines for the use of modifiers in Superpave mixtures: Executive summary." *Evaluation of SBS modifier. State Job 99052793.* Florida Department of Transportation, Tallahassee, FL, 2004.

Sadd, M. H., Dai, Q., Parameswaran, V., and Shukla, A. (2003). "Simulation of Asphalt Materials Using a Finite Element Micromechanical Model with Damage Mechanics." *Transportation Research Board*, 1832, pp. 86-95.

Sebaaly, P., Hitti,H. and Weitzel, D. (2002). "Effectiveness of Lime in Hot Mix Asphalt Pavements." 82nd Annual Meeting of the Transportation Research Board, November 12, 2002.

Sengoz, B., and Isikyakar, G. (2008). "Evaluation of the Properties and Microstructure of SBS and EVA Polymer Modified Bitumen." *Construction and Building Materials*, 22, pp 1897–1905.

Shukla, R. S., Singh, V. K. P., and Bhanwala, R. S. (2003). "Polymer modified bitumen for construction of heavy traffic density corridors." *Indian Highways*, 31(4), 55–66.

Solaimanian, M., Kennedy, T. W., and Elmore, W. E. (1993). "Long-term Evaluation of Stripping and Moisture Damage in Asphalt Pavements Treated With Lime and Anti-Stripping Agents." *Final Report, CTR 0-1286-1F,* Texas Department of Transportation.

Stuart, K.D. (1990). "Moisture Damage in Asphalt Mixtures: a State of Art Report." *Research Development and Technology*, Turner-Fairbank Highway Research Center.

Tarefder, R. A., Zaman, M. M., and Hobson, K. (2002). "Laboratory Assessment of Binders' Contribution to Rutting Susceptibility." *International Journal of Pavement*, Vol. 1, No. 2, pp. 36-47.

Takallou, H.T., Hicks, R.G., and Wilson, J.L., "Evaluation of Stripping Problems in Oregon." ASTM STP 899, *American Society for Testing and Materials*, 1985.

Thomas, R. C., Houston, J. E., Crooks, R. M., Kim, T. and Michalske, T. A. (1995). "Probing Adhesion Forces at the Molecular Scale." *Journal of the American Chemical Society*, 117, 3830-3834.

Terrel, R.L. and Al-Swailmi, S. Water Sensitivity of Asphalt – Aggregate Mixes: Test Selection. Report SHRP-A-403, *Strategic Highway Research Program, National Research Council*, Washington, D.C., 1994.

Tian, Z., Jiao, N., Liu, L., Wang, Y., Dong, Z., Xi, N, and Li W. (2004). "An AFM Based Nanomanipulation System With 3D Nano Forces Feedback." *International Conf. on Intelligent Automation on Mechatronics*, China.

Transportation Research Board (TRB), February 2003, Moisture Sensitivity of Asphalt Pavements, A National Seminar, San Diego, California.

USGS Annual Commodity Mineral Yearbook, Lime, Table 4, 2004.

Vaidya, A., and Chaudhury, M. K. (2002). "Surface Studies on Polyurethanes Containing Perfluoropolyether, Polydimethylsiloxane and Polyethyleneglycol Segments." *J. Colloid Interface Sci*, 249, 235.

Vezenov, D., Noy, A., and Lieber, C. (2008). "Chemical Force Microscopy: Force Spectroscopy and Imaging of Complex Interactions in Molecular Assemblies", *Handbook of Molecular Force Spectroscopy*, Springer US, pp 123-141.

Wardlaw K.R, Shuler S. (1992). "Polymer Modified Asphalt Binders." *American Society for Testing Materials*, ASTM STP 1108, Philadelphia, PA.

Wasiuddin, N. M., Zaman, M. M. and O'Rear, E. A. (2008). "Effect of Sasobit and Aspha-Min on Wettability and Adhesion Between Asphalt Binders and Aggregates." *Journal of Transportation Research Board*, TRB, Vol. 2051, pp. 80-89.

Wegan, V., and Nielsen, B. C. (2001). "Microstructure of polymer modified binders in bituminous mixtures." Report Number 87-90145-85-8. Danish Road Directorate, Roskilde, Denmark, 2001.

Wikipeia website <http://en.wikipedia.org/wiki/Error_bar> (November, 2010).

Witczak, M. W., Hafez, I., and Qi, X. (1995). "Laboratory characterization of Elvaloy® modified asphalt mixtures: vol. I – Technical report." College Park, Maryland: University of Maryland. *Dupont* < http://www.dupont.com/asphalt/link5.html> (November, 2010).

Western Research Institute. Fundamental properties of asphalts and modified asphalts, Volume 1: Interpretive report. Report: DTFH61-99C-0022. Laramie, Wyoming, 2003.

Yildirim, Yetkin (2007). “Polymer modified asphalt binders.” *Construction and Building Materials,* Vol 21, No. 1, 66-72.

Yoon, H., and Tarrer, A. (1988). "Effect of Aggregate Properties on Stripping," Transportafion Research Record 1171, National Research Council. Transportation Research Record, pp 37-43.

Zaniewski, J and Viswanathan, A. (2006). “Investigation of Moisture Sensitivity of Hot Mix Asphalt Concrete.” *Asphalt Technology Program*, West Virginia University, Publication no: AAT 1431455.

Zvejnicks, A. (1958). “Progress with Adhesion – Improving Bitumen Additives.” *Highway Res Board Bull*, 192, pp 26–32.

Appendix A1 Elvaloy and Lime modified binder raw data

	Dry adhesion (nN)						Wet adhesion (nN)				
Sample/Tip	COOH	NH_3	CH_3	OH	Si_3N_4		COOH	NH_3	CH_3	OH	Si_3N_4
Elvaloy 0.5%: Lime 0.5%	390.39	334.22	145.73	291.72	76.46		495.40	296.16	401.99	643.77	74.72
Elvaloy 0.5%: Lime 1.0%	398.34	342.02	151.09	417.78	88.05		527.14	242.58	443.03	707.00	132.70
Elvaloy 0.5%: Lime 1.5%	415.38	304.05	165.51	247.13	93.16		527.64	274.10	257.91	665.15	92.69
Elvaloy 0.75%: Lime 0.5%	407.85	345.73	139.79	331.94	96.88		392.50	206.25	375.35	305.41	89.08
Elvaloy 0.75%: Lime 1.0%	400.70	366.90	166.26	298.78	76.89		451.83	265.14	354.37	464.21	63.03
Elvaloy 0.75%: Lime 1.5%	397.69	237.61	188.67	341.77	92.63		490.82	250.22	292.01	662.37	80.04
Elvaloy 1.5%: Lime 0.5%	404.45	247.09	121.79	315.99	82.95		353.12	200.52	261.54	379.68	74.46
Elvaloy 1.5%: Lime 1.0%	400.93	208.30	92.65	371.16	71.04		354.96	195.45	327.06	485.20	80.71
Elvaloy 1.5%: Lime 1.5%	367.03	203.24	109.75	409.26	68.80		381.34	200.18	248.02	552.62	67.94
Elvaloy 2.0%: Lime 0.5%	379.54	197.84	109.90	259.12	56.25		449.55	235.82	305.95	484.58	53.45
Elvaloy 2.0%: Lime 1.0%	404.38	243.81	120.01	390.80	61.79		379.94	205.13	315.51	257.60	59.69
Elvaloy 2.0%: Lime 1.5%	385.95	256.78	93.10	333.75	71.89		432.42	213.13	561.40	370.35	57.04

Appendix A2 Elvaloy and klingbeta modified binder raw data

	Dry adhesion (nN)						Wet adhesion (nN)				
Sample/Tip	COOH	NH_3	CH_3	OH	Si_3N_4		COOH	NH_3	CH_3	OH	Si_3N_4
Elvaloy 0.5%: KB 0.25%	179.94	214.24	197.32	113.95	135.93		296.69	366.01	309.91	227.14	263.79
Elvaloy 0.5%: KB 0.5%	150.47	203.78	190.50	173.34	158.09		354.06	317.44	252.38	203.50	261.53
Elvaloy 0.5%: KB 0.75%	115.34	203.10	198.45	184.54	170.87		444.84	331.11	237.41	217.83	255.53
Elvaloy 0.75%: KB 0.25%	255.24	142.95	212.63	137.87	168.32		281.48	327.62	310.27	187.03	263.43
Elvaloy 0.75%: KB 0.5%	220.86	132.09	170.75	119.23	173.60		327.12	348.14	287.03	214.22	204.74
Elvaloy 0.75%: KB 0.75%	251.70	126.99	178.01	131.98	170.23		308.52	310.55	288.67	205.72	209.71
Elvaloy 1.5%: KB 0.25%	219.79	219.46	180.93	115.51	170.02		281.91	332.77	283.72	152.24	228.37
Elvaloy 1.5%: KB 0.5%	232.79	190.97	177.70	111.59	204.69		300.53	164.01	304.46	163.54	223.77
Elvaloy 1.5%: KB 0.75%	205.17	182.66	158.94	102.59	207.53		314.81	272.54	246.22	169.80	228.20
Elvaloy 2.0%: KB 0.25%	114.08	150.84	151.29	141.81	143.00		203.44	204.49	224.11	143.66	231.49
Elvaloy 2.0%: KB 0.5%	133.03	147.73	180.64	166.77	137.21		442.02	286.48	238.56	178.96	292.90
Elvaloy 2.0%: KB 0.75%	163.44	134.98	177.58	152.75	112.99		274.92	242.49	258.91	164.32	269.55

Appendix A3 Elvaloy and Wetfix modified binder raw data

	Dry adhesion (nN)						Wet adhesion (nN)				
Sample/Tip	COOH	NH_3	CH_3	OH	Si_3N_4		COOH	NH_3	CH_3	OH	Si_3N_4
Elvaloy 0.5%: WtFx 0.25%	267.62	230.60	200.82	161.83	226.68		307.64	373.54	260.12	205.21	320.61
Elvaloy 0.5%: WtFx 0.65%	286.22	220.76	158.68	197.62	232.09		315.92	315.92	221.35	243.11	289.44
Elvaloy 0.5%: WtFx 1.0%	276.20	210.83	202.01	192.64	212.41		316.00	384.45	264.54	198.32	355.60
Elvaloy 0.75%: WtFx 0.25%	301.65	207.24	206.70	126.18	161.30		386.84	340.56	303.47	214.14	312.53
Elvaloy 0.75%: WtFx 0.65%	333.07	103.32	191.83	161.85	219.20		341.34	313.27	246.27	205.15	291.59
Elvaloy 0.75%: WtFx 1.0%	333.30	164.63	160.27	164.15	141.98		244.73	257.86	203.46	170.63	257.28
Elvaloy 1.5% WtFx 0.25%	282.03	142.30	162.79	142.28	186.56		243.06	234.84	246.58	157.04	246.59
Elvaloy 1.5% WtFx 0.65%	276.88	204.42	168.86	172.42	166.16		263.79	218.32	284.90	177.12	329.79
Elvaloy 1.5% WtFx 1.0%	247.85	157.35	150.87	154.60	185.27		272.34	253.47	256.85	189.25	235.09
Elvaloy 2.0%: WtFx 0.25%	253.18	133.39	144.44	144.60	208.32		283.39	347.26	219.57	190.77	285.33
Elvaloy 2.0%: WtFx 0.65%	226.89	127.88	168.35	159.10	224.97		267.86	327.79	259.09	175.55	261.53
Elvaloy 2.0%: WtFx 1.0%	259.83	169.25	153.50	151.26	246.51		275.68	233.94	228.33	166.31	284.91

Appendix A4 Elvaloy and Morlife modified binder raw data

	Dry adhesion (nN)						Wet adhesion (nN)				
Sample/Tip	COOH	NH_3	CH_3	OH	Si_3N_4		COOH	NH_3	CH_3	OH	Si_3N_4
Elvaloy 0.5%: Morlife 0.25%	533.59	304.65	137.71	837.29	78.48		455.69	260.58	301.57	610.72	236.80
Elvaloy 0.5%: Morlife 0.6%	676.96	400.41	178.75	463.33	112.36		319.74	217.68	286.11	757.04	138.97
Elvaloy 0.5%: Morlife 1.0%	692.88	240.92	152.43	620.87	111.13		312.14	243.80	269.29	663.18	157.53
Elvaloy 0.75%: Morlife 0.25%	572.64	268.87	122.83	532.73	97.62		436.55	323.46	318.26	474.81	142.82
Elvaloy 0.75%: Morlife 0.6%	520.38	205.45	200.20	634.79	116.00		509.35	243.70	337.47	382.44	122.72
Elvaloy 0.75%: Morlife 1.0%	651.48	357.57	109.00	556.82	93.05		449.55	271.32	246.32	336.76	129.53
Elvaloy 1.5%: Morlife 0.25%	433.00	295.24	105.14	345.65	97.84		460.89	269.99	280.62	375.43	81.07
Elvaloy 1.5%: Morlife 0.6%	538.95	274.70	102.47	436.65	88.80		548.37	318.58	318.67	465.79	85.75
Elvaloy 1.5%: Morlife 1.0%	515.15	212.19	166.41	354.92	96.35		510.69	234.27	295.61	398.67	141.71
Elvaloy 2.0%: Morlife 0.25%	366.26	317.37	133.40	328.45	64.98		293.10	278.33	258.54	742.21	193.70
Elvaloy 2.0%: Morlife 0.6%	499.12	262.13	144.25	396.31	78.06		425.79	302.90	230.77	460.89	133.77
Elvaloy 2.0%: Morlife 1.0%	376.54	323.89	108.11	478.53	57.85		449.39	264.89	178.27	366.44	121.03

Appendix A5 Elvaloy and Unichem modified binder raw data

	Dry adhesion (nN)						Wet adhesion (nN)				
Sample/Tip	COOH	NH_3	CH_3	OH	Si_3N_4		COOH	NH_3	CH_3	OH	Si_3N_4
Elvaloy 0.5%: Uncm 0.25%	467.38	261.84	150.80	342.66	69.44		418.93	323.29	284.33	581.78	124.04
Elvaloy 0.5%: Uncm 0.8%	436.60	208.53	142.61	355.25	77.63		537.85	281.52	334.65	581.57	97.07
Elvaloy 0.5%: Uncm 1.5%	465.21	257.66	134.28	280.25	86.89		373.76	321.82	250.12	534.78	102.92
Elvaloy 0.75%: Uncm 0.25%	468.81	303.21	166.71	309.19	85.08		540.58	298.69	266.47	497.60	78.44
Elvaloy 0.75%: Uncm 0.8%	411.96	263.51	181.71	331.59	83.80		375.08	273.89	310.28	593.63	95.42
Elvaloy 0.75%: Uncm 1.5%	361.21	238.57	186.63	451.51	87.09		543.43	311.56	260.50	169.92	90.41
Elvaloy 1.5%: Uncm 0.25%	397.70	216.58	123.28	389.68	76.04		400.38	261.92	233.24	401.17	79.24
Elvaloy 1.5%: Uncm 0.8%	357.69	222.54	115.99	349.32	76.36		441.94	259.42	235.30	351.97	84.30
Elvaloy 1.5%: Uncm 1.5%	391.55	235.60	133.84	384.85	63.38		506.84	305.46	297.18	307.06	96.66
Elvaloy 2.0%: Uncm 0.25%	396.05	253.69	107.37	278.06	82.84		432.33	256.33	231.80	425.21	55.45
Elvaloy 2.0%: Uncm 0.8%	342.89	218.74	117.04	143.08	59.77		415.11	226.95	205.78	340.71	66.48
Elvaloy 2.0%: Uncm 1.5%	378.04	172.90	76.73	277.08	60.83		527.20	249.33	293.29	339.40	77.65

Determining Hardness and Elastic Modulus of Asphalt by Nanoindentation

Rafiqul A. Tarefder, M.ASCE[1]; Arif M. Zaman[2]; and Waheed Uddin, M.ASCE[3]

Abstract: Nanoindentation is a relatively new technique which has been used to measure nanomechanical properties of surface layers of bulk materials and of thin films. In this study, micromechanical properties such as hardness and Young's modulus of asphalt binders and asphalt concrete are determined by nanoindentation experiments. Indentation tests are conducted on a base binder and two polymer-modified performance grade (PG) binders such as PG-70-22 and PG76-28. In addition, two Superpave asphalt mixes such as SP-B and SP-III are designed using these PG binders, and the corresponding mixes are compacted to prepare asphalt concrete. Aggregate, matrix (Materials Passing No. 4 sieve) and mastic (Materials Passing No. 200 sieve) phases of each asphalt concrete sample are indented using both Berkovich and Spherical indenters. In nanoindentation, an indenter penetrates into asphalt material and the load (milli-Newton) and the depth (nanometers) of indentation are recorded continuously. Indentation load versus displacement data are analyzed using Oliver and Pharr method to measure hardness and Young's modulus. The unloading data of base binder is a straight line and therefore could not be analyzed using Oliver and Pharr's method. However, the indentation data of the PG grade binders are successfully analyzed. Young's modulus value is less than 3 GPa for mastic, 3 to 12 GPa for matrix, and greater than 12 GPa for aggregate studied herein. Based on the hardness data, mastic is 2 to 15 times softer than matrix materials, and matrix is 10 times softer than aggregate materials. The fact that the properties of the mastic can be measured while in the mixture, this study has great potential for realistic characterization of asphalt mixture components. In this study, spherical indenter is found to be suitable for asphalt binders based on the fact that the spherical indenter produces higher indentation depths than the Berkovich indenter. The study contributes significantly to the use of nanoindentation for transportation material characterization.

DOI: 10.1061/(ASCE)GM.1943-5622.0000048

CE Database subject headings: Nanotechnology; Micromechanics; Asphalts; Binders, material; Concrete; Young's modulus.

Author keywords: Nanoindentation; Micromechanics; Asphalt binder; Concrete; Hardness; Young's modulus; Berkovich; Spherical.

Introduction

There has been a long history of research into the macroscale and in some cases micromechanical behavior of asphalt in literature (Xu and Solaimanian 2009; Sadd et al. 2004; Papagiannakis et al. 2002; Guddati et al. 2002; Buttlar and You 2001). Micromechanics methods or models such as discrete element modeling or Huet-Sayegh model uses the properties of the individual particle and matrix as model parameters to predict the properties of the composite materials such as asphalt concrete (Masad et al. 2001; Roque et al. 1999; Little et al. 1999; Uddin 2003; Huet 1963; Sayegh 1965). Asphalt concrete being a stone-based asphaltic composite, the mechanical properties of asphalt binder film, mastic (binder filled by aggregates smaller than 0.075 mm), and aggregate significantly influence the stress-strain behavior of asphalt concrete composites. For example, Young's modulus and hardness of asphalt binder film affect the low-temperature fracture properties of asphalt concrete significantly (Desai 2007; Park et al. 1999; Chang and Meegoda 1997). Similarly, mastic affects the healing behavior of asphalt concrete and aggregate plays a significant role in the durability of asphalt pavements (Allen and Searcy 2001; Li et al. 1999; Roberts et al. 1996). Over the last two decades, asphalt researchers have expressed considerable interest in the micromechanical characterization of thin film, mastic, and aggregate to understand complex mechanical behavior such as fracture, healing, and durability (Masad et al. 2001; Roque et al. 1999; Little et al. 1999; Aglan et al. 1994). Surprisingly, there is little understanding of the fundamental properties of the binder and mastic at the submicron or nanoscale. To date, the micromechanical models of asphalt are insufficient due to difficulty in determining constitutive parameters based on aggregates, mastic, and asphalt interactions and properties (Buttlar and You 2001; Desai 2001). With the advent of nanoindenter, it is now possible to measure the mechanical properties of thin film asphalt, and small volume or phase of an asphaltic composite which is the main topic of discussion in this paper.

In a nanoindentation test, an indenter is used to indent a sample surface and the movement of the indenter is measured with an increasing load. Time, force, and displacement are recorded throughout the test. The shape of the loading and unloading curves depends on the elastic and plastic properties of the sample material. This technique is similar to classical indentation,

[1]Assistant Professor, Dept. of Civil Engineering, Univ. of New Mexico, MSC01 1070, Albuquerque, NM 87131 (corresponding author). E-mail: tarefder@unm.edu

[2]Graduate Research Assistant and Ph.D. Candidate, Dept. of Civil Engineering, Univ. of New Mexico, MSC01 1070, Albuquerque, NM 87131. E-mail: arif@unm.edu

[3]Professor of Civil Engineering, Univ. of Mississippi, University, MS 38677-1848. E-mail: cvuddin@olemiss.edu

Note. This manuscript was submitted on June 20, 2009; approved on November 3, 2009; published online on May 14, 2010. Discussion period open until November 1, 2010; separate discussions must be submitted for individual papers. This paper is part of the ***International Journal of Geomechanics***, Vol. 10, No. 3, June 1, 2010. ©ASCE, ISSN 1532-3641/2010/3-106–116/$25.00.

but is capable of producing contact areas and penetration depths characterized by submicrometer or nanometer dimensions for materials (Zhu and Bartos 2000; Bucaille et al. 2002). Nanoindentation is suitable for testing interface and specific component materials in a composite (VanLandingham et al. 2000) because nanoindentation can be performed at a much smaller scale and uses extremely low indentation forces. The forces involved are usually in the milli-Newton range and are measured in order of resolution of a few nano-Newtons. The depths of penetration are in order of nanometers. Apart from the displacement scale (10^{-9} m or nanometer) involved, the distinguishing feature of the most indentation testing is the indirect measurement of the contact area, which is the area of contact between the indenter and the specimen. In conventional indentation tests, the area of the contact is calculated from the direct measurements of the residual impression left in the specimen surface upon removal of load (Franco et al. 2004; Giannakopoulos et al. 1994). In nanoindentation tests, the size of the residual impression is too small to be conventionally measured directly (Hebbache 2003). The contact area is measured indirectly from the depth of penetration of the indenter into the specimen surface and known geometry of the indenter (Pharr et al. 1992; Oliver and Pharr 1992). For this reason, nanoindentation is also termed as depth sensing indentation.

To date, nanoindentation tests on asphalt have been reported in the literature by only a very few researchers in Europe (Ossa and Collop 2007; Ossa et al. 2005; Pichler et al. 2005). Nanoindentation is a powerful technique to obtain values of hardness and Young's modulus of a material (Pethica 1982; Loubet et al. 1984; Newey et al. 1982; Stone et al. 1988). Young's modulus, E is an intrinsic material property and fundamentally related to atomic bonding. E measures the resistance of a material to elastic (recoverable) deformation under load. A stiff material has a high Young's modulus and changes its shape only slightly under elastic loads (Beake et al. 2006; Igarashi et al. 1996). A soft material has a low Young's modulus and changes its shape considerably (e.g., rubbers). Young's modulus is one of the most widely used material properties for micromechanical modeling. For example, the operational principle of many micromechanical components is based on the elastic behavior and Young's modulus of the material (Pätzold et al. 1997). In this study, hardness and Young's modulus of asphalt binder, mastic, and aggregate are determined using nanoindentation tests. However, asphaltic materials create significant challenges to measure E accurately using indentation testing. Asphalt binders are very soft. In soft materials, it is difficult to measure the material response due to low system compliances (Lucas 1998). This difficulty is related to the load resolution, typically not better than $\pm$ 1 nN and to detect initial contact loads less than 0.1 nN. In this study, nanoindentation tests are conducted on three asphalt binder films, namely, PG 70-22, PG 76-28, and PG 58-22. The smallest maximum loads required for successful indentation tests on these soft binders are determined. Indentation data are analyzed based on elasticity (Oliver and Pharr 1992). In addition, indentation tests are conducted on the aggregate and mastic phases of two asphalt concretes which are designed based on Superpave technology. The viscous behavior of asphaltic composite can be captured through a nanoindentation creep test which is not addressed in this study.

Objectives

The main objectives of this study are to:

- Determine the characteristics of the load-displacement curves of asphalt binder, mastic, matrix, and aggregates in asphalt composite;
- Determine the fundamental properties such as Young's modulus and hardness of asphalt binders from nanoindentation experiments; and
- Determine fundamental properties such as Young's modulus and hardness of aggregate, matrix, and mastic phases in intact asphalt concrete.

Review of Past Research

Nanoindentation work directly related to asphalt, and some other materials such as polymer, cement, and concrete is discussed below.

Jäger et al. (2007) conducted nanoindentation creep test using a Berkovich tip on B50/70 bitumen to determine viscoelastic properties. They derived a viscoelastic solution modifying the existing elastic solution of the indentation problem. Three creep models such as the single dash-pot, the Maxwell, and the three-parameter model are used to simulate creep data generated by nanoindentation. The influences of loading rate, maximum load, and temperature on the model parameters are investigated and the respective model parameters are identified. An increase in the maximum load resulted in a decrease in values for the model parameters due to the heterogeneity of the bitumen microstructure consisting of both high-viscous strings embedded into a low-viscous matrix. Their study related indentation creep data to the viscosity of asphalt binders and described the temperature dependence of the viscosity by an Arrhenius law.

Stangl et al. (2007) studied the effect of styrene-butadiene-styrene (SBS) modification on the characteristics of bitumen using nano- and microindentation tests. These tests produce viscosities in the microrange corresponding to large-scale rheological properties. Two bitumen, one plain bitumen and one polymer-modified bitumen, are considered in the experimental program. The viscoelastic material properties of bitumen are identified from the holding phase using a single dash-pot model.

Pichler et al. (2005) studied the viscoelastic behavior and microstructure of bitumen and cement paste by nanoindentation. An indentation test was performed on a number of points to determine the spatial distribution of the mechanical properties based on viscosity gradient. Their study related the viscosity of bitumen to the nanomechanical properties of bitumen. In addition, they showed that the microstructure of bitumen is related to the material behavior.

Cheng et al. (2005) performed nanoindentation experiments on polymers: polystyrene (PS) and polyvinyl alcohol (PVOH) by a spherical-tip indenter. They proposed a linear viscoelastic analytical solution of indentation on a semi-infinite solid with a spherical-tip indenter. The Poisson's ratios for these polymers are assumed 0.3 and 0.4, respectively. The maximum load is 200 μN at a 50 N/s rate. Indentation depth is less than 400 nm. The comparison of results obtained from their model for indentation from the initial elastic unloading curve and the viscoelastic model for creep shows that the analytical solutions derived in both models work well when the materials are relatively elastic.

Ossa et al. (2005) investigated spherical microindentation response of 50 pen bitumen both experimentally and via an analytical model. Their study is limited to using a spherical indenter with a relatively large 40-mm diameter with loading ranges from 550 N, depth of 1.5 mm, and 30-s time. They concluded that the monotonic indentation response of the bitumen exhibits a power-

law dependence on the indentation force while the continuous cyclic response is primarily a function of the mean indentation load. Their model is successful in capturing the indentation recovery behavior of the bitumen and shown to be in reasonable agreement with periodic pulse loads over a wide range of test conditions. Monotonic, continuous cyclic, and cyclic pulse loading experiments are conducted over a range of temperatures. The results show that the continuous cyclic response depends mainly on the mean applied indentation load and the cyclic pulse loading behavior depends strongly on the recovery behavior of bitumen.

Cross et al. (2005) studied polystyrene polymer with a sharp Berkovich tip and blunt spherical indenters. They investigated the mechanical state of polymer flows induced by wide area thermal nanoimprint. Polystyrene films of narrow distribution molecular weight both slightly above and well above the chain entanglement weight spacing are imprinted with a range of feature shapes under nominally equivalent flow conditions. The maximum load is 700 mN with indentation depth of 500 nm. They find the elastic modulus range 10–150 GPa and hardness is 0.1–0.3 GPa for the polymers. The modulus behavior increases monotonically with indentation depth demonstrating the expected strong substrate influence on the long range elastic field. The proximity of the rigid, hard substrate is found to strongly influence the mechanical properties measured by the indenter. The results of both local and nonlocal investigations of imprinted polystyrene films showed no evidence of hardening due to the forming process. Bucaille et al. (2002) introduced a new method to identify the viscoplastic behavior of a polymer by using the force-penetration curves during nanoindentation testing. They used two indenters, a Berkovich indenter and a cone indenter with a semiangle of $\theta=30°$, for polycarbonate polymer. The nanoindentation tests are performed with three strain rates. The maximum applied load is 2000 μN and penetration depth is 2 μm.

Mondal et al. (2007) determined the mechanical properties of hardened and early aged cement paste by a nanoindenter. Berkovich and cube corner tips are used to determine elastic modulus and hardness of Portland cement paste. The loading range is 500–1500 μN and the loading rate is 100 to 300 μN/s, with correspondence penetration depth of 250 to 500 nm. A Poisson's ratio of 0.24 is assumed for all calculations. It is shown that the elastic modulus can be divided into three different groups of cement paste based on the decreasing values with the distance from the unhydrated particles. Saha and Nix (2002) studied the effects of the substrate on the determination of mechanical properties of thin films by nanoindentation with a Berkovich tip. Aluminum, glass, silicon, and sapphire are used as substrate in this study. They studied both soft films on hard substrates and hard films on soft substrates and assessed the effects of elastic and plastic heterogeneity as well as material pileup on the nanoindentation response. Compared to hardness, the nanoindentation measurement of the elastic modulus of thin films is more affected by the substrate. They concluded that the effect of the substrate hardness on the film hardness is negligible.

Theory of Determining Modulus and Hardness from Indentation Tests

In an indentation test, a tip with a defined shape penetrates into a sample surface and the indentation load (P) and penetration depth (h) are measured as a function of time. A schematic of the load-indentation depth curve recorded during indentation is presented in Fig. 1(a). The quantities shown are the peak indentation load

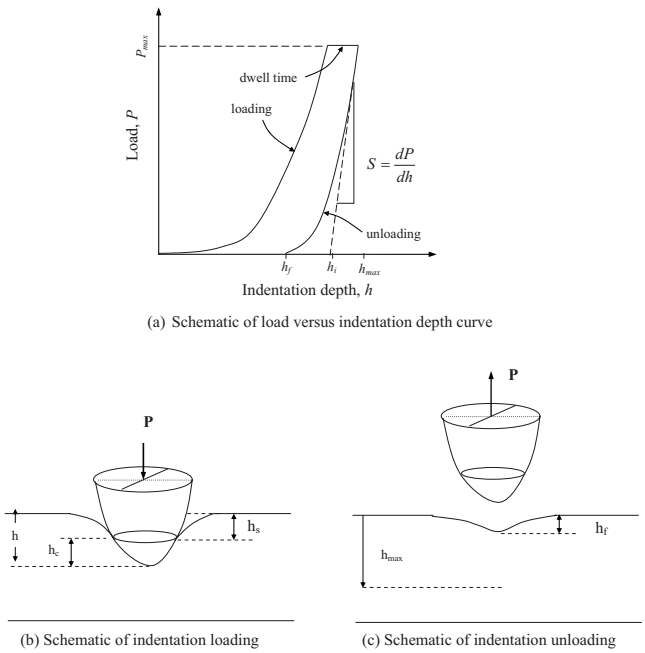

(a) Schematic of load versus indentation depth curve

(b) Schematic of indentation loading

(c) Schematic of indentation unloading

Fig. 1. Schematic of nanoindentation

(P_{max}), the depth a peak load (h_{max}), the final depth of the contact impression after unloading (h_f), and the initial unloading stiffness (S). It can be noted that at peak load h becomes h_{max}. These quantities are used to calculate modulus and hardness.

Fig. 1(b) shows the shape of sample during loading. Fig. 1(c) shows the final impression of the surface at the end of unloading. Solution of elastic indentation problem, i.e., a rigid indenter penetrating the elastic surface goes back to the experimental and theoretical work in the field of contact mechanics (Hertz 1881; Boussinesq 1885; Tabor 1951; Sneddon 1965; Johnson 1985). Stilwell and Tabor (1961) found the diameter of the contact impression in the surface formed by indenters does not recover during unloading. That is, plasticity affects the elastic unloading data. Stilwell and Tabor (1961) accounted for this issue by considering the shape of the perturbed surface in the elastic analysis. They defined a reduced modulus E_r to account for effects of nonrigid indenter on the load-indentation behavior through the following equation:

$$\frac{1}{E_r} = \frac{1-\nu_s^2}{E_s} - \frac{1-\nu_i^2}{E_i} \tag{1}$$

where E_s=Young's modulus of the sample; ν_s=Poisson's ratio of the sample (e.g., for asphalt materials ν_s=0.40); E_i=Young's modulus of indenter tip (e.g., for Berkovich tip E_i=1,141 GPa); ν_i=Poisson's ratio of indenter (e.g., for Berkovich tip ν_i=0.07); and E_r=reduced modulus. By recording data of the whole indentation procedure, Eq. (1) can be used to determine the Young's modulus of the sample.

The reduced modulus (E_r) is related to the unloading portion of the load-indentation curve according to the following equation (Doerner and Nix 1986; Pharr et al. 1992):

$$E_r = \frac{\sqrt{\pi}}{2}\frac{S}{\sqrt{A}} \tag{2}$$

where $S=dP/dh$=initial unloading stiffness and A=contact area. Therefore, measurement of modulus relies on how initial unload-

ing stiffness S and contact area A are determined from indentation data.

How to Find S—Oliver and Pharr (1992) determined the initial unloading stiffness S by fitting the depth versus loading-unloading data using the following power-law function:

$$P = \alpha(h - h_f)^m \tag{3}$$

where h=any depth of penetration; h_f=unrecoverable or plastic depth; and α and m=constants. Here, m is a power-law exponent that is related to the geometry of the indenter. Values of m equal to 1 for a flat-ended cylindrical indenter, 1.5 for a paraboloid of revolution, and 2 for a cone. The initial unloading slope S is determined by differentiating Eq. (3) and evaluating the derivative at the peak load and displacement.

How to Find A—Oliver and Pharr (1992) calculated contact area from the contact depth at peak load and the geometry of the indenter. They defined the contact area A by an area function $f(h_c)$ which relates the cross-sectional area of the indenter to the distance from its tip. From Fig. 1(b), at anytime during loading, the total displacement, h can be written as

$$h = h_c + h_s \tag{4}$$

where h_c=vertical depth along which contact is made and h_s=displacement of the surface at the perimeter of the contact. To determine contact depth h_c from the experimental data, Oliver and Pharr (1992) extrapolated the tangent line to the unloading curve at the maximum loading point down to zero load. This yields an intercept value for depth h_i which estimates the h_s and relates the contact depth h_c associated with the maximum loading point as follows:

$$h_c = h_{\max} - \varepsilon \frac{P_{\max}}{S} \tag{5}$$

where ε=geometric constant. The value of ε is 0.72 for conical indenter, 0.75 for a Berkovich indenter, and 0.85 for spherical indenter (Sneddon 1965; Doerner and Nix 1986; Oliver and Pharr 1992).

The hardness (H) value is defined by the mean pressure the material will support under loading. Hardness is computed from

$$H = \frac{P_{\max}}{A} \tag{6}$$

where A=projected area of contact at the peak load and $P_{\max}$ was previously defined. Hardness measurement technique is analogous to the well-known classic indentation tests (Brinell 1901). The unit of hardness is given in N/m^2=Pa. NanoTest Material Testing Platform software (MicroMaterials Ltd., Wrexham, U.K., 2007) makes use of the method of Oliver and Pharr (1992), described above to compute the hardness and reduced modulus. This software is employed in this study.

Nanoindentation Experiments

Materials Description

Asphalt Binders

Three asphalt binders were used for nanoindentation experiments. The binders were collected from a local supplier in New Mexico in cooperation with the New Mexico Department of Transportation (DOT). One of them is base asphalt, and the others are polymer-modified asphalt binders. The polymer-modified binders are designated as Superpave performance grade (PG) binders of PG 70-22 and PG 76-28. It can be noted that polymers are mixed with base asphalt binders so that its resistance to flow (viscosity) is less affected by temperature change. The PG 70-22 binder is expected to have small permanent deformation up to 70°C (usually summer), whereas it is expected to show small low-temperature cracking up to −22°C (usually in winter).

Table 1. Mix Properties

Sieve size (mm)	Percent passing	
	Mix SP-B	Mix SP-III
25	100	100
19	94	96
12.5	85	75
9.5	77	69
2.36	41	29
1.18	32	21
0.6	24	16
0.30	14	11
0.075	5.6	4.8
Binder percent	5.7	5.2
PG	PG 70–22	PG 76–28
Air voids (%)	4	4
Aggregate type	Limestone	Dolomite

Asphalt Concrete

Superpave mixes that used the aforementioned PG binders were collected from the local plant also. The mix properties are listed in Table 1. Mix SP-III is a coarse mix, and mixed SP-B is a fine mix. No mixes that use base binders are readily available from the plant or DOT. Therefore, base mixtures are not included in the nanoindentation tests on asphalt concrete. Each of the mixes is compacted into 15 cm (6 in.) diameter cylinders by a Superpave gyratory compactor using a 600 kPa (87 psi) vertical pressure (AASHTO T312 2002). Using a water-cooled laboratory saw, 1-in.-thick disc is sliced from the center of each cylinder in an attempt to acquire samples with uniform air voids. Disks are prepared at a target low air voids of 4%.

Sample Preparation

Asphalt Binder Films

Fig. 2(a) shows a laboratory prepared asphalt film on glass substrate. As a first step, a glass slide surface is wrapped with a high temperature resistant tape. Two strips of tape are placed in parallel by keeping a small gap between them. Next, the hot polymer-modified liquid asphalt is poured into the gap between the two strips of tape. It can be noted that polymer-modified binders are melted by heating them to 163°C for an hour. The asphalt coated glass substrate is then placed in the oven at 163°C for 10 min in order to have a smooth surface. Next the glass substrate is removed out of the oven, cooled down to room temperature, and peeled off the tapes. The final thickness of the film is kept in the range of 15–20 μm (micrometer) so that an indentation (i.e., 8 μm maximum depth) is not affected by the glass substrate.

Asphalt Concrete Sample

Fig. 2(b) shows a polished asphalt concrete cube that is used for nanoindentation testing. Fine laboratory saws at Geology Depart-

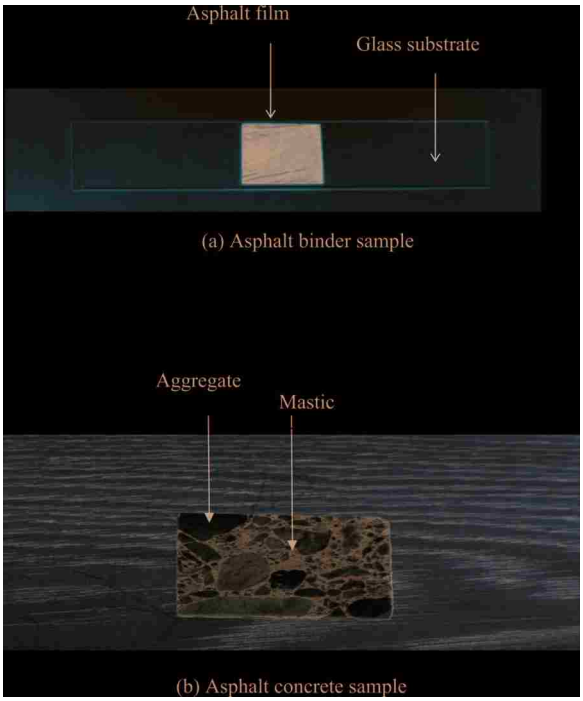

Fig. 2. (Color) Asphalt samples for nanoindentation tests

ment are used to cut and prepare thin ac cubes (12 mm $\times$ 12 mm $\times$ 6 mm). Smooth surface of the cube is very important for nanoindentation experiment. Because the contact area is measured indirectly from the depth of penetration, a rough surface may cause errors in the determination of the area of contact between the indenter and the specimen (Johnson 1985). Therefore, the cube surfaces are polished by a grinding machine rotating at angular speed of 150 rpm with a sequence of SiC papers of decreasing abrasiveness (100, 200, 400, 800, 1,000, 1,200 and 1,400 grit) under continuous water cooling. Each step is carried out for 150 s. Only one phase (surface) of the cube sample is polished. Finally, the specimens are washed in a water bath to remove any remaining dusts.

Laboratory Testing

Test Equipment

Nanoindentation tests were conducted using a nanoindenter supplied by MicroMaterials Ltd. Wrexham, U.K. (MicroMaterials 2007). The indenter is equipped with both pyramidal Berkovich and spherical tips and the direction of indentation is horizontal. Both the Berkovich and spherical indenters are made of diamond. The load and displacement resolution of the indenter are 1 nN (nano-Newton) and 0.01 nm (nanometer) respectively. Both load and depth-controlled tests are conducted on asphalt. Indentations on randomly selected areas are performed on each asphalt binder and asphalt concrete samples. The indents are located at least 40 μm (micrometer) apart to avoid the influence of residual stresses from adjacent impressions. On the asphalt concrete sample, the locations of aggregate and mastic are determined using the nanopositioner attached with our nanoindenter equipment. All testing is conducted at room temperature (23.8°C) controlled by the temperature chamber attached with the nanoindenter.

Indenter Tips

Berkovich Tip

Three-sided pyramidal Berkovich tip with a semiangle of 65.27° (i.e., face angle with the central axis of the indenter) is used for nanoindentation testing. It has sharp and well-defined (pyramid defined by face angle 65.3°) tip geometry. This tip is good for brittle materials (Fischer-Cripp 2004). In this study, a Berkovich tip is used on the mastic and aggregate samples only. Several attempts are made to indent asphalt binder using a Berkovich indenter in this study; however those attempts are not successful.

Spherical Tip

The spherical indenter used in this study has a nominal tip radius of 10 μm. This tip is also known as a "blunt" tip. While working on soft materials such as asphalts it is important to keep the stress in the contact region low, to do meaningful experiments without considerable deformation of the asphalt film or mastic surface. The purpose of using the blunt tip is to reduce the stress at the contact, thereby generating plastic deformation at low contact stress. As it described later in this study, spherical tip is suitable for measuring hardness and modulus of asphalt binder materials. In all indentation on asphalt binder, the maximum indentation depth is kept below 8,000 nm.

Loading Configuration

As it is described previously, based on Oliver and Pharr (1992), Young's modulus E is obtained from the initial slope S of the unloading curve at maximum depth. It is important that the unloading curve is not affected by the viscous response of asphalt materials. Therefore, it is required to ensure that either the unloading rate is large enough to exclude viscous material response or that the material exhibits asymptotic creep behavior and the dwelling phase lasted long enough for the creep response to subside (Pichler et al. 2005). To avoid such errors in hardness and modulus measurement, Chudoba and Richter (2001) recommended that the maximum load should be retained for a period of 10 to 60 s before the onset of unloading. Our testing cycle consisted of three segments: the loading segment, the peak load holding segment, and the unloading segment [see Fig. 1(a)]. The duration of the dwell at maximum load is 30 s. Indentation experiment can be done either in-depth-controlled or load controlled or first condition methods. Depth-controlled indentation is done by setting the maximum depth of indentation value, whereas the load controlled indentation is done by setting the maximum load. In the first condition, maximum depth and load values are specified, and tip penetration stops are based on whichever of the depth or load reaches first to its maximum value.

Results and Discussions

Asphalt Binder Study

Load-Displacement Characteristics

For asphalt binders, depth-controlled tests were performed, where the maximum load is set to 0.045 mN (milli-Newton) at different depth gains and loading rates. Figs. 3(a and b) show the indentation load versus depth curves of asphalt binders using spherical indenter at different gains and loading rates. Here, two-gain means two different trials or depths. In this study, different

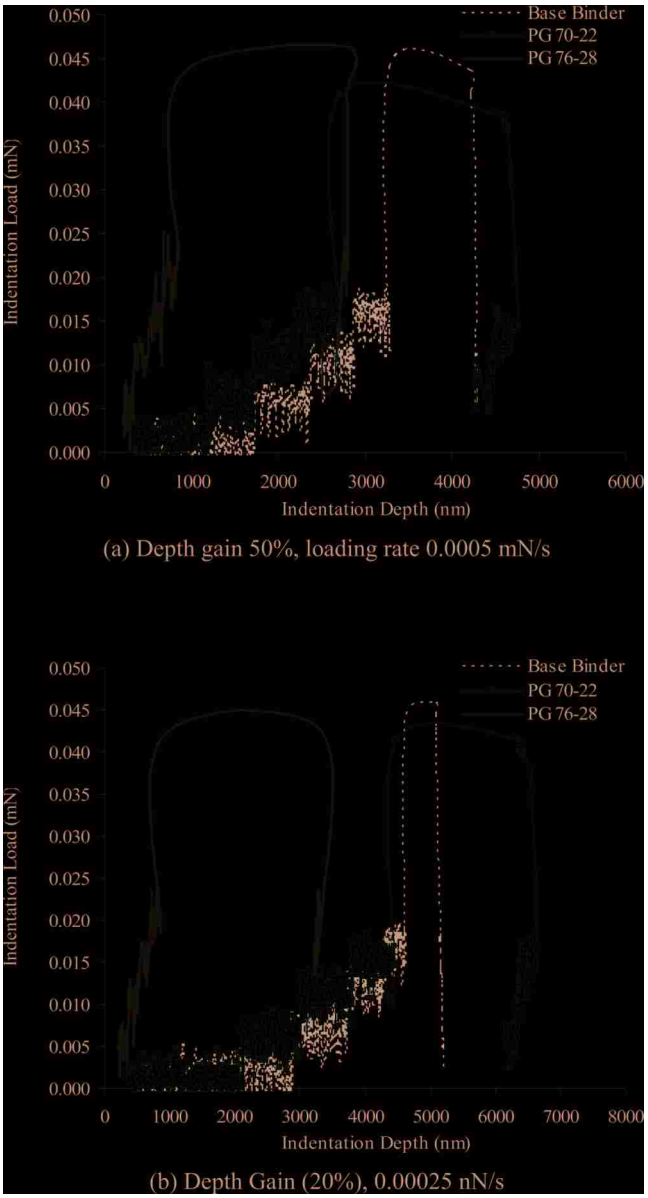

Fig. 3. (Color) Load versus depth on asphalt binders using spherical indenter

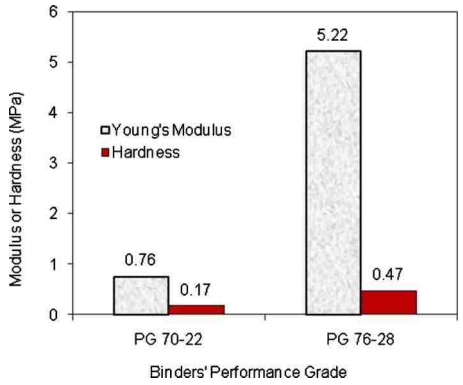

Fig. 4. Young's modulus and hardness of PG asphalt binders

trails are attempted for successful indentation results. Both Figs. 3(a and b) show hysteresis at the beginning and after certain depth the data becomes regular. There is a gradual increase in depth and indentation load up to 0.02 mN (milli-Newton) and resolution of data are not very good. Then there is a sharp increase in load from 0.02 to 0.045 mN. This seems like the indenter is being held at a fixed position while the load is being increased. It is possible that the elastic deformation in the whole sample is not being converted to plastic deformation in the region of indenter, rather healing the indenter region resulting in increased load at constant depths. In the dwell period porting portion of the curve, load is constant (approximately) while depth increases. But for asphalt binder, it is noticeable from Figs. 3(a and b) that there is a slight decrease in load during the dwell period. The applied load might decrease during the dwell creep period through decrease in contact area due to delayed (viscous) flow of asphalt binders at the indentation location. Also, due to a minute scale or nano-Newton level load carrying the capacity of the asphalt binders and binder softening, keeping the maximum applied load constant is virtually impossible.

Figs. 3(a and b) show that the unloading curve of base binder differs from those of the PG binders. For base binders, the unloading curve of the base binder is a downward straight line starting from the end of the dwell period to the horizontal axis ($P=0$). It is possible that the dwell period used for base binder is not long enough and therefore, base binder is deforming plastically by creep faster than it is elastically recovering as the load is reduced. However, this is not the case for PG grade binders which clearly show an unloading path. Overall, it can be said that creep behavior is predominant in asphalt binders. In this regard, it worthwhile to mention that this study has observed that nanoindentation on asphalt binders is very challenging. Nanoindentation tests have been performed routinely on hard materials (e.g., silicon and tin), but submicron level penetrations and/or small nano-Newton loads become critical for success when nanoindentation is done on soft viscoelastic materials such as asphalt binders. Asphalt binders pose two major challenges. The first challenge is related to the low load resolution and capacity of the nanoindenter system. The second challenge is getting an unloading curve to apply the Oliver and Pharr (1992) method to measure stiffness and hardness accurately from the indentation data. Generally, it may be appropriate to conduct several tests at one specific indentation load or depth and then perform repeatability study but this is not done in this study. Rather, the repeated nanoindentations are done on asphalt film or concrete samples, and the resulting data that meet the second challenge that is, if the unloading data can be analyzed using the Oliver and Pharr (1992) method, are reported in this study for exhibiting characteristics of binder films or mastic or aggregate. The discrepancy in the unprocessed data, that do not follow the Oliver and Pharr (1992) analysis, may occur due to asphalt's healing and/or delayed flow behavior. It can be noted that though the tests were performed at room temperature in this study, the viscous feature of bitumen may still play a role in the test results.

Hardness and Modulus Values

Fig. 4 is a bar plot of modulus and hardness values of asphalt binders. It can be seen that the base binder's modulus and hardness are not shown. In fact, analysis of base binder data using Oliver and Pharr (1992) method failed to produce meaningful results. For base binder, the elastic recovery is 0, and the plastic depth is equal to the maximum depth of penetration. The hardness value calculated using Eqs. (6) is found to be very low. Similarly,

Table 2. Elastic Young's Modulus, Hardness, and Poisson's Ratio of Construction Materials

Material	Elastic modulus (GPa)	Hardness (GPa)	Poisson's ratio
Si (substrate)	170–180	10–12	0.17
Diamond	1070	65	0.07
Steel	210	4–9	0.26
Fused silica	72.5	8–10	0.17
Aluminum	70.5	0.58	0.24
Glass	70	3–5	0.23
Granite	50–70	2.27	0.1–0.26
Marble	50–70	30	0.06–0.22
Limestone	25–55	—	0.18–0.25
Sandstone	10–20	—	0.21–0.38
Concrete	10–17	—	0.1–0.2
Wood	7–14	0.3	0.40
Polystyrene (polymer)	2.2–4.0	5	0.340
Lime stabilized soils	0.21–0.42	—	0.15–0.20
Clay soils	0.35–0.10	—	0.40–0.45
Silty soils	0.35–0.15	—	0.40–0.45

Note: References: Franco et al. (2004) and Fischer-Cripp (2004).

the reduced modulus calculated using Eq. (2) is found to be very high compared to the values listed in Table 2 for general construction and polymer materials. From Fig. 4, it can be seen that PG 76-28 is almost three times harder than the PG 70-22 binders which is expected. Hardness indicates a resistance to permanent deformation. Ideally, higher grade PG binders are used in warmer climate pavements to prevent permanent deformation of asphalt concrete subjected to high summer temperatures. Fig. 4 shows that stiffness of PG 76-28 binder is approximately six to seven times higher than that of the PG 70-22 binders. High stiffness is a concern for low-temperature cracking in asphalt.

Indentation Depth Recovery

Images of indented surface are taken using atomic force microscope before and after indentation. Fig. 5(a) shows indentation induced-blister of a PG 76-28 film on glass substrate immediately after indentation. Fig. 5(b) shows the image of the same sample 30 min after indentation. Through visual inspection, it is determined that 30% of the indentation depth has recovered during this time. No in-depth analysis of these images is presented in this paper. However, it is evident from images that indentation technique allows for observation and assessment of minute scale deformation and deformation recovery. It may be possible to get a

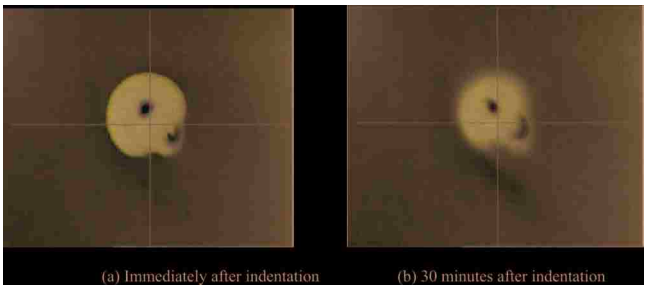

Fig. 5. (Color) Depth recovery of PG 76–28 asphalt binder (spherical indenter)

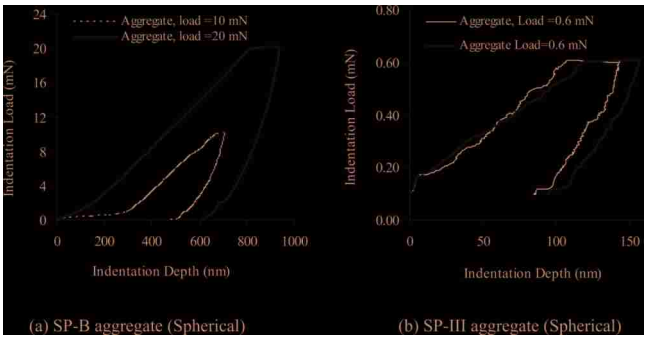

Fig. 6. (Color) Indentation load-depth characteristics of aggregates

sense of microstructural phenomena such as molecular nucleation or dislocation phenomenon due to the heterogeneous stress field that arise in asphalt binders under the loading of an indenter.

Asphalt Concrete Study

Load-Displacement Characteristics of Aggregate, Matrix, and Mastic

In this section, the experimental results are discussed with an overview of the characteristics of the load-displacement curves for aggregate, matrix, and mastic phases of an asphalt concrete. Mastic is a mixture of asphalt binder and fines passing #200 sieve, whereas matrix is defined as the mixture of asphalt binder and fine aggregates retained on #200 sieve. Generally fines passing #200 sieve being trapped inside a binder film increases the thickness of asphalt binder film, whereas the fine aggregates are coated by asphalt binders or mastic in an asphalt mix.

Figs. 6(a and b) show the load-displacement characteristics of SP-B (limestone) and SP-III aggregates (dolomite) using a spherical indenter. For both aggregates dwell time is set for 30 s to minimize time dependent plastic effect. For SP-B aggregate, two maximum loads 10 and 20 mN are specified at two different loading rates 1.75 and 1.0 mN/s, respectively. Fig. 6(a) clearly shows that the penetration depth is higher at higher loading rates. Also, total penetration (i.e., 937 nm) at 20 mN maximum load is larger than the total penetration (i.e., 703 nm) at 10 mN maximum load. From Fig. 6(b), it can be seen that total penetration in SP-III aggregate is only about 143 nm because the sample is loaded to a small maximum load at 0.6 mN. The unloading curve is nonlinear for the SP-B aggregate and linear for SP-III based on the load applied in this study. It can be noted that a seating load of 0.1 mN is used for all tests.

Figs. 7(a and b) show the load, load-displacement characteristics of SP-B and SP-III matrix materials. The SP-B aggregate is loaded up to 10 mN with a loading rate of 1.00 mN/s, and the SP-III sample is loaded up to 0.6 mN at a loading rate of 0.025 mN/s (different for two curves shown in each plot). Two tests data are plotted in each of the Figs. 7(a and b). It can be seen that the loading curve differs in two tests for a specific matrix. However, from careful examination it can be seen that the shapes of the unloading curves are almost same for a specific matrix.

Figs. 8(a and b) show the load and load-displacement characteristics of SP-B and SP-III mastics. It can be seen that the mastic materials show a very small amount of elastic recovery during unloading. The mastic is very soft which is apparent from the high value of depth attained at the maximum load (0.6 nN) for both SP-B and SP-II mastics. The maximum amount of displacement is in the range of 1,775 to 1,990 nm (nanometer) is SP-B

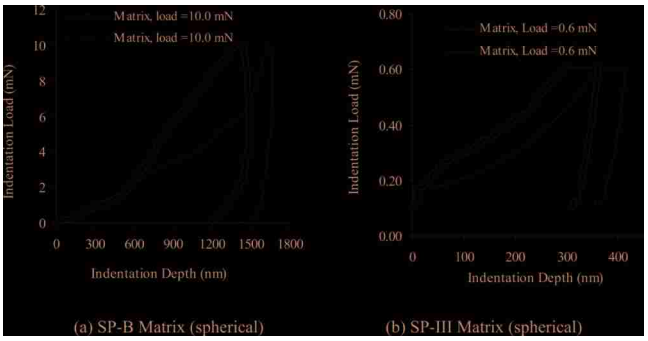

Fig. 7. (Color) Load versus indentation depth for matrix

mastics and 925 to 950 nm in SP-III mastic. Therefore, mastic SP-B is softer than the mastic SP-III. It can be noted that 5.7% (optimum) PG 70-22 binder is used in the SP-B mix and 5.2% (optimum) PG 76-28 binder is used in the SP-III mix. In general, the PG 70-28 is stiffer binder than the PG 70-22 although the nanoindentation tests are done in this study at 23.8°C. This demonstrates that nanoindentation tests can differentiate the softness or hardness of different mastic materials while they are parts of the parent asphalt concrete samples. Such study has not yet been reported in the asphalt literature. Some researchers have tested macro scale sand-asphalt mix or mastic sample but they have not tested mastic as a part of the intact asphalt concrete sample.

Figs. 9(a and b) show the difference in load-displacement characteristics of the three phases of an asphalt concrete using Berkovich and Spherical indenters, respectively. Fig. 9(a) shows that the these three phases such as aggregate, matrix, and mastic are subjected to descending order of loads, yet mastic shows larger plastic deformation than the matrix and/or aggregate. Similarly, matrix is softer than the aggregate. Fig. 9(b) shows the similar trend of deformation at an equal load using a spherical indenter.

In this study, both the Berkovich and spherical indenters produced meaningful results from aggregate, mastic, and matrix phases. The Berkovich indenter is sharper than the spherical tip (blunt tip). Fig. 10 compares the load-displacement characteristics obtained by Berkovich and spherical indenters. In aggregate [Fig. 10(a)], both Berkovich and spherical indenters produces approximately the same amount of indentation depth. In soft materials such as matrix and mastic [Fig. 10(b)], the Berkovich indenter shows larger indentation depths than the spherical indenter. However, this really depends on the response of the specimen material.

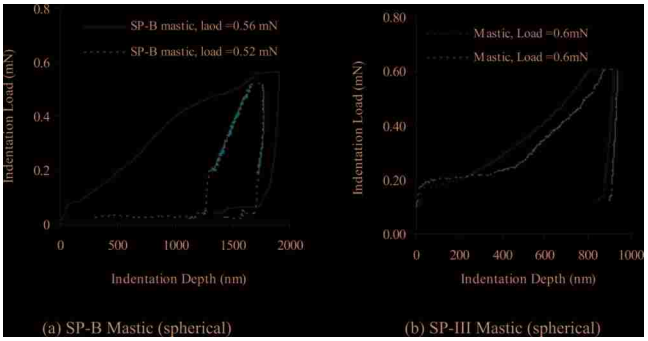

Fig. 8. (Color) Load versus indentation depth for mastics

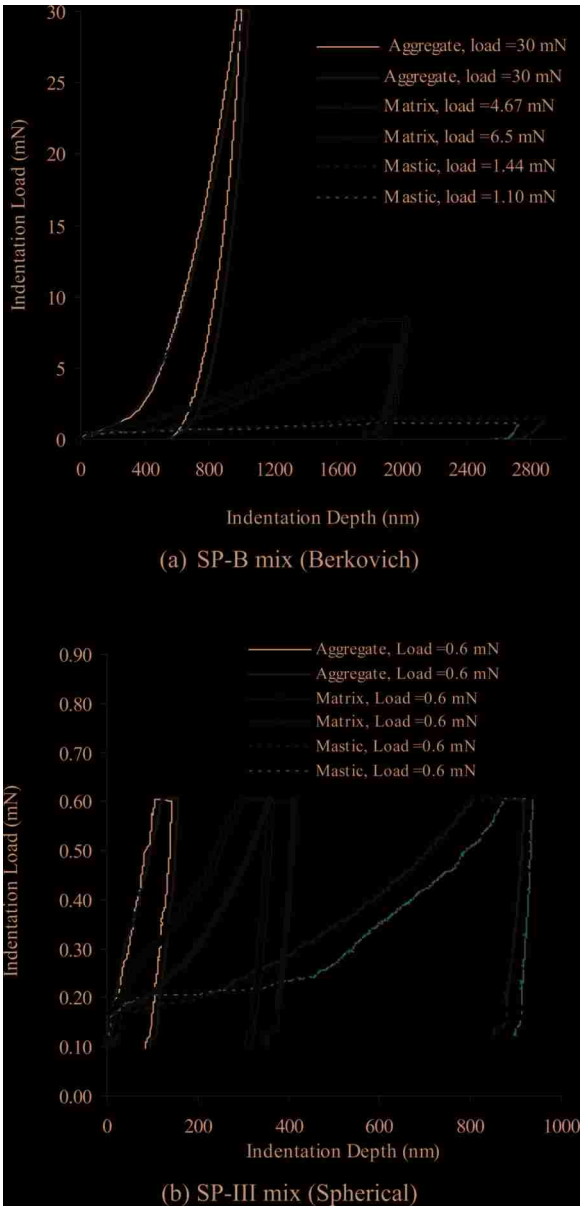

Fig. 9. (Color) Comparing aggregate, matrix, and mastic (spherical) indentation

Hardness and Modulus Values of Aggregate, Matrix, and Mastic

From Fig. 11(a), the average hardness value of aggregate is 1.24 GPa for SP-B and 2.52 GPa for SP-III.; the average value of hardness of matrix is 0.153 GPa for SP-B mix and 0.54 GPa for SP-III mix; the average modulus value of mastic is 0.007 for SP-B mix and 0.031 for SP-III mix. Overall the SP-III mix is harder and stiffer than the SP-B mix. The hardness and modulus values of SP-B and SP-III are compared in Figs. 11(a and b). From Fig. 11(b), the average modulus value of aggregate is 26.5 GPa for SP-B and 23.6 GPa for SP-III; the average value of modulus of matrix is 6.7 GPa for SP-B mix and 9.6 GPa for SP-III mix; the average modulus value of mastic is 0.74 for SP-B mix and 2.29 for SP-III mix. For the sake of comparison, the hardness and modulus values of the asphalt concrete components such as aggregate, matrix, and mastic are separated. Clearly, the modulus and hardness values differ at different phases of asphalt concrete. SP-III uses dolomite and PG 76–28, whereas SP-B

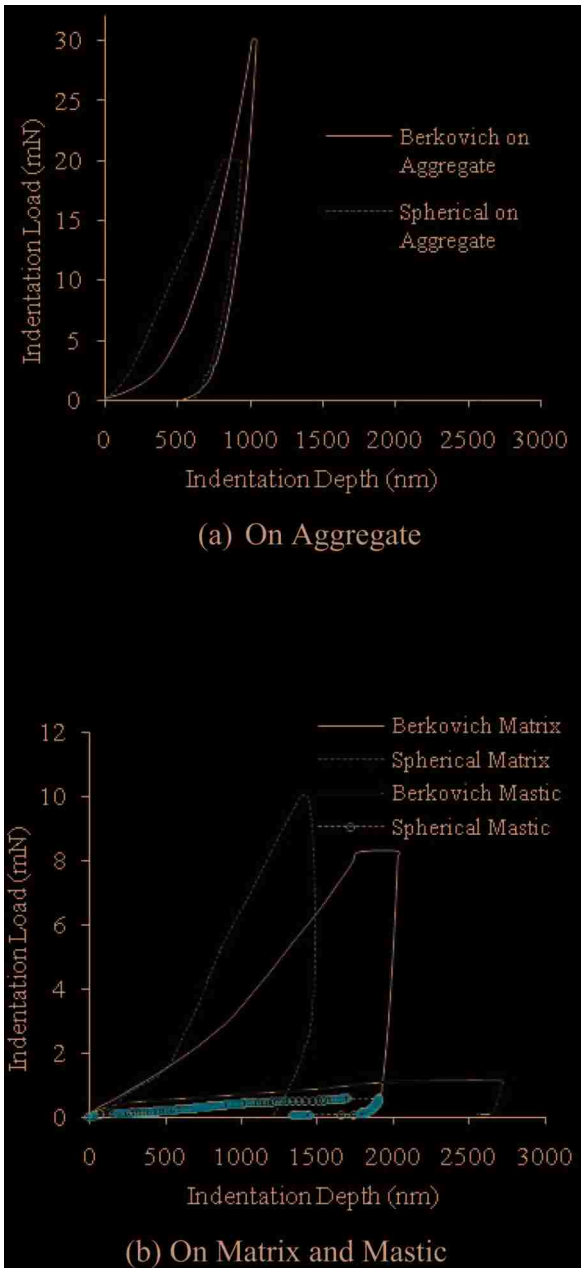

Fig. 10. (Color) Comparing indentation results of Berkovich versus spherical (SP-B mix)

mixes uses limestone and PG70-22 binders. Therefore, dolomite's hardness value is higher than the limestone's hardness value. However, Young's modulus value of dolomite is slightly smaller than that of the limestone. For the matrix and mastic materials, hardness and Young's modulus of SP-III are consistently higher than those of the SP-B mix. The higher PG grade binder has significantly contributed to the higher values of modulus and hardness in matrix and mastic.

Table 2 shows the typical values of modulus and hardness of some common materials (Li et al. 1999). It can be seen from Fig. 11 that limestone and dolomite's hardness values determined from indentation tests fall within the rock hardness and modulus values reported in the literature. For the mastic and matrix materials, no literature is available yet on the hardness and Young's modulus values. Fig. 12 shows results of 60 indentation tests (10×6 grids) on the asphalt concrete using a Berkovich indenter.

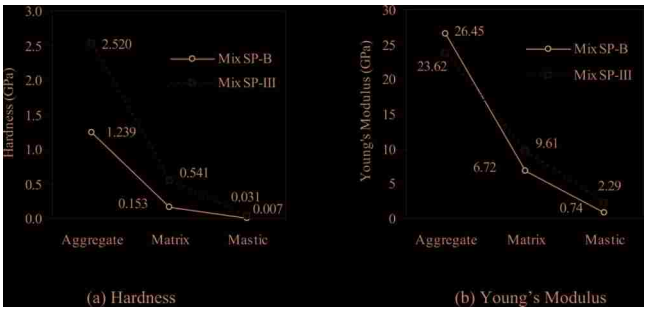

Fig. 11. (Color) Modulus and hardness of asphalt mixes

Some of the test points are taken on mastic, some points on matrix, and many points on aggregate using the nanopositioner attached with nanoindenter. Data are sorted in ascending order of Young's modulus values before plotting in Fig. 12. It can be seen that overall the hardness value increases as the Young's modulus value increases. The hardness and modulus values found to be as expected: low values in the mastic (less than 50 MPa), intermediate values in the matrix (100 to 800 MPa), and high values (above 1 GPa) in aggregate phases. Based on the nanoindentation results, presented in this study, it is revealed that Young's modulus is less than 3.0 GPa for mastic, 3 to 12 GPa for matrix, and 12 to 38 GPa for aggregate used in this study.

Application Note

This paper has made a significant contribution to the use of nanoindenter for testing asphalt binder, mastic, and aggregate to measure modulus and hardness of the materials. The results are particularly useful for characterization of thin film asphalt binders. Currently, there is no standard method available for direct measurements of modulus and hardness of asphalt binder film. Nanoindentation can be applied to better characterize asphalt film. For example, the method can compare the stiffness of asphalt binder films before and after aging, healing, and/or moisture damage.

It is evident from this study that nanoindentation provides micromechanical properties of mastic, aggregate, and matrix without separating them from the asphalt concrete. Thus the properties from nanoindentation test may provide more realist inputs for the micromechanical models such as discrete element model for characterization of fracture, damage, healing, and aging behavior of asphalt concrete. The nanoindentation technique has high poten-

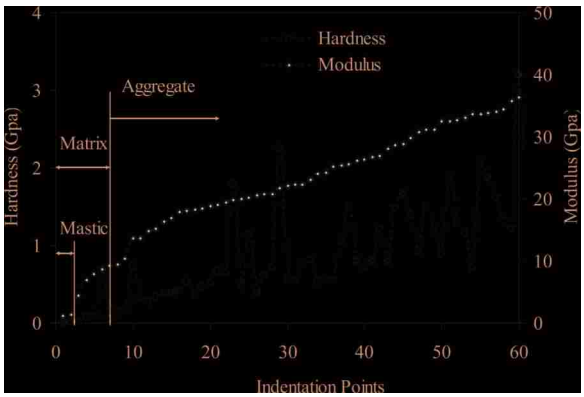

Fig. 12. (Color) Young's modulus and hardness of different components of an asphalt concrete

tial for identifying the mechanical effects of the elementary chemical components of the asphalt binder at the scale where physical chemistry meets mechanics (chemomechanics).

Currently, modulus of asphalt concrete is used in the mechanics based pavement design procedure. Only rheological properties of binders are used, while the properties of mastic are not used in such pavement design. Nanoindentation has the potential to incorporate more mechanics into the existing mechanistic-empirical pavement design method through incorporating the nanomechanical properties of mastic and binder film to account for moisture damage, healing, and aging related distress which are yet unsolved in asphalt pavement engineering.

Conclusions

The following conclusions are made:

- Based on the results of nanoindentation tests on asphalt binders, it is observed that the base binder is too soft for successful indentation experiment based on the load and displacement range and resolution capacity of the nanoindenter used in this study. For the base binders, the unloading data are linear and vertical, which could not be analyzed using existing analytical tools (Oliver and Pharr method). However, nanoindentation tests using a spherical indenter are successful on the PG binders;
- The PG 76-28 binder has shown to be harder and stiffer compared to the PG 70-22 binder. Although this outcome meets the expectation built on PG binder characteristics literature, currently there is no standard method available for direct mechanical characterization of asphalt binder films. This study for the first time has made significant contribution to the use of nanoindenter for characterization of thin film asphalt binder;
- It is shown that both Berkovich and spherical indenters can be used on asphalt concrete for successful indentation experiments and results to be analyzed by Oliver and Pharr method. Overall, the Berkovich indenter penetrates into asphalt sample more than a spherical indenter under the same amount of load;
- Based on the results of nanoindentation tests on asphalt concrete, the average value of the modulus of limestone and dolomite aggregate obtained from nanoindentation tests is within the range of commonly accepted values from the literature. Aggregate's modulus value is much higher than the matrix and mastic materials in an asphalt concrete. Average Young's modulus of mastic is less than 3 GPa and average Young's modulus of matrix is in between 3 to 12 GPa. Construction aggregate's Young's modulus value is above 12 GPa. The fact that properties of mastic can be determined while in the mixture or composite provides great potential for realistic characterization of asphalt mixture components;
- There is a clear difference in the hardness value of aggregate, matrix, and mastic phases of an asphalt concrete. The hardness value ranged 100–800 MPa for matrix, less than 50 MPa for mastic, and above 1 GPa for aggregate in an asphalt concrete; and
- Hardness increases as the Young's modulus value increase however, not proportionally. Modulus and hardness of asphalt can be measured from nanoindentation experiments at several different peak loads and loading rates.

Acknowledgments

This project is funded by the National Science Foundation (NSF) through prestigious CAREER program. NSF Grant No. 0644047 and Program: Infrastructure Materials and Structural Mechanics. Thanks to Mr. Robert Meyers and Mr. Parveez Anwar of NMDOT and Mr. John Galvin of the Lafarge North America Quality Assurance Laboratory in obtaining the material needed for this study. Finally, the writers thank Mr. Evan Kias at the University of New Mexico for his assistance in the laboratory.

References

Aglan, H., Othman, A., and Figueroa, L. (1994). "Processing conditions-fracture toughness relationships of asphalt concrete mixtures." *J. Mater. Sci.*, 29(18), 4786–4792.

Allen, D. H., and Searcy, C. R. (2001). "A micromechanical model for a viscoelastic cohesive zone." *Int. J. Fract.*, 107, 159–176.

Beake, B., et al. (2006). *Micro materials manual*, Micromaterials, Wrexham, U.K.

Boussinesq, J. (1885). *Applications des potentiels à l'etude de l'équilibre et du mouvement des solides élastiques*, Gauthier-Villars, Paris, 508.

Brinell, J. A. (1901). *Congrès international des méthodes d'essai des matériaux de construction*, Vol. 2, Paris, 83–94.

Bucaille, J., Felder, E., and Hochstetter, G. (2002). "Identification of the viscoplastic behavior of a polycarbonate based on experiments and numerical modeling of the nano-indentation test." *J. Mater. Sci.*, 37(18), 3999–4011.

Buttlar, W. G., and You, Z. (2001). "Discrete element modeling of asphalt concrete: A micro-fabric approach." *Transportation Research Record. 1757*, Transportation Research Board, National Research Council, Washington, D.C.

Chang, G. K., and Meegoda, J. N. (1997). "Micromechanical simulation of hot mixture asphalt." *J. Eng. Mech.*, 123(5), 495–503.

Cheng, L., Xia, X., Scriven, L., and Gerberich, W. (2005). "Spherical-tip indentation of viscoelastic material." *Mech. Mater.*, 37(1), 213–226.

Chudoba, T., and Richter, F. (2001). "Investigation of creep behaviour under load during indentation experiments and its influence on hardness and modulus results." *Surf. Coat. Technol.*, 148(2–3), 191–198.

Cross, G., O'Connell, B., Pethica, J., Schulz, H., and Scheer, H. (2005). "Instrumented indentation testing for local characterization of polymer properties after nanoimprint." *Microelectronic Engineering*, 78–79, 618–624.

Desai, C. S. (2001). *Mechanics of materials and interfaces: The disturbed state concept*, CRC, Boca Raton, Fla.

Desai, C. S. (2007). "Unified DSC constitutive model for pavement materials with numerical implementation." *Int. J. Geomech.*, 7(2), 83–102.

Doerner, M. F., and Nix, W. D. (1986). "A method of interpreting the data from depth-sensing indentation measurements." *J. Mater. Res.*, 1(4), 601–609.

Fischer-Cripp, A. (2004). "Nanoindentation." *Mechanical engineering series*, 2nd Ed., Springer, New York.

Franco, A., Pintaúdeb, G., Sinatoraa, A., Pinedoc, C., and Tschiptschina, A. (2004). "The use of a Vickers indenter in depth sensing indentation for measuring elastic modulus and Vickers hardness." *Mater. Res.*, 7(3), 483–491.

Giannakopoulos, A. E., Larsson, P. L., and Vestergaard, R. (1994). "Analysis of Vickers indentation." *Int. J. Solids Struct.*, 31(19), 2679–2708.

Guddati, M. N., Feng, Z., and Kim, R. (2002). "Toward a micromechanics-based procedure to characterize fatigue performance of asphalt concrete." *Transportation Research Record. 1789*, Transportation Research Board, National Research Council, Washington, D.C., 121–128.

Hebbache, M. (2003). "Nanoindentation: Depth dependence of silicon

hardness studied within contact theory." *Phys. Rev. B*, 68(12), 125310.
Hertz, H. (1881). "On the contact of elastic solids (Zeitschrift fur die reine und angewandte Mathematik)." *J. fuer reine und angewandte Mathematik*, 92, 156–171 (in German).
Huet, C. (1963). "Etude par une méthode d'impédance du comportement viscoélastique des matériaux hydrocarbones." Ph.D. thesis, Faculté des Sciences de Paris, France.
Igarashi, S., Bentur, A., and Mindess, S. (1996). "Characterization of the microstructure and strength of cement paste by microhardness testing." *Adv. Cem. Res.*, 8(30), 87–92.
Jäger, A., Lackner, R., and Eberhardsteiner, J. (2007). "Identification of viscoelastic properties by means of nanoindentation taking the real tip geometry into account." *Meccanica*, 42, 293–306.
Johnson, K. L. (1985). *Contact mechanics*, Cambridge University Press, Cambridge, U.K.
Li, G., Li, Y., Metcalf, J. B., and Pang, S. (1999). "Elastic modulus prediction of asphalt concrete." *J. Mater. Civ. Eng.*, 11(3), 236–241.
Little, D. N., Lytton, L. R., Williams, D. A., and Kim, Y. R. (1999). "An analysis of the mechanism of microdamage healing based on the application of micromechanics first principles of fracture and healing." *Asph. Paving Technol.*, 68, 501–542.
Loubet, J. L., Georges, J. M., Marchesini, O., and Meille, G. J. (1984). "Vickers indentation curves of MgO." *J. Tribol.*, 106(1), 43–48.
Lucas, B. N. (1998). "Thin-films-stresses and mechanical properties. VII 505." *Mater. Res. Soc.*, 505, 97.
Masad, E., Niranjanan, S., Bahia, H., and Kose, S. (2001). "Modeling and experimental measurements of localized strain distribution in asphalt mixes." *J. Transp. Eng.*, 127(6), 477–485.
Mondal, P., Shah, S., and Marks, L. (2007). "A reliable technique to determine the local mechanical properties at the nanoscale for cementitious materials." *Cem. Concr. Res.*, 37(10), 1440–1444.
Newey, D., Wilkens, M. A., and Pollock, H. M. (1982). "An ultra-low-load penetration hardness tester." *J. Phys. E: J. Sci. Instrum.*, 15(1), 119–122.
Oliver, W. C., and Pharr, G. M. (1992). "An improved technique for determining hardness and elastic modulus using load and displacement sensing indentation experiments." *J. Mater. Res.*, 7(6), 1564–1583.
Ossa, E. A., and Collop, A. C. (2007). "Spherical indentation behavior of asphalt mixtures." *J. Mater. Civ. Eng.*, 19(9), 753–761.
Ossa, E. A., Deshpande, V. S., and Cebon, D. (2005). "A spherical indentation behavior of bitumen." *Acta Mater.*, 53, 3103–3113.
Papagiannakis, A. T., Abbas, A., and Masad, E. (2002). "Micromechanical analysis of viscoelastic properties of asphalt concretes." *Transportation Research Record. 1789*, Transportation Research Board, National Research Council, Washington, D.C., 113–120.
Park, S. W., Kim, Y. R., and Lee, H. J. (1999). "Fracture toughness for microcracking in a viscoelastic particulate composite." *J. Eng. Mech.*, 125(6), 722–725.
Pätzold, G., Linke, A., Hapke, T., and Heermann, D. (1997). "Computer simulation of nanoindentation into polymer films." *Z. Phys. B: Condens. Matter*, 104(3), 513–521.
Pethica, J. B. (1982). *Ion implantation into metals*, Pergamon, Oxford, 147–156.
Pharr, G. M., Oliver, W. C., and Brotzen, F. R. (1992). "On the generality of the relationship among contact stiffness, contact area, and elastic modulus during indentation." *J. Mater. Res.*, 7(3), 613–617.
Pichler, C., Jäger, A., Lackner, R., and Eberhardsteiner, J. (2005). "Identification of material properties from nanoindentation: Application to bitumen and cement paste." *Proc., 22nd DANUBIA-ADRIA Symp. on Experimental Methods in Solid Mechanics, Das2005*, Monticelli Terme, Parma, Italy.
Roberts, F., Kandhal, P., Brown, E., Lee, D., and Kennedy, T. (1996). *Hot mix asphalt materials, mixture design, and construction*, 2nd Ed., National Asphalt Pavement Association Research and Education Foundation, Lanham, Md.
Roque, R., Zhang, Z., and Sankar, B. (1999). "Determination of crack growth rate parameters of asphalt mixtures using the Superpave IDT." *Asph. Paving Technol.*, 68, 404–433.
Sadd, M. H., Dai, Q., and Parameswaran, V. (2004). "Microstructural simulation of asphalt materials: Modeling and experimental studies." *J. Mater. Civ. Eng.*, 16(2), 107–115.
Saha, R., and Nix, W. (2002). "Effects of the substrate on the determination of thin film mechanical properties by nanoindentation." *Acta Mater.*, 50(1), 23–38.
Sayegh, G. (1965). "Contribution à l'étude des propriétés viscoélastiques des bitumes pur et bétons bitumineux." Thèse de Docteur-Ingénieur, Sorbonne, France.
Sneddon, N. (1965). "The relation between load and penetration in the axisymmetric Boussinesq problem for a punch of arbitrary profile." *Int. J. Eng. Sci.*, 3(1), 47–57.
Stangl, K., Jäger, A., and Lackner, R. (2007). "The effect of styrene-butadiene-styrene modification on the characteristics and performance of bitumen." *Monatshefte für Chemie*, 138, 301–307.
Stilwell, N. A., and Tabor, D. (1961). "Elastic recovery of conical indentation." *Physicis Proc. Soc*, 78(2), 169–179.
Stone, D., LaFontaine, W. R., Alexopoulos, P., Wu, T-W., and Li, C-Yu. (1988). "An investigation of hardness and adhesion of sputter-deposited aluminum on silicon by utilizing a continuous indentation test." *J. Mater. Res.*, 3(1), 141–147.
Tabor, D. (1951). *The hardness of metals*, Oxford University Press, Oxford, U.K.
Uddin, W. (2003). "Viscoelastic characterization of polymer-modified asphalt binders of pavement applications." *Appl. Rheol.*, 13(4), 191–1999.
VanLandingham, M., Villarubia, J., Guthrie, W., and Meyers, G. (2000). "Nanoindentation of polymers: An overview." *Polym. Prepr. (Am. Chem. Soc. Div. Polym. Chem.)*, 41(2), 1412–1413.
Xu, Q., and Solaimanian, M. (2009). "Modelling linear viscoelastic properties of asphalt concrete by the Huet-Sayegh model." *Int. J. Pavement Eng.*, 10(1), 1–22.
Zhu, W., and Bartos, P. J. M. (2000). "Application of depth-sensing microindentation testing to study of interfacial transition zone in reinforced concrete." *Cem. Concr. Res.*, 30(8), 1299–1304.